Shear Loading of the Lumbar Spine: Modulators of Motion Segment Tolerance and the Resulting Injuries

by

Vanessa Rose Yingling

A thesis
presented to the University of Waterloo
in fulfilment of the
thesis requirement for the degree of

Doctor of Philosophy

in

Kinesiology

Waterloo, Ontario, Canada, 1997

0-612-22252-7

Canadä

The University of Waterloo requires the signatures of all persons using or photocopying this thesis. Please sign below, and give address and date.

Abstract

The general theme of this thesis was to determine the modulators of biomechanical tolerance values and to quantify the specific resulting injuries of spinal motion segments exposed to pure shear loading. A porcine model was used for all experimental testing due to its similarity in structure to human specimens. A specially designed jig which isolated shear loading was coupled to an Instron 8511 hydraulic testing machine to test the specimens. Several experiments were performed to specifically examine the effects of loading rate, loading direction and posture on the failure behavior of porcine motion segments. As well, serial destruction of anatomical components was performed prior to a second series of tests which attempted to identify the contributions of each structure during applied shear loading. Biomechanical modelling techniques were used to illustrate possible mechanisms of the load sharing strategies as well as illustrate the mechanism of injury of the structures comprising the motion segment during shear loading. The major findings were that following the removal of the posterior ligaments and the facet joints, the intervertebral disc was found to account for the majority of the shear load resistance under both anterior and posterior loading. The posterior elements were involved in either increasing the stiffness of the entire structure, which was the function of the pars during anterior shear loading, or increasing the deformation to failure of the structure, which was the role of the capsular ligaments and the pars under posterior shear loading. A flexed posture increased the moment arm of the pars which resulted in higher ultimate shear load

values as well as a larger deformation at failure. The resulting injuries from mechanical tests were similar to those found in clinical conditions and in in-vitro testing. Anterior shear loading resulted in pars fractures with endplate avulsions occurring at higher loading rates and following the preconditioning cycles. Posterior loading injuries were primarily endplate avulsions with edge fractures and facet face avulsions occurring at higher loading rates and following preconditioning cycles. These data begin to identify the different functioning of the intervertebral disc and the posterior elements under anterior shear loading compared to posterior shear loading. The results of the mechanical tests along with the injuries resulting from the tests suggest that the posterior elements may function to protect the disc from injury, however, more evidence is needed to support this hypothesis.

Acknowledgements

Dedicated

To Women

Just like moons and like suns,

With the certainty of tides,

Just like hopes springing high,

Still I'll rise.

Maya Angelou

Table of Contents

List of Tables

List of Figures

Chapter Seven

Reader's Guide to this Thesis

This theme of this thesis was to elucidate the injuries which result from external shear loading on a spinal motion segment and to determine the modulators which affect injury. Several experiments were performed to identify the structural properties of the motion segments, these experiments shared a common methodology. For this reason, Chapter Three covers all common material pertaining to the methodology while specific methods for each test were described in the appropriate chapter. Chapter Two has been submitted for publication. Chapter Four through Chapter Six will be submitted as a mechanical properties paper. Chapter Seven will be submitted with more of a focus on the injuries which result from shear loading. Specific content within each chapter is as follows:

Chapter One: "Introduction" A general introduction which identifies the importance of shear loading as a factor in the etiology of spine injuries.

Chapter Two: "Is the porcine cervical spine a reasonable model of the human lumbar spine: An anatomical, geometrical and functional comparison." A submitted paper which gives evidence on the suitability of using a porcine model for mechanical testing.

Chapter Three: "General Methodology" This is a general methodology chapter discussing factors which are common between all the mechanical tests, such as the characteristics of the

specimens (3.2.1), specimen mounting (3.2.2), shear loading jig (3.2.3) and the definition of failure (3.2.4). A review of literature concerning types of loading, biomechanical modelling techniques, specimen storage and preload on specimen behavior is included. The protocols for the different mechanical tests is given (3.2.5) as well as for the data analyses (3.2.6) and the statistical analyses (3.2.7).

Chapter Four: "The effect of anterior vs posterior shear loading" This chapter discusses the difference in the mechanical properties between anterior and posterior shear loading, including a review of relevant literature, a list of hypotheses, a brief protocol specific to the specimens involved in this series of testing and a discussion including a list of key findings.

Chapter Five: "The effect of the rate of loading on motion segment behavior under anterior and posterior shear loading." This chapter discusses the effect of the rate of loading on the mechanical properties between anterior and posterior shear loading, including a review of relevant literature, a list of hypotheses, a brief protocol specific to the specimens involved in this series of testing and a discussion including a list of key findings.

Chapter Six: "Identification of the mechanical roles of individual structures of the motion segment under shear loading" This chapter discusses the contribution of the major structures of the motion segment involved in resisting applied shear loads. The chapter includes a review of relevant literature, a list of hypotheses, a brief protocol specific to the specimens involved in this series of testing and a discussion including a list of key findings.

2

Chapter Seven: "Documentation of specific injuries resulting from shear loading of the motion segment" This chapter discusses the resulting injuries from all of the mechanical testing protocols. Identifying the difference in injury due to the direction of loading, the rate of loading and finally the injuries resulting from each structure in isolation. The chapter includes a review of relevant literature, a list of hypotheses, a brief protocol specific to the specimens involved in this series of testing and a discussion including a list of key findings.

Chapter Eight: "Summary" This chapter summarizes the main findings of the studies and suggests future research directions in this area.

Chapter One

1.0   Introduction

Low back problems are a serious concern in society. This concern has motivated much research focussing on understanding the mechanisms of low back injury with the ultimate objective of improving prevention and rehabilitation approaches. There is little conclusive evidence to suggest that compression is the most important mode of loading in the etiology of lumbar spine injuries. Yet, the majority of research has focussed on compressive loading leaving a void of understanding about the effect of bending, torsional and shear loading on lumbar spine injury etiology. The purpose of this project was to determine the modulators of biomechanical tolerance values and resultant injuries of spinal motion segments exposed to pure shear loading using a porcine model.

Research is beginning to identify shear loading as a risk factor in low back problems. For example, slipping and landing on the buttocks causes a rapid posterior shear load to the lumbar motion segments and has been hypothesized to lead to shear failure (McGill, 1997). Excessive anterior shear loading may cause pars fractures, a commonly identified injury in clinics. This type of anterior shear may occur in landing in gymnastics due to the excessive lordotic posture in the lumbar spine. Load handling task may also apply an anterior shear load on the lumbar spine (Figure 1). Moreover, a recent case-control study involving a large
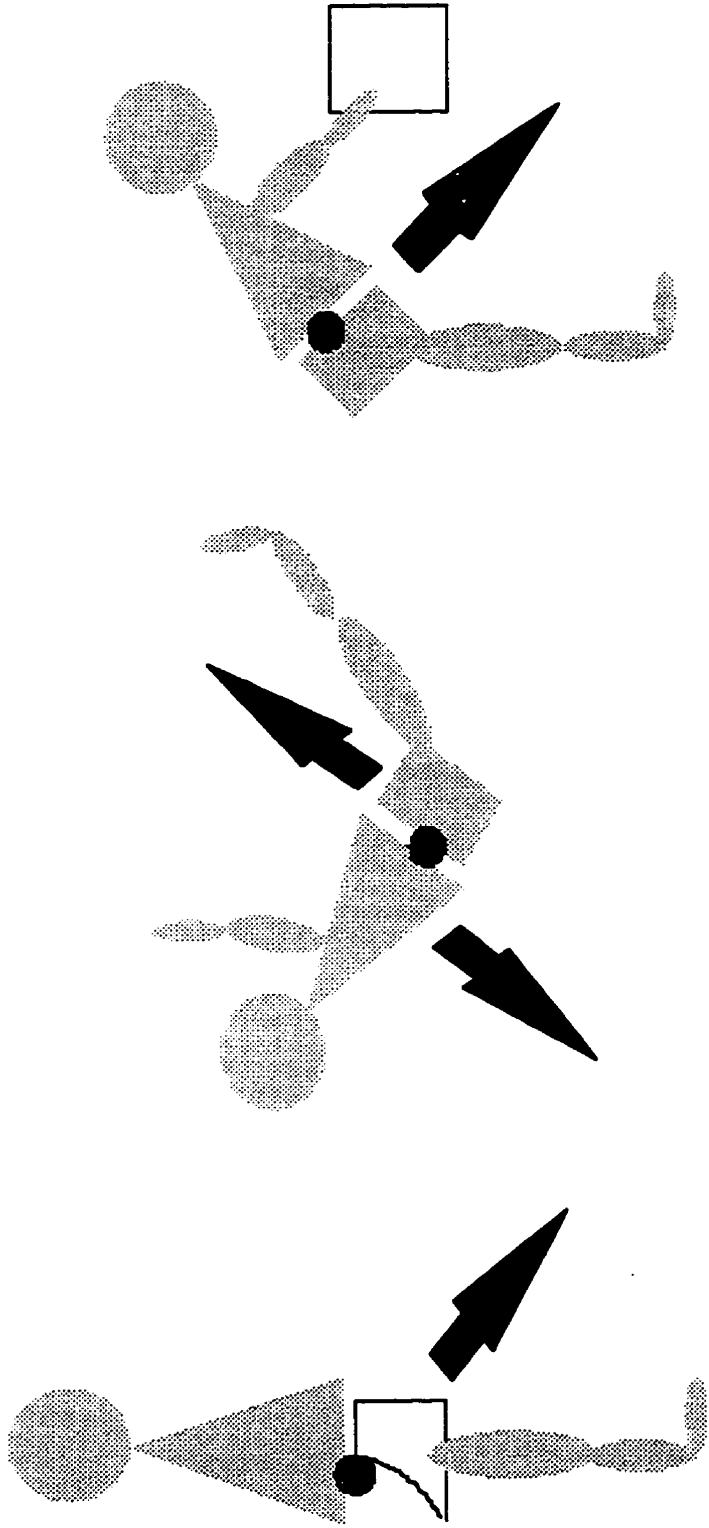
(A) Lordosis   (B) Falling/Slipping   (C) Lifting

Figure 1: Examples of shear loading on the lumbar spine during activities. (A) The lordotic curve of the lumbar spine imposes a shear load. (B) slipping and falling on the buttocks applies a posterior shear load to the lumbar spine. (C) lifting tasks apply an anterior shear to the spine.

5

automotive plant investigating the incidence of low back pain reports in industry has identified shear force magnitude as a strong predictor of low back pain (Norman, Wells, Neumann, Kerr, Frank & Shannon, 1997). Finally, studies involving the quantification of the risk of injury due to changes in the posture of the spine indicate that the margin of safety is often smaller in shear than in compression. For example, in a single lift the margin of safety for shear tolerance is greatly decreased at full lumbar spine flexion while the margin of safety for compressive loading remains unchanged. Specifically, McGill and Norman (1987) and Potvin et. al. (1991) demonstrated that fully flexing the spine can increase the shear component of the lumbar motion segment up to three-fold independent of the size of the load lifted.

Biomechanical models suggest that the lumbar spine experiences a wide range of reaction shear load. For example, reaction shear loads have been estimated to range from 400 N in a static flexed posture to a maximum of 3539 N for some male power lifts (Cholewicki, McGill, & Norman, 1991; Potvin, McGill, & Norman, 1991). These applied shear loads increase due to the acceleration and inertia of the load and the upper body mass, and passive tissue involvement associated with spine flexion (Potvin, McGill, & Norman, 1991). Muscular activity can increase and/or oppose anterior shear loading. The psoas muscle at the L5-S1 level may add significantly to the anterior shear load on the motion segment (Santaguida & McGill, 1995), however, the pars lumborum fibers of longissimus thoracis and iliocostalis lumborum of the erector spinae muscles may oppose anterior shear loading (McGill & Norman, 1987). It is becoming more clear that shear loading is important and requires investigation to elucidate injury mechanics.

6

Basically, injury to the spine occurs when loading on the spine exceeds its material and/or structural mechanical tolerance to the specific type of applied load. To fully understand the injury mechanisms of the intervertebral joint to shear loading, the tolerance of the joint must be identified, as well as, the variables which modulate this tolerance. Engineers consider a variety of factors in their attempts to design a failure resistant structure, including the geometry of the structure, the mechanical properties of the materials which make up the structure and the location, direction and magnitude of the loads which are applied to the structure (Hayes & Myers, 1994). A similar approach can be used to examine the failure of a motion segment under applied shear loading, which is affected by the structure of the motion segment itself as well as the external loading applied to the segment.

The intrinsic characteristics of the motion segment which are designed to resist shear loads are the geometry of the motion segment and the material properties of the tissues which comprise the structure. The alignment of the facet joints, which are perpendicular to the plane of the disc, the elliptical shape of the disc and the alignment of the posterior ligaments suggest a role of the motion segment in shear load resistance. The variety of tissues: cortical and cancellous bone in the vertebral body, collagenous tissue in the ligaments and annulus, and a mucoprotein gel in the nucleus making up the structure exhibit different responses to external loading. Therefore, these tissues are expected to have different responses to different types of external loading.

The second factor affecting the failure tolerance of a motion segment is the external load applied to the structure. The external load varies in the direction of application (anterior or posterior), the rate of loading, the magnitude of the load and the type of loading (impact

7

loading or repetitive loading). The posture of the motion segment during loading also affects the tolerance of the motion segment. It appears that anterior shear loading is resisted by the annulus and facet joints, whereas posterior shear loading is resisted by soft tissue including the annulus and the capsular and interspinous ligaments. These different tissues may be responsible for the different response between anterior and posterior shear loading. The motion segment is made up of viscoelastic materials: bone, ligament, nucleus and the collagenous annulus suggesting a load rate effect on its tolerance. In a flexed posture the facet joints of a vertebral motion segment are misaligned, with only the facet tips sustaining load (Cailliet. 1995; Yang & King. 1984). Both the intrinsic features of the motion segment and the external loading conditions are important in the injury mechanisms of shear loading.

The tolerance values for the spine under shear loading, in the literature. are quite variable possibly due to differing testing protocols and some inconsistency between the specimens used. Some preliminary data suggest that the facet joints may resist between 3100-3600 N of shear load with the intervertebral disc resisting less than 900 N (Farfan. 1988). Another test concluded that facets fail near 2500 N with the discs resisting 77% of the applied load at that instant of failure (Cripton, Berleman, Visarius, Begeman, Nolte, & Prasad. 1995).

The substantial range of both in-vivo and in-vitro applied shear load values applied to the motion segment, indicates a need for a comprehensive analysis of factors which modify the tolerance of a motion segment. Furthermore, little is known about the injuries resulting from shear loading and the mechanisms of occurrence. As a result two major questions were addressed in this work:

1) What are the factors which modulate the tolerance of lumbar spinal motion segments exposed to shear loading?

2) What injuries result from shear loading?

1.1   Statement of Purpose

The purpose of this project was to determine the modulators of biomechanical tolerance values and the resultant injuries of lumbar spinal motion segments exposed to pure shear loading using a porcine model. The first objective was to assess the suitability of the porcine model to represent human spines. The porcine model is advantageous in low back injury research. Human tissue may have the advantage of size which may allow more accurate absolute mechanical test results. However, human tissue is not homogeneous and studies with large sample sizes are not feasible. Large controlled studies can be carried out to identify the modulators of tolerance values and identify the resulting injuries using porcine tissue and human tests can be used to verify the injury sites as well as to scale the resulting mechanical tolerance values. Then, the relative contribution of each of structure of the spinal motion segment in the resistance of shear loading was quantified. These structures included: the disc, facet joints, and the posterior ligaments (supraspinous and interspinous). Biomechanical modelling techniques were then used to link the physical properties of the

9

individual components to the total behavior of the motion segment, and recreate the effect of external shear loading on the lumbar motion segment.

1.2   Statement of Hypotheses

The following hypotheses were examined to understand the factors which may affect the tolerance of the motion segment. The use of a hydraulic testing machine limits the relevance of the following tests to normal daily activity, not to an impact situation such as slipping and falling. The fastest loading rate, 10810 N/s, may mimic fast lifting in an occupational setting.

Hypothesis 1:

The ultimate shear load at failure will be higher under anterior shear loading than under posterior loading.

Hypothesis 2:

A flexed posture will sustain a lower ultimate shear load at failure compared with a neutral posture.

Hypothesis 3:

Cyclic preconditioning, both anterior and posterior, decreases the ability of the

motion segment to resist shear loading.

Hypothesis 4:

Stiffness and the ultimate shear load at failure of the spinal motion segment will increase as load rate increases.

Hypothesis 5:

Facet joints will resist a greater proportion of an external anterior shear load compared with the disc and posterior ligaments (interspinous and supraspinous).

1.3   Limitations

In vitro studies are intended to replicate as closely as possible, the in-vivo situation but in reality fall short of this objective. Thus, in-vitro study results should be interpreted with the following limitations:

1. In-vitro studies fail to include the effect of muscle and other tissues surrounding the spinal column in resisting loading. Anatomical descriptions of the erector spinae muscles have shown that the orientation of the muscles is such that they would resist anterior shear of the superior vertebra with respect to the inferior vertebra.

2. The porcine spine is not an exact replica of the human spine. however. the porcine cervical vertebrae is structurally similar to the human lumbar vertebrae (Chapter Two). Furthermore, a porcine model has the benefit of testing a homogeneous population with similar genetics, activity level, age. weight and diet, which is a distinct limitation when using human material.

3. The use of specimens with normal, healthy gelatinous intervertebral discs may not reflect the disc status in the general human population. The specimens which will be used in this thesis only represent young, healthy discs. A natural loss of fluid and increasing fibrosity of the intervertebral disc occurs with age. The intention of the thesis is to determine the modulators of the tolerance value of the material and structure of the motion segment without the confounding effects of age induced changes.

4. The application of a pure shear load to the motion segment does not imitate the complex loading experienced by the motion segment in-vivo. However, in order to understand the ability of the motion segment to resist shear loading other loading modes will be controlled. to avoid confounding variables.

5. The motion segments are always under load due to body weight and muscle activity in-vivo. Further, cadaveric material requires a preload to balance fluid distribution and achieve viscoelasticity commiserate with in-vivo conditions. A static preload is applied to all specimens before loading during in-vitro testing.

Chapter Two

Is the Porcine Cervical Spine a Reasonable

Model of the Human Lumbar Spine:

An Anatomical, Geometrical and Functional

Comparison.

Vanessa R. Yingling, MS, Jack P. Callaghan, MSc, Stuart M. McGill, PhD

August 1997

.

2.0   Abstract

Study Design: Anatomical, geometric and functional characteristics of the porcine cervical spine were compared to the human lumbar spine.

Objectives: To assess whether the porcine cervical model is a reasonable analog for studying human lumbar injuries.

Summary of Background Data: Controlled studies of identical specimens are not possible using human vertebrae. An animal model offers the asset of assembling a cohort where control can be exercised over age, weight, physical activity and genetic background of the specimen donor. Given this asset, the question is asked; "Is the porcine cervical spine a reasonable model of the human lumbar spine?".

Methods: Three porcine cervical spines (C2-C7) were assessed for geometrical characteristics then a larger cohort (N= 24) were loaded to failure under either compressive or shear loading. Also, in-vivo loading was computed and compared between the human low back (biped) and the porcine neck (quadruped).

Results: Generally, the porcine vertebrae are smaller in all dimensions. They also have anterior processes unlike humans, but they have similar ligamentous structure and facet joint orientation. Stiffness values (compression and shear) are similar and comparable injuries resulted from both applied compressive and shear loads.

Conclusions: Porcine cervical spines appear to be a reasonable analog for studying human lumbar injury due to the similarity of mechanical characteristics and injuries. The porcine

model will allow large control studies which can identify injury mechanisms.

Precis: Anatomical, geometric and functional characteristics of the porcine cervical spine were compared to the human lumbar spine, to assess whether the porcine model is a reasonable analog. Porcine cervical spines appear to be an analog for studying human lumbar injury which will provide a homogeneous specimen for large control studies.

Key Words: Injury, porcine, spine, low back

2.1   Introduction

Study of spine injury is hindered by the inability to collect a cohort of identical

human specimens for controlled testing. Therefore, injury research would be best served by

the use of both human and animal tissue to identify injury processes, but each approach has

different assets and liabilities. While it is impossible to obtain a homogeneous sampling of

human specimens, samples may be acquired from animal specimens where control is

exercised over genetic make-up, age, weight, physical activity levels and diet. For example,

little would be known about cancer and other disease processes if animal models were not

utilized. As well, animal tissue is typically harvested from healthy animals, where as human

tissue is generally obtained from elderly or diseased populations. While controlled

experiments are only possible using an animal model, they suffer from the drawback of

scaling the results to apply to human tissue. The critical issue addressed in this study was

whether the porcine cervical spine is a reasonable analog for furthering our knowledge of

injury mechanisms in the human lumbar spine.

Oxland et. al. (1991) described qualitatively the similarities between porcine cervical

vertebrae and human lumbar vertebrae. They determined that the facets shared a similar

orientation and there was a "consistency" of the posterior interspinous and supraspinous

ligaments. Furthermore, Sikoryn and Hukins (1990) reported similarities between the human

and porcine ligamentum flavum after dissection. The maximum stress found in porcine

ligamentum flavum, 2.6 -3.0 mPa (Sikoryn & Hukins. 1990) was somewhat lower than

16

values found from human ligaments, 4.4 MPA. (Nachemson & Evans. 1968). Also the porcine vertebrae were characterized by ossification centers as determined through x-ray. which were similar to a child or adolescent spine (Oxland. Panjabi. Southern. & Duranceau. 1991), but still appear to be useful in research investigating the mechanical function of the lumbar spine.

The purpose of this study was to compare the anatomy, geometry and functional characteristics of human lumbar vertebrae to porcine cervical vertebrae to assess whether the porcine model is a reasonable analog for studying human lumbar injuries. Anatomical and geometrical parameters and load-deformation and failure characteristics of porcine cervical vertebrae were collected in the laboratory. Human vertebral geometry and functional behavior were gathered from the literature. Finally, to address the issue of comparing a biped to a quadruped. some analytical modelling was performed to assess the hypothesis that loading experienced by the human lumbar spine is similar to the porcine cervical spine in-vivo.

2.2   Methods

Three methodological approaches were conducted to compare pig cervical and human lumbar spines.

Geometrical Measurements:

Calipers were used to measure nine parameters of the porcine vertebrae: four parameters of the vertebral body, the width and depth of both the upper and lower endplates (UEW, LEW, UED, LED) (Figure 1); seven parameters of the posterior elements, the pedicle width (PEDW), pars height (PH), pars width (PW), spinal canal depth and width (SCD, SCW).

A specially designed gimbal was used to measure two orientation angles of the facet joint (Figure 2). The sagittal facet angle was the orientation of the facet face with the sagittal plane and the transverse angle was the orientation of the pars and facet face with the horizontal plane (Figure 3). The vertebrae were oriented using two site lines and the angles were measured via protractors attached to the gimbal.

Endplate areas were determined using two methods. The endplates of both human and porcine vertebrae resemble an ellipse (Figure 4). Therefore, the formula for the surface area of an ellipse ($\pi/4 * a * b$) (Hutton & Adams. 1982) was used to estimate the surface area of the endplate of a vertebral body. A second method utilized an electronic
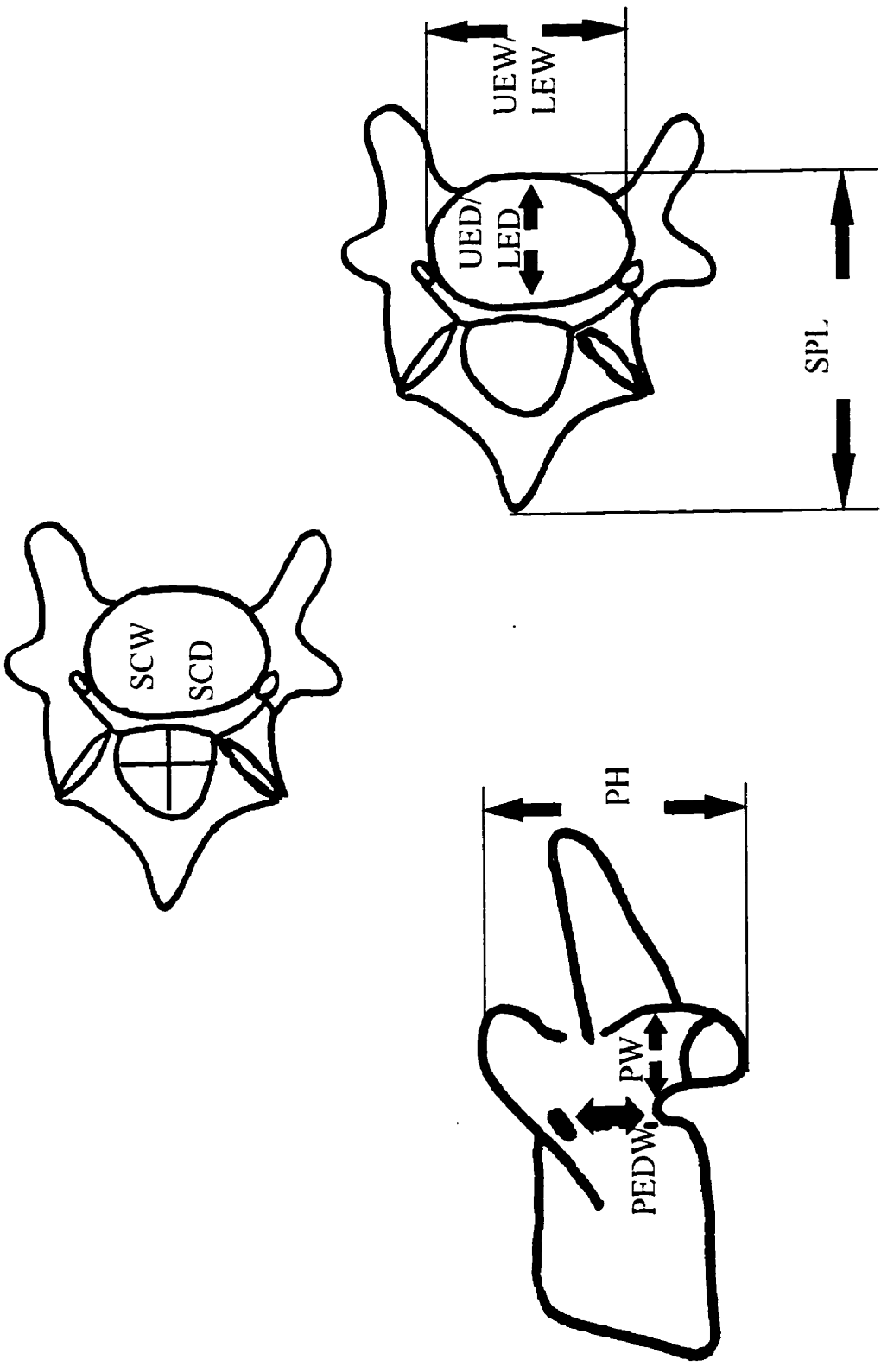
Figure 1: Schematic top and side view of a porcine lumbar vertebra illustrating the measured parameters. Width and depth of both the upper and lower endplates (UEW,LEW,UED,LED), the pedicle width (PEDW), pars height (PH), pars width (PW), spinal canal depth and width (SCD, SCW).
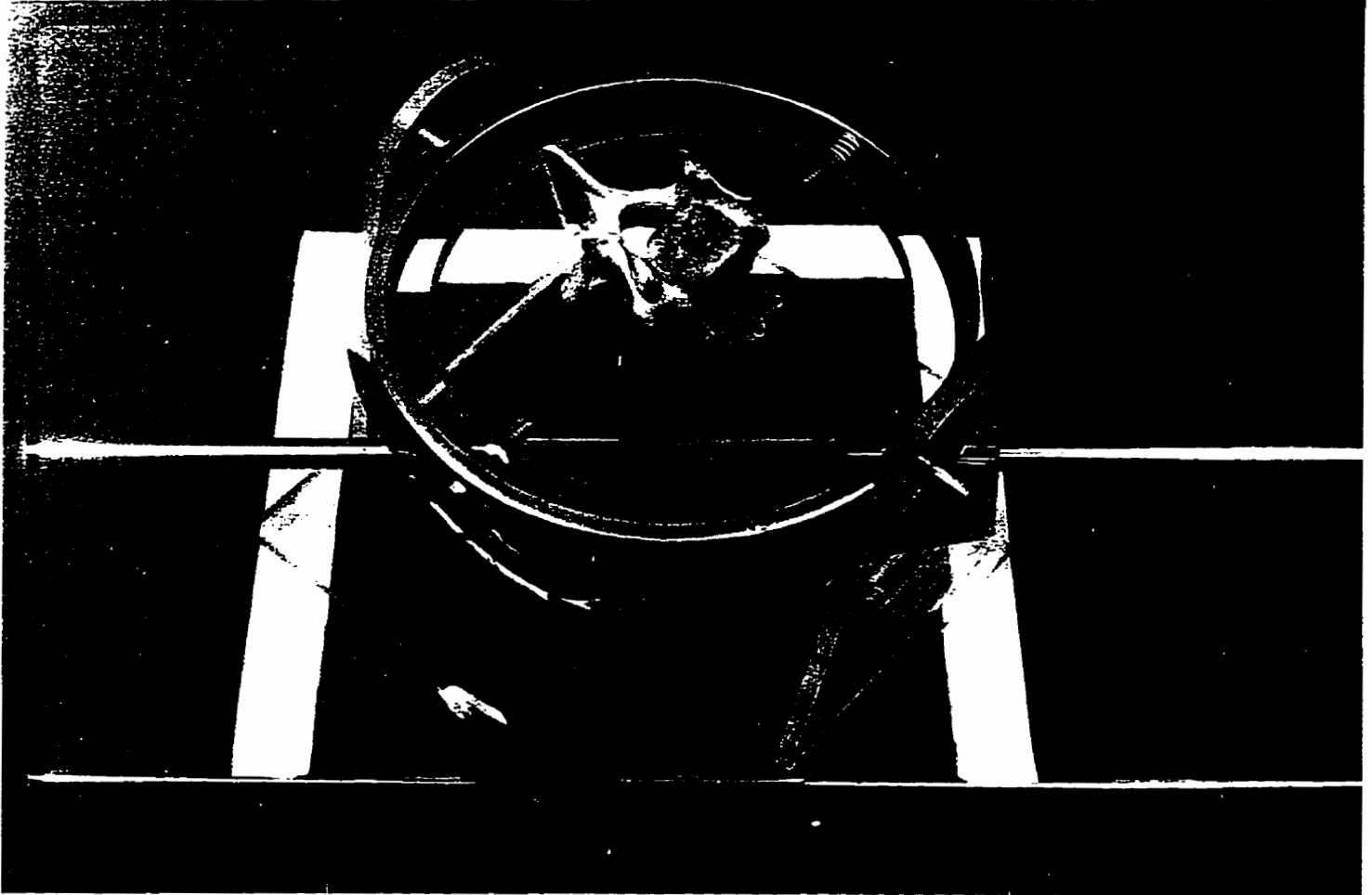
Figure 2: Angle measurement gimbal with three angular degrees of freedom and measurement.

Transverse Angle
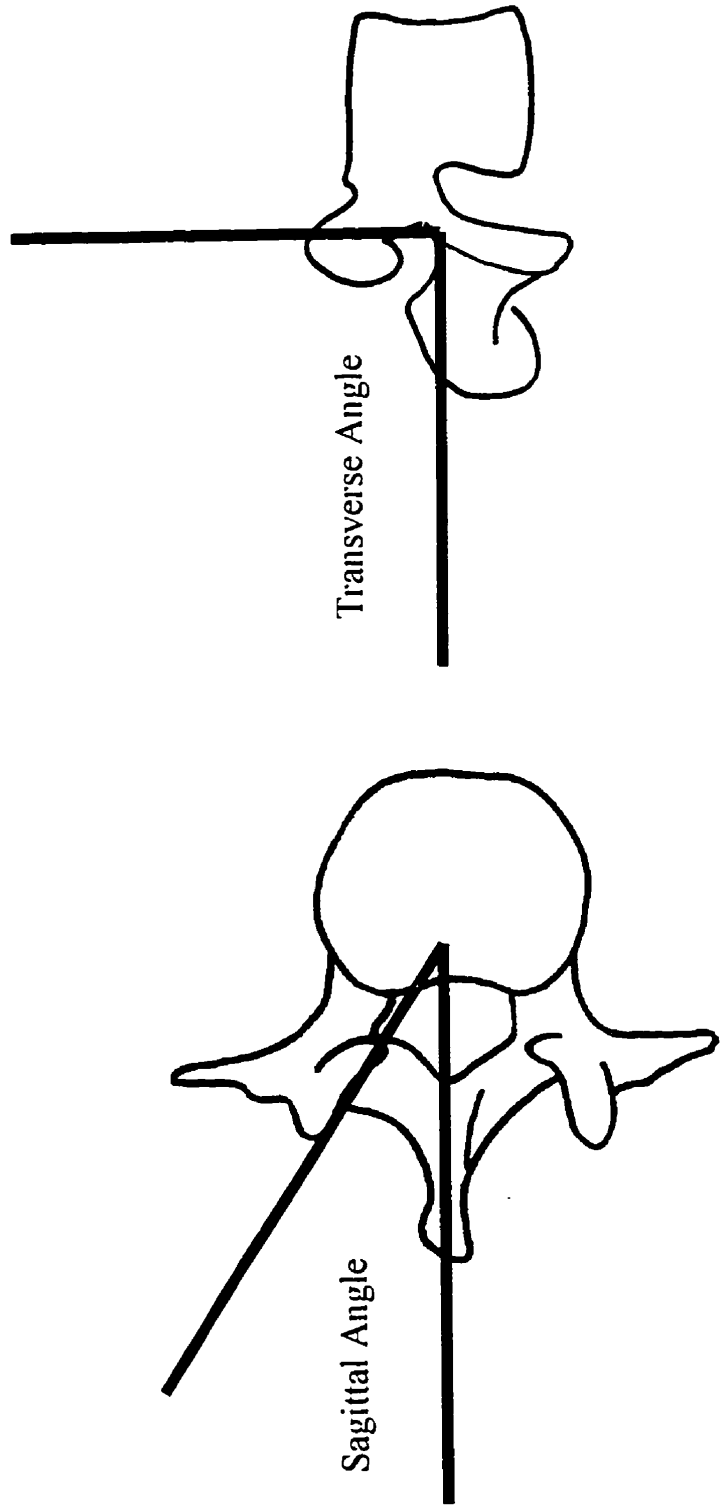
Sagittal Angle

Figure 3: Schematic diagram of the sagittal and transverse facet angles

21
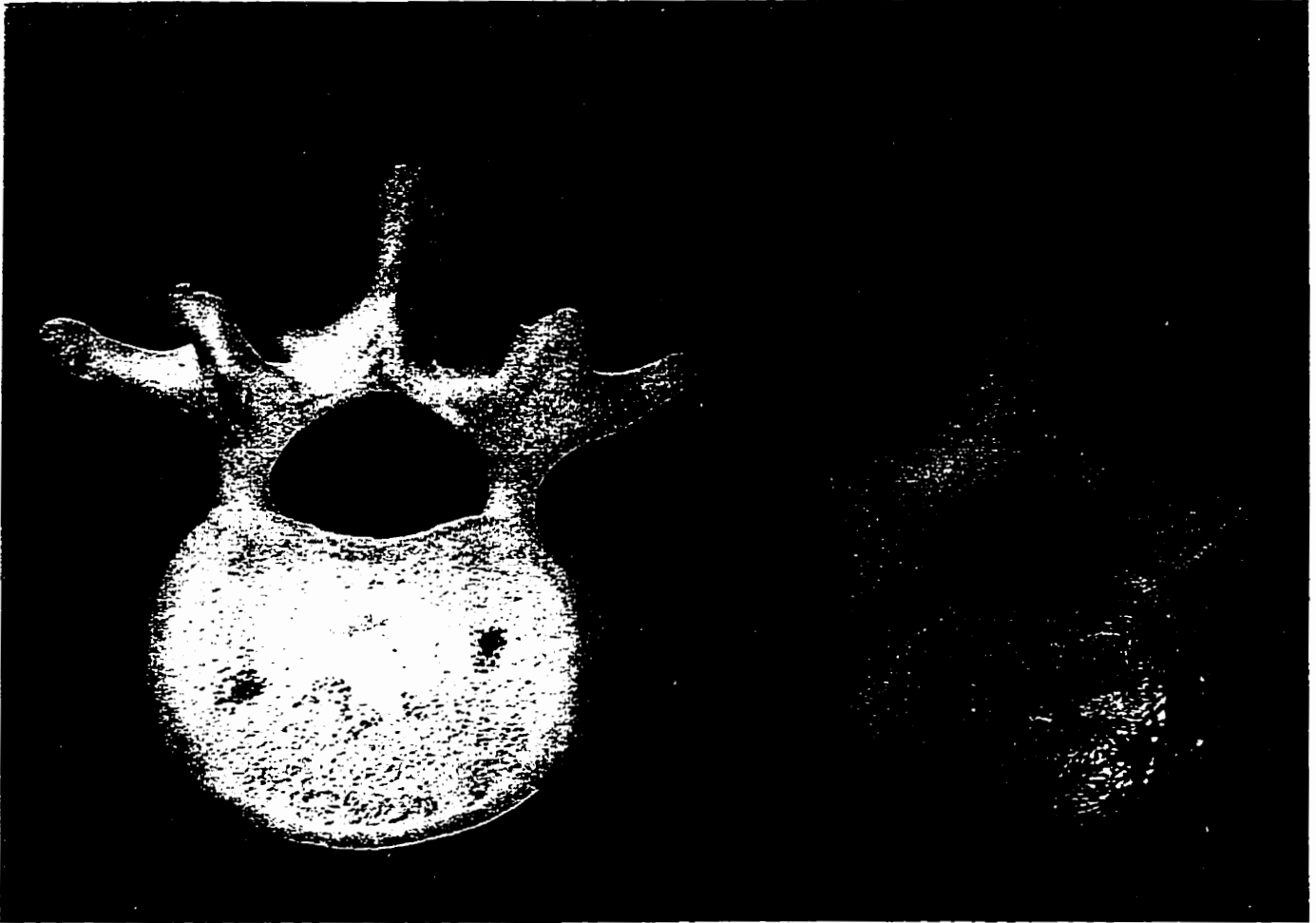
Figure 4: Top view of a human lumbar vertebra and a porcine cervical vertebra.

digitizing tablet (Summasketch 010, Summagraphics, Seymour, CT), which determined the area of the endplate from the digitized perimeter using an area integration algorithm. Scaled photographs of both upper and lower endplates were taken and digitized using the digitizing tablet.

Mechanical Properties:

A servo-hydraulic dynamic testing machine (Instron Model 8511, Instron Canada Inc. Burlington, ON) was used to determine the mechanical properties of the porcine cervical motion segments under both shear (N=10) and compressive (N=14) loading. The specimens were mounted in stainless steel cups and fixed with dental plaster (Denstone, Miles Inc. South Bend, IN, USA). For the compressive tests, the specimens consisting of 3 vertebrae, were placed in the cups with the central vertebrae endplates parallel to the cups to avoid a bending moment during testing. Three vertebrae were used to avoid the effects of the potting material on the outer vertebrae. A specially designed jig was used for the testing which applied only a compressive load onto the specimens. A compressive preload of 300 N was applied for 15 minutes to the specimens to precondition and produce an equilibrium state in the creep response. The spines were then loaded to failure at different load rates, 100 N/s, 3000 N/s, 10,000 N/s 16,000 N/s. Failure was defined as a drop in the load feedback signal, 3.125% indicating structural failure. The choice of the drop is important since too large a drop would not detect the first stages of failure (injury) and allow progression to massive tissue destruction.

23

The specimens subjected to shear loading, which consisted of two vertebrae, were mounted into stainless steel cups using dental plaster with steel wire looped around the pedicles and the anterior processes to secure the specimens. A jig, compatible with the Instron machine, constrained the motion of one vertebral joint to a pure shear load. A compressive preload, 300 N, was applied to the motion segment through a spring mechanism. The spines were then loaded to failure, which was defined as a drop in the load feedback signal, 6.25%. Load deformation curves were sampled at 50-100 Hz and processed with a 486 computer to obtain the mechanical parameters of the specimens which included, the energy stored at failure, the deformation to failure, the ultimate compressive load at failure and the stiffness of the specimen.

Finally, the measured parameters and functional test values of the porcine cervical vertebrae were compared with values found in the literature on human thoracic and lumbar vertebrae. As well, an analytical model was used to provide evidence that the quadruped porcine cervical spine bears loads in a similar way to the human lumbar spine (the head-neck of an 80 kg pig was used to determine the modelling parameters needed for analysis).

2.3   Results

Qualitatively, the porcine vertebrae appear to be quite similar to the human lumbar vertebrae except for the anterior processes of the pig. The prominent features of the human lumbar vertebrae include a large body and facet joints which are perpendicular to the plane of

24

the body. These structures of the human are similar to porcine vertebrae, but the porcine vertebral body is smaller than the human lumbar vertebral body.

A comparison of the four vertebral body parameters from porcine specimens to human values found in the literature demonstrates that both the endplate depth and width (Figure 1) of the porcine specimens are on average 10 mm less than the human vertebrae (Table 1). Consequently, the endplate areas are smaller in the porcine with an average area of 500 mm^2 likened to an average area of 1000 mm^2 for human lumbar vertebra (Table 2). There was no statistical difference between the estimated endplate area using the ellipse formula and the area measured by the digitizing tablet suggesting that the ellipse seems to be a good representation of the shape of the vertebral endplate.

A comparison of the posterior elements of the porcine cervical vertebrae to the human lumbar vertebrae (Table 3) demonstrated that the pars interarticularis, an important structure in resisting shear loads, is smaller in the porcine vertebrae. The pedicle of the vertebra, also a structure of the neural arch involved in resisting both applied shear loads and bending moments, compared well with values from human lumbar vertebrae (Table 3). The spinal canal dimensions were similar to human lumbar vertebrae, but the spinal canal width (SCW) was smaller (Table 3).

The facet joints of the human lumbar motion segments are oriented perpendicular to the vertebral body (transverse facet angle), which enables the facet joints to resist shear loading (Table 3). The facet faces are also angled approximately 45° from the sagittal plane (sagittal facet angle) (White & Panjabi. 1990) which permits the facets to resist torsional loading.

25

The mechanical characteristics of porcine cervical vertebrae under applied shear loading appear to have similar values to human samples (Table 4). Our data from porcine specimens and that from Cripton et. al. (1995) on human specimens presented similar trends for anterior and posterior shear stiffness. Under destructive constrained shear testing Cripton et. al. (1995) found an ultimate load to failure of approximately 2500 N under anterior loading compared to 1980 N (160 N) found in our porcine specimens from this study. The fracture of the pars interarticularis below the facet face found through dissection and planar x-ray on porcine specimens compare to injuries found in human specimens following in-vitro tests (Figure 5) (Cripton, Berleman, Visarius, Begeman, Nolte, & Prasad, 1995).

Compressive load tests under quasi-static and dynamic load rates have resulted in similar trends between human and porcine vertebrae (tolerance values for compressive tests on human and porcine vertebrae are shown in Table 5). Injuries resulting from compressive loading using human and porcine motion segments were similar. endplate fractures were the common injury in both specimens (Figure 6). Specifically, at lower load rates, stellate endplate fractures were recurrent, however, at higher load rates edge fractures of the vertebral bodies appeared (Figure 7).

There are two final issues regarding the similarity of loading between the two animals: the first is to compare the neck loads of a biped to an anatomically similar quadruped; the second is to compare the demands on the human lumbar spine and the porcine cervical spine. Upon first consideration, many would expect a biped neck to experience higher compressive loads than a quadruped. This is not the case. The human neck supports the mass of the head, approximately 60 N of compression in an 80 kg person in upright

standing. If one were to bend forward to simulate a quadruped posture and assuming the

head center of mass to be cantilevered 7cm from the fulcrum of the C4-C5 joint. an extensor

tissue moment arm of 2.32 cm (Moroney. Scultz. & Miller. 1988) then the compressive load

increases approximately three-fold to 180 N. Now to compare the applied loads on a human

lumbar spine to a pig cervical spine, in upright quiet standing and assuming an upper body

mass of 40 Kg, the human lumbar spine would experience approximately 400 N of

compressive load. In contrast, during quiet standing the quadruped pig has the head/neck

cantilevered in front of the body requiring and extensor moment for support (Figure 8).

Using the head-neck of an 80 kg pig the following measurements were obtained: a mass of

17.7 Kg for the head to the C4-C5 segment, a center of mass residing 12.8 cm anterior of C4-

C5. and an extensor moment arm of 12.9 cm (with a slight posterior shear orientation due to

serratus ventralis cervicis and splenius). The resulting compressive load at C4-C5 would be

126 N. This is a substantial load. but still smaller than the upright human lumbar static load.

However. the pig has well developed extensor muscles for uprooting food. which would

impose much larger compressive forces on the cervical spine. This analysis helps to explain

the functional similarity of the porcine cervical spine and the human lumbar spine as well as

the greater need for load bearing in the quadruped neck.

Figure 5: Pars interarticularis injury resulting from in-vitro shear loading of a porcine vertebra.

Figure 6: Porcine endplate fracture resulting from compressive loading.
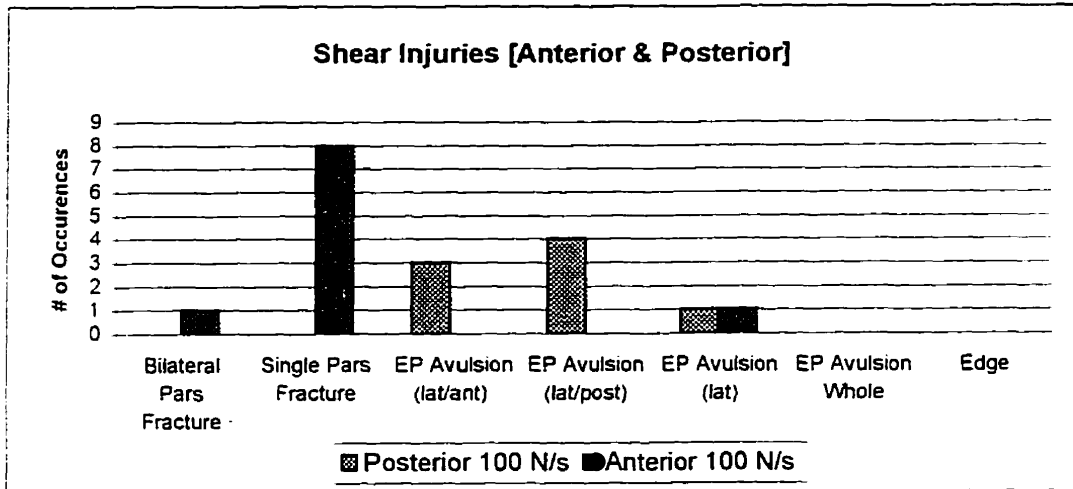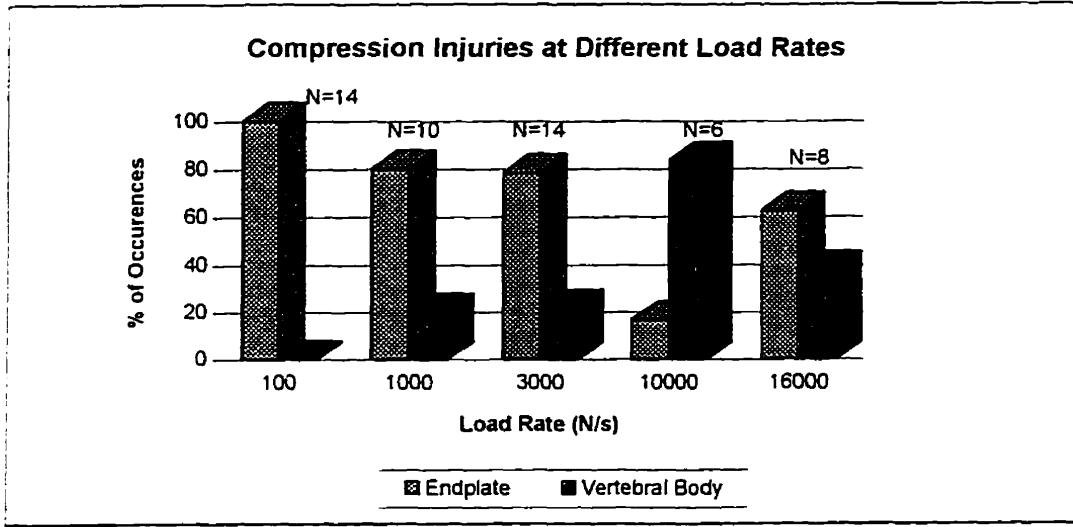
Figure 7: Compressive and shear injuries resulting from in-vitro testing of porcine vertebrae.

Figure 8: The quadruped porcine must support the cantilevered head with an extensor moment creating approximately 126 N of ompressive load.

Table 1: Human - Porcine Comparison of Vertebral Body Dimensions. mean (sd).

Variable	Porcine Vertebra C3-C7	Nissan & Gilad(1986) Human L1-L5 (Radiographs)	Cotterill et. al. (1986) Human L3	White & Panjabi (1990) Human T12
Endplate Depth UED(mm)	22.28 (2.54)	L1: 33.5 (2.9)		32.8
		L2: 34.4 (2.9)		
		L3: 34.7 (2.7)	*L3: 32.7 (6.1)	
		L4: 34.4 (2.7)		
		L5: 34.2 (2.7)		
(LED) (mm)	22.53 (2.67)	L1: 34.1 (2.9)		33.4
		L2: 34.7 (3.0)		
		L3: 34.6 (2.8)		
		L4: 34.9 (2.8)		

32

L5: 33.9 (2.7)

Endplate Width UEW(mm)	31.17 (3.97)	n.a.	*44.3 (7.4)	39.0
LEW(mm)	34.41 (3.55)			42.1

Table 2: Comparison of Upper Endplate Area (UEA) and Lower Endplate Area (LEA) using both the formula of an Ellipse and Simograph.

Cervical Spinal Level	C3	C4	C5	C6	C7
UEA (mm^2) Ellipse Formula	501.72 (129.33)	572.23 (132.17)	580.91 (133.54)	570.03 (130.36)	534.79 (133.81)
UEA (mm^2) Scanned	535.27 (136.28)	539.01 (127.00)	573.36 (132.08)	586.68 (144.50)	529.75 (102.02)
LEA (mm^2) Ellipse Formula	594.10 (133.06)	622.37 (139.72)	656.88 (146.81)	629.99 (150.55)	573.91 (159.21)
LEA (mm^2) Scanned	649.01 (150.64)	558.83 (140.19)	598.37 (141.92)	597.21 (144.40)	567.65 (144.75)

Table 3: Human - Porcine Comparison of the Posterior Elements and the Spinal Canal

Dimensions, mean (sd).

Variable	Porcine		Cotterill et. al. (1986)	White & Panjabi (1990)	Berry et. al. (1987) Human L1-	
Pedicle Width (PEDW) (mm)	Right 8.67 (1.21)	Left 8.91 (.95)	8.4 (2.0)	8.8	Right	Left
					L1: 7.0 (1.9)	L1: 6.9 (1.7)
					L2: 7.4 (1.6)	L2: 7.5 (1.5)
					L3: 9.2 (1.3)	L3: 9.1 (1.6)
					L4:10.3(1.6)	L4: 10.4(1.6)
					L5:10.9(3.4)	L5:10.5(2.9)
Pars Height (PH)(mm)	Right 28.81 (2.94)	Left 29.34 (1.99)	n.a.	n.a.	Right	Left
					L1:47.6(3.7)	L1:47.3(3.7)
					L2:45.2(3.6)	L2:44.8(4.6)
					L3:48(3.2)	L3:48.6(3.3)
					L4:48.5(2.7)	L4:49.1(3.5)
					L5:41.5(4.4)	L5:42.2(3.7)

Pars Width (PW) (mm)	<u>Right</u> 8.48 (.89)	<u>Left</u> 8.35 (.92)	n.a.	n.a.	
Sagittal Facet Angle (degree)	<u>Right</u> 45.0 (7.7)	<u>Left</u> 47.4 (7.8)	57.8 (7.3)	45	n.a.
Transverse Facet Angle (degree)	<u>Right</u> 81.2 (6.2)	<u>Left</u> 81.7 (4.3)	87.2 (4.2)	90	n.a.
Spinal Canal Depth SCD (mm)	9.78 (1.68)		12.1 (1.5)	18.1	L1: 17.2 (1.3)
					L2: 16.0 (2.6)
					L3: 16.2 (2.6)
					L4: 16.1 (1.5)
					L5: 17.3 (2.9)
Spinal Canal Width SCW (mm)	17.92 (1.84)		21.5 (1.7)	22.2	L1: 22.1 (2.3)
					L2: 23.0 (2.3)
					L3: 22.7 (1.7)
					L4: 22.0 (1.8)
					L5: 26.0 (2.5)

Table 4: Comparison of the mechanical properties of the human and porcine motion segments under shear loading, mean (sd).

Shear Loading	Human Lumbar Vertebrae Cripton et. al. (1995)	Porcine Cervical Vertebrae
Anterior Stiffness N/mm	155	212 (42)
Anterior Loading Ultimate Load to Failure N	2500	1980 (160)
Posterior Stiffness N/mm	104	164 (24)

Table 5: Comparison of the mechanical properties of the human and porcine motion segments under compressive loading, mean (sd).

Compressive Loading	Human Lumbar Vertebrae Genaidy et. al. (1993) Porter et. al. (1989)	Porcine Cervical Vertebrae Yingling et. al.	
		Quasi-static	Dynamic
Stiffness N/mm	N/A	1720 (280)	2780 (620)
Ultimate Compressive Load N	4000 - 8000[**] 13954[-]	6750 (1180)	8890 (1440)

[**]Average values from a motion segment
[-] Maximum value from one specimen

38

2.4   Discussion

The current study assessed the structural and functional properties of porcine cervical vertebral motion segments and human lumbar vertebral motion segments and found them to be quite similar although the values may have to be scaled to replicate human values. Consequently, the use of a porcine model appears to provide a reasonable surrogate of the human lumbar spine to perform controlled studies. Furthermore, given the similarity in the manner in which the specimens fail and are injured, it appears that human injury mechanisms and the spine's capacity to resist different loading conditions may be investigated using a porcine model.

Two main limitations should be realized for interpretation of the results of the current study. First, the number of porcine spines used for the quantitative geometry comparison was small (N=3 spines, 18 vertebrae), however, the repeatability of the porcine dimensions indicated that a larger sample size was not necessary. Second, the porcine vertebrae were harvested from a homogeneous population and were compared to human tissue which was acquired from a variable and uncontrolled population. The human specimens varied in age, gender, race and disease state at the time of death. These factors have been found to affect the tolerance of the spine and geometric differences and pedicle inclination have been found to differ between different racial populations (Cheung, Ruan, Chan, & Fang. 1994).

The spinal column is subject to different loading conditions; compressive and shear forces and torsional and bending moments. The anisotropic motion segment has different

load-deformation characteristics for each loading condition. The pars interarticularis, pedicles, facet angle, annulus, and posterior ligaments are the structures believed to oppose applied anterior and posterior shear loading. The similarities between these structures in human and porcine vertebrae suggest similarity in their functional ability to resist applied shear loading. Oxland et. al. (1991) indicated a similarity between porcine and human interspinous and supraspinous ligaments. The facet angles of the porcine are oriented approximately 90° from the endplate and 45° in the sagittal plane comparable to human lumbar vertebral bodies. The pedicle widths were also comparable between the two types of vertebrate.

The ultimate compressive strength of the spine has been found to be affected by the age, race, gender, body weight, level of disc degeneration and physical activity of the specimen donor, as well as the testing protocol used. These factors affect the direct comparison of tolerance values between porcine and human vertebrae, however, the geometrical similarities, the trends in the mechanical properties and the injury mechanisms can be compared. The alignment of the facet joints and the elliptical shape of the vertebral body and endplate signify the usefulness of a porcine model for compressive loading testing. Researchers (Hutton, Cyron, & Stott, 1979; Kazarian & Graves, 1977) using human specimens found increases in the stiffness and the ultimate compressive loads of lumbar vertebrae and decreases in the deformation to failure between quasi-static and dynamic compressive loading tests. Kazarian et. al. (1977) using three deformation rates which increased by 100 times (.21, 21, 2100 in/min) found the ultimate compressive load to increase, (8.76 kN, 12.1 kN, 14.9 kN). The stiffness also increased as strain rate increased

40

(2966 N/mm, 4234 N/mm, 5360 N/mm). A study using porcine cervical vertebrae (Yingling, Callaghan, & McGill, 1997) found similar trends to the human tests; the stiffness increased from 1700 N/mm to 3000 N/mm with an increase in load rate from 100 N/s to 16,000 N/s. The maximum compressive load also increased from 7000 N to 9700 N.

Common compressive injuries resulting from in-vitro compressive loading of human tissue are endplate failures or stellate fractures which are two or more cracks running from the center of the endplate to the periphery (Brinckmann, Biggemann, & Hilweg, 1989). As the compressive load is applied to the joint, and as the pressure in the gelatinous nucleus increases, the annulus and the endplate begins to bulge, the fracture occurs when the pressure of the endplate on the cancellous bone exceeds its tolerance. The stellate fractures are sometimes accompanied by an intrusion of nuclear gel into the trabecular bone, Schmorle's Nodes. These injuries are difficult to detect in-vivo and are typically documented post-mortem or using laminograms. These same stellate fractures are commonly found in porcine spines after compressive loading (Figure 6).

A second type of injury due to compressive loading found in humans (Brinckmann, Biggemann, & Hilweg, 1989), and in porcine spines, are edge fractures of the vertebral body. These are wedge-like fractures at the edge of the vertebral body similar to a bone avulsion injury in a bone-ligament-bone complex. These fractures were more prevalent during higher load rate compressive testing of porcine material (Figure 7). At higher load rates (but not impacts) the bony attachment of the annulus to the cortical vertebral body is weaker than the collagenous fibers of the annulus and the annulus ruptures at its bony attachment resulting in an edge fracture.

41

Shear loading results primarily in injuries to the pars interarticularis, a fracture originating at the posterior facing aspect of the superior facet below the facet face and on the anterior portion of the inferior facet above the facet face (Cyron, Hutton, & Troup, 1976). Previously it was thought that genetic factors predisposed individuals to pars defects which resulted in fractures (Krenz & Troup, 1973), however, mechanical factors are currently associated with fractures of the pars interarticularis. An applied shear loading to the intervertebral joint introduces a bending moment on the pars interarticularis and the pedicles resulting in failure (Figure 5). The bending moment about the pars interarticularis is larger than the bending moment about the pedicles; Cyron et. al. (1976) found a majority of pars interarticularis fractures with about 1/3 as many fractures across the pedicles from in-vitro testing. Fractures of the pars interarticularis have been also found in-vitro on porcine spines following shear loading. The porcine pars fractures were located in the same location as injuries on human vertebrae. Pars injuries are not only found in-vitro, injuries found in-vivo on cricket bowlers are typically pars interarticularis defects. The study of 22 bowlers resulted in 6 bilateral and 6 unilateral pars defects being detected (Hardcastle, Annear, Foster, et al. 1992). Injuries found in-vivo in clinical assessments of Spondylolisthesis patients also suggest injuries of the pars interarticularis (Newman, 1963; Grobler, Novotny, Wilder, Frymoyer, & Pope, 1994). As well, a study of skeletons from Alaskan natives verified that every second skeleton showed one or more defective neural arches. The defects were considered defects of the neural arch but did not specify whether they were defects to the pedicle or to the pars interarticularis. The fracture in the pars interarticularis is difficult to detect using radiographs unless the fracture is a massive injury since the fracture is typically

42

not through the entire thickness of the pars interarticularis. A segmental analysis of the pars interarticularis found two dense layers of cortical bone and the anterior face of the inferior process to the inferior border of the pedicle and on the posterior portion of the superior process extending into the lamina (Krenz & Troup. 1973). The cortical bone which is stronger than cancellous bone is hypothesized to be in portions of the pars which are subject to tensile stress from bending moments placed on the pars interarticularis and pedicle. Porcine in-vitro shear testing also resulted in annular avulsions, a tearing of the endplate from the vertebral body. Cripton et. al. (1995) reported avulsion injuries on human vertebrae after in-vitro testing.

In conclusion, the porcine cervical vertebral motion segment appears to be a useful model in research investigating injury mechanics of the human lumbar spine. While porcine specimens offer the asset of homogeneity for controlled scientific inquiry, human samples are affected by unmatched age, disease state etc. However, observations and conclusions obtained from a porcine model must be scaled to match human magnitudes.

Chapter Three

General Methodology

3.0   Review of Literature

3.0.1   Type of Loading

The lumbar motion segments are subjected to extremely complex loading situations during sport, daily activities and even at rest. The physiological load profile during these activities is very difficult to recreate in a laboratory setting, therefore, the research community tends to study individual loading conditions and to use modelling techniques to integrate the information. This suggests that the development of a tolerance value for application to daily living may not be a single value but rather a function.

The spine may experience many modes of loading including compressive loading, flexion moments, torsional moments and shearing forces. Axial compressive loading of the motion segments which result from gravity, muscular and ligament tension, and external forces is the most commonly studied mode of loading. An increase in nuclear pressure and the tensile load on the annular fibers transfer the compressive load between vertebrae. However, indirect measures of the facet joints under compressive loading found that 3-40% of the applied load was resisted by the facet joints dependant on the posture of the motion segment (Yang & King. 1984; Hakim & King. 1976).

The motion segments are also able to resist flexion and extension moments: flexion moments being the most common. During flexion, the posterior elements of the motion segment are placed in tension while the anterior portion of the motion segment is in compression. After systematic testing on 18 human lumbar vertebrae (16-74 yrs of age), Adams et. al. (1994) concluded that the posterior elements seem to be the predominant structures resisting a flexion moment (Adams, Green, & Dolan, 1994). The posterior elements resisted 81% of the bending moment applied to the specimens and limited the intervertebral discs to 79% $\pm$ 9% of their full range of safe motion.

Previous work by Adams et. al. (1980) suggested that the capsular ligaments and intervertebral discs are the important structures in resisting flexion moments, resisting 39% and 29% of a bending moment respectively but a methodological oversight in their earlier work necessitates a prudent interpretation of their data. A compressive load prior to testing (preload) was not included in the protocol for these earlier studies (but was corrected for all subsequent work). Specimens were obtained from routine necropsies and were frozen at -20°C until testing. Swelling is associated with specimens immediately after death (Johnstone, Urban, Roberts, & Menage, 1992) and may increase the tensile load on the ligaments of the motion segment. Application of a preload to the segments prior to testing decreased the height of motion segments, indicating a reduction in excess fluid within the specimen (Adams, Green, & Dolan, 1994). This earlier work of Adams et. al. (1980, 1983), in which they did not preload the specimens, resulted in a decreased range of flexion compared with later studies when a preload was employed, which led to the conclusion that the contribution of the interspinous and supraspinous ligaments was trivial in resisting flexion moments (Adams, Hutton, & Stott,

45

1980; Adams & Hutton. 1983).

One study focusing on torsional loading, a third type of loading on the motion segment, found the load required to produce failure in the facet joints was relatively low with 2-3 degrees of motion before fracture (Farfan, Cossette, Robertson. Wells. & Kraus. 1970). The intervertebral disc and the facet joints provided 90% of the torsional resistance of the motion segment, equally distributed between the two structures. The authors suggested that the torsional strength of the disc depends on its shape and area and the integrity of the annulus fibrosus. The oval shape of the lumbar discs, which would decrease their capacity for torsional resistance, is compensated by their greater surface area. The facet joints are loaded asymmetrically during torsional loading. One facet joint is under compressive load and the other under tensile load. The facet joint function is similar to conditions for the joints under shear loading.

The lumbar motion segment appears to be designed to resist shear loading; the facet joints are perpendicular to the plane of the intervertebral disc and the interspinous and supraspinous ligaments are nearly parallel to the plane of the disc. As well, the fiber angle in the annulus suggests a role in shear load resistance. The applied shear load on the spine may range from 400 N in static standing to over 3000 N for power lifting (Cholewicki, McGill. & Norman. 1991; Potvin, Norman, & McGill. 1991). The tolerance values from static and dynamic testing are extremely varied. Miller et. al. (1986) did not detect failure in 14 male human motion segments (18-41 yr) exposed to anterior and posterior shear loads up to 980 N in magnitude. Many studies have combined flexion and shear loading which have yielded thresholds for injury from static loading of 486 N and 430 N for dynamic loading (Osvalder,

46

Neumann, Lovsund, & Nordwall. 1993). Failure occurred at 620 N for static loading and 600 N for dynamic loads. In a recent symposium proceeding, Cripton et. al. (1995) investigated shear loads placed on human lumbar vertebrae under quasi static, dynamic and destructive loading conditions, however, the study used human vertebrae ranging in age from 31 to 71 years, therefore the disc status could not be controlled which may affect any absolute tolerance values reported. The maximum load at failure was found to range between 2 - 2.4 KN for dynamic testing. However, Farfan (1988) estimated the shear tolerance of the facet joints at 3100-3600 N with the intervertebral disc resisting less than 900 N. Cyron et. al. (1976) found the disc to resist the majority of an applied shear load with the facet joints only resisting 1/3 of the total load. The large range of results for shear tolerance may be due to the specimens being tested or the difference in the testing protocol.

3.0.2   Biomechanical Modeling: Models of Motion Segment

To understand the load sharing capabilities and etiology of injury within the spinal motion segments, it is important to understand the contribution of both the geometrical aspects of the individual structures as well as the material properties of these structures. Biomechanical modelling techniques allow hypotheses of load sharing strategies to be tested and further developed.

Various modelling approaches have attempted to understand the mechanics and mechanisms of injury in the lumbar spine. For example, finite element models attempt to

47

accurately represent the geometry and the material properties of the elements making up the motion segment during loading. Although these models are usually geometrically detailed. this approach relies on many assumptions about tissue behavior. An alternative is the lumped parameter approach which may be less concerned with the details of the distribution of deformation and may represent parts of the motion segment as a continuum. Both modelling approaches are used to investigate extreme loading on the body without the threat of injury to human participants. an important issue during in-vivo testing. These modelling approaches for the spinal motion segment have been validated through in-vitro testing of specimens as well as in-vivo intra-discal pressure measurements.

The entire lumbar region (L1-L5 and the pelvis) may be modelled but with a different objective from models of the motion segment. Models encompassing the entire lumbar region estimate joint forces during external loading conditions. whereas models of the motion segment focus on injury mechanisms of tissues within the motion segment. Both types of modeling in conjunction with in-vitro testing may help clarify injury mechanisms and the tolerance of the tissues to different loading conditions. However, few models have included an accurate account of shear loading. Models of the lumbar region were originally single equivalent muscle models, the representation of the back musculature consisted of one muscle running perpendicular to the plane of the disc. This perpendicular alignment completely eliminates the resistance of an external anterior shear load by the erector spinae muscles (Potvin, Norman. & McGill. 1991; Potvin, McGill, & Norman. 1991; McGill & Norman. 1987). More advanced models included the effects of the disc, ligaments and a more accurate representation of the muscles role in spinal mechanics (McGill & Norman. 1986) which enabled the analysis of

48

shear loading.

Models of the motion segment or intervertebral disc mainly replicate the interaction of the segments under axial compressive loading (Broberg & vonEssen. 1980) with little effort directed at shear loading. Shirazi-Adl et. al. (1984) developed a three dimensional finite element model of the motion segment under compression and went on to adapt the model for use in the study of applied torque to the motion segment (Shirazi-Adl, Shrivastava, & Ahmad. 1984; Shirazi-Adl, Ahmed, & Shrivastava. 1986). These models did not account for the load rate dependence of the motion segment. Complex loading, including shear loading, was modeled using the lumped parameter approach (Miller, Haderspeck, & Schultz. 1983) but the facet joints, supraspinous, interspinous, intertransverse (spanning adjacent transverse processes) and the ligamentum flavum were all represented by one stiffness value. Estimates for this stiffness were arguable due to the lack of sufficient data. This approach cannot identify injury mechanisms between the various structures of the posterior element of the motion segment. In summary, modelling can be advantageous in the understanding of injury mechanisms and the modulators of shear loading of the spinal motion segment. However, more accurate stiffness values for the motion segment are needed as well as the relative contribution of each structure making up the motion segment in the resistance of shear loads.

3.0.3   Specimen Storage

Many in-vitro studies attempt to replicate in-vivo conditions as closely as possible. At

times due to transportation logistics and/or testing complexity, the specimens cannot always be tested immediately after harvesting. Freezing specimens has become common practice, yet controversy still remains whether the mechanical properties are changed by this storage method. The motion segment includes cortical and trabecular bone, collagenous tissue and the gelatinous nucleus. Cortical bone was found to have no significant changes in its mechanical properties after freezing the specimen at -20°C and thawing (Sedlin & Hirsch. 1966). The appearance of the stress-strain curves of pig ligaments was not affected by freezing (Hukins. Kirby, Sikoryn, Aspden, & Cox. 1990). Freezing does not affect the orientations of the collagen fibers in connective tissue, however, ligaments were found to fail at reduced stress possibly due to the formation of ice crystals within the tissue (Hukins. Kirby, Sikoryn, Aspden. & Cox. 1990). Testing cn motion segments found no difference in the hysteresis and stiffness of the tissue after freezing and thawing (Smeathers & Joanes. 1988). The cadaver motion segments were tested both fresh and after freezing at -18°C for 5 days. More recently, Callaghan & McGill (1995) found an increase in the compressive strength and the energy absorbed at failure in specimens which were frozen prior to testing compared with fresh specimens (Callaghan & McGill. 1995). Although studies appear to contradict one another, testing specimens which have been stored in an identical manner may impose a constant bias into the data, but will not affect the relative results between the testing conditions.

3.0.4   Specimen Preload

Close replication of in-vivo conditions provides some validation for the results and conclusions from in-vitro studies. A compressive load, due to the weight of the upper body. is always present on the motion segments. The curvature of the spine necessitates that the ligaments and the musculature offset the flexion moment created by the curvature which further places a compressive burden on the motion segment. Specimens harvested post-mortem will swell (Johnstone, Urban, Roberts, & Menage. 1992) and disturb the elastic equilibrium of the structures of the motion segment specifically ligament and disc laxity. In order to accurately replicate in-vivo conditions this continual loading on the motion segment needs to be simulated.

Previous researchers have applied a compressive preload to account for the load of the body weight, ligaments and muscles. This compressive preload affects the stiffness results of motion segments loaded in flexion, axial rotation and anterior shear loading (Janevic. Ashton-Miller, & Schultz. 1991). Preload values ranging from 300 N to 4400 N with time durations ranging from 5 - 30 minutes have been used in testing. A comparison of three compressive preloads (0 N, 2200 N, 4400 N) followed by anterior shear loading found that the deformation in the specimen decreased as the preload magnitude was increased (Janevic. Ashton-Miller, & Schultz. 1991). Average shear displacement for a 2200 N and 4400 N preload compared with zero preload decreased by a factor of 6.16 and 26.8 respectively. Anterior shear loading following a preload of 2200 N with posterior elements intact showed

displacement to decrease by a factor of 6.9, whereas with the posterior elements excised, displacement was only decreased 1.9 times compared to zero preload. Impingement of posterior elements, mainly the facet joints likely play a role in the decrease in displacement. It would appear that shear load testing must have a preload which simulates in-vivo conditions but which does not impinge the posterior elements.

3.1   Methods

This next section discusses the common methods associated with the specimen testing.

3.1.1   Specimens

Cervical spines of domestic pigs (mean live weight of 80 kg) were collected immediately after death with all soft tissue in place. The specimens were similar in age, weight, genetic make-up, diet and physical activity. The spines were then frozen (-20°C) until testing. The musculature was then stripped from the spine exposing the osteo-ligamentous structure prior to testing to minimize dehydration of the motion segments. Each spine was thawed immediately before testing at room temperature. Then each spine was separated into two specimens for testing, consisting of two vertebral bodies and the intervening intervertebral

disc (C3-C4, C5-C6). The exposed intervertebral discs were examined for degeneration. only specimens satisfying the Grade I classification (Galante. 1967) were used in testing. Galante's classification criteria (1967) are as follows:

Grade 1: Normal discs. Annulus shiny white and free from rupture. nucleus shiny white and gelatinous.

Grade 2: The appearance is normal but the nucleus exhibits a more fibrous structure. A clear boundary is present between annulus and nucleus.

Grade 3: Isolated fissures in the annulus. The nucleus is dry and occasionally discolored. The boundary between the nucleus and annulus is not distinct.

Grade 4: Severe changes. Ruptures and sequestrae in both the annulus and nucleus. Marginal osteophytes often found.

3.1.2   Specimen Mounting

The specimens were potted in stainless steel cups and fixed with dental plaster (Denstone Miles Inc. South Bend, IN. USA) (Figure 1). Wires were looped around the pedicles and anterior processes and then secured to the mounting cups to ensure secure fixation. The spacing between the cups was on average 1 mm which minimized bending moments applied to the specimen due to the shear loading. The cups with the mounted specimens were then placed into a custom designed jig which applied a pure shear load to the motion segment. Set screws were tightened to secure the cups into the jig. No relative movement was detected between the cup and the fixed vertebrae during testing. After

53

removing the specimens from the cups, the dental plaster was still solid and uncracked.

3.1.3   Shear Loading Jig

The specimens were positioned in a custom jig designed to isolate shear loading on the motion segments along the plane of the intervertebral disc for the mechanical testing protocols. The jig was adapted to an Instron Servo-Hydraulic Dynamic Testing Machine Model 8511, a large steel base was attached to the testing machine to securely interface the loading jig (Figure 2 & 3). The motion segment lay horizontally in the jig with one end of the motion segment remaining stationary while the other end moved in a casing mounted on linear bearings for low friction movement. External set screws secured the cups into the jig. The space between the cups after mounting the cups into the jig is less than 1 mm on average, this minimizes any bending moments applied to the specimen from the shear load. The jig applied a constrained shear load meaning that the specimens did not have any free movement at their ends. The lumbar vertebrae in-vivo are partially constrained by the load of the upper body as well as the increase in compressive load by muscle contraction. A compressive preload was applied to the motion segment via two calibrated springs mounted on the sides of the casing which can be tightened to 300 N. The preload was applied to create physiologic loading during testing where as, preconditioning cycles are used to create repeatable tests from the tissue specimens. The jig also has capabilities of flexing and extending the motion segment prior to testing. The external screws are designed to secure the motion segment into a flexed posture up to 10

degrees. A 4448 N load cell was in series with the actuator and was attached to the movable casing in order to measure the shear load resisted by the specimen. The Instron testing machine has an accuracy of 1% of the load cell capacity.
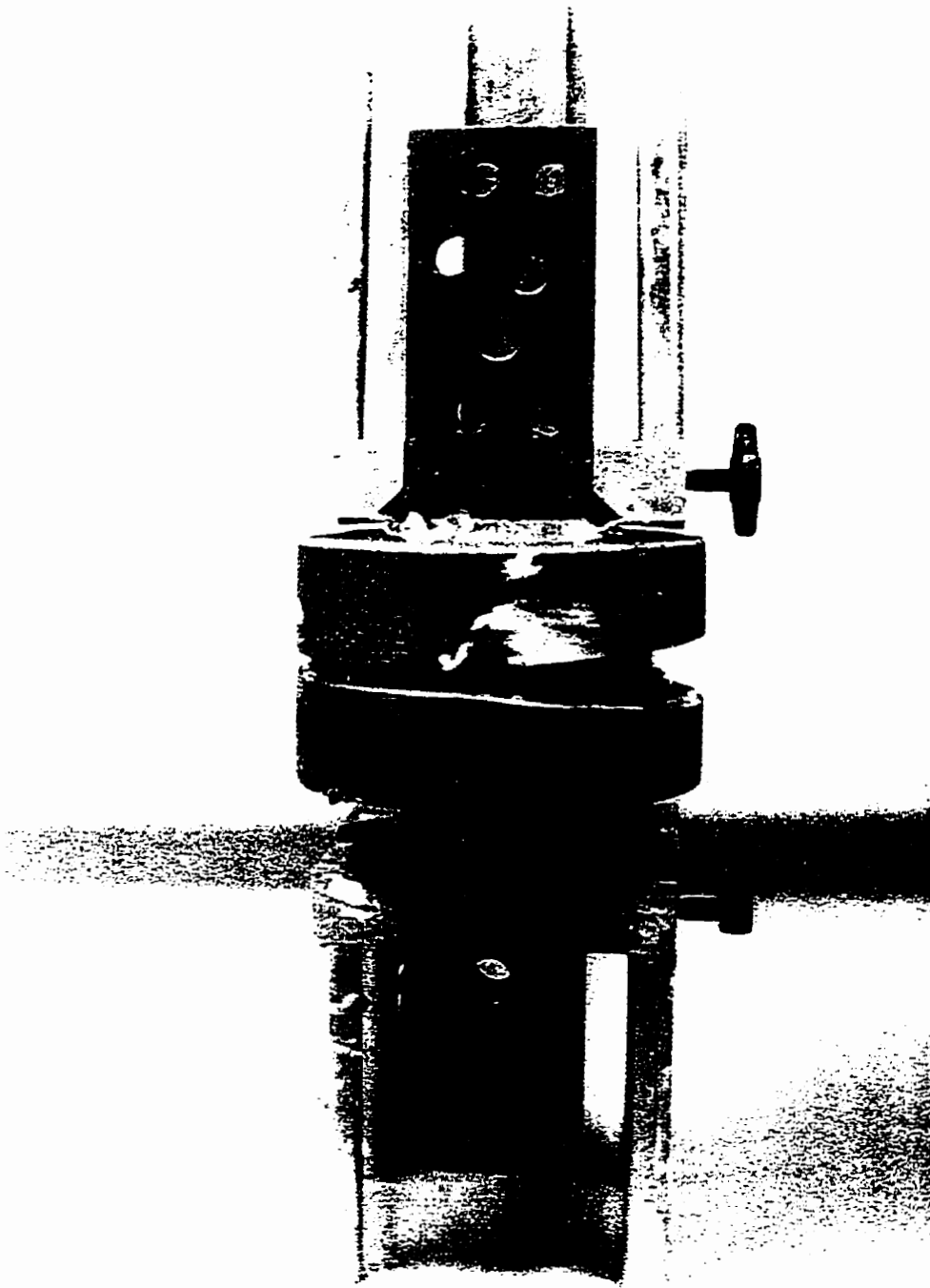
Figure 1: Stainless steel potting cups which housed the motion segment. One vertebra was potted into one cup (A). the specimen was aligned so the intervertebral disc was parallel to the top of the cup. The other vertebra was potted into the second cup (B). The spacing between the cups (A) and (B) was on average less than 1 mm which minimized any bending moments occurring from the applied shear load.
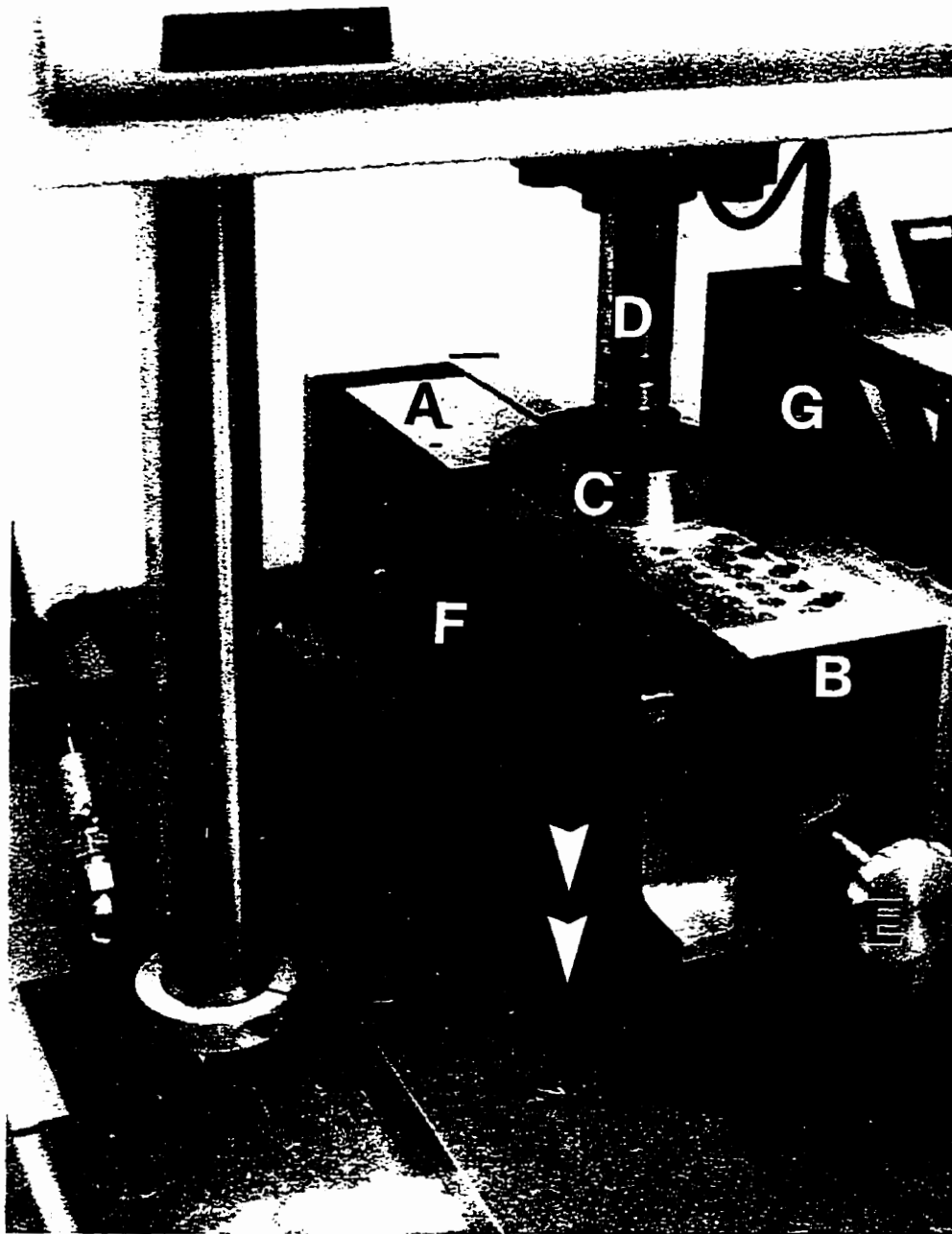
Figure 2: The shear loading jig was designed to apply a pure shear load to a motion segment. The motion segment was placed in the jig with one vertebra mounted in a stationary casing (A) and the other vertebra mounted in a movable casing (B). The load cell (C) is in series with the movable casing which is attached to the actuator (D). The movable casing is mounted on linear bearings (G) to provide low friction movement. The cups holding the specimen are less than 1 mm apart to minimize bending moments (F). A 300 N compressive preload was applied to the specimens using calibrated springs (E).
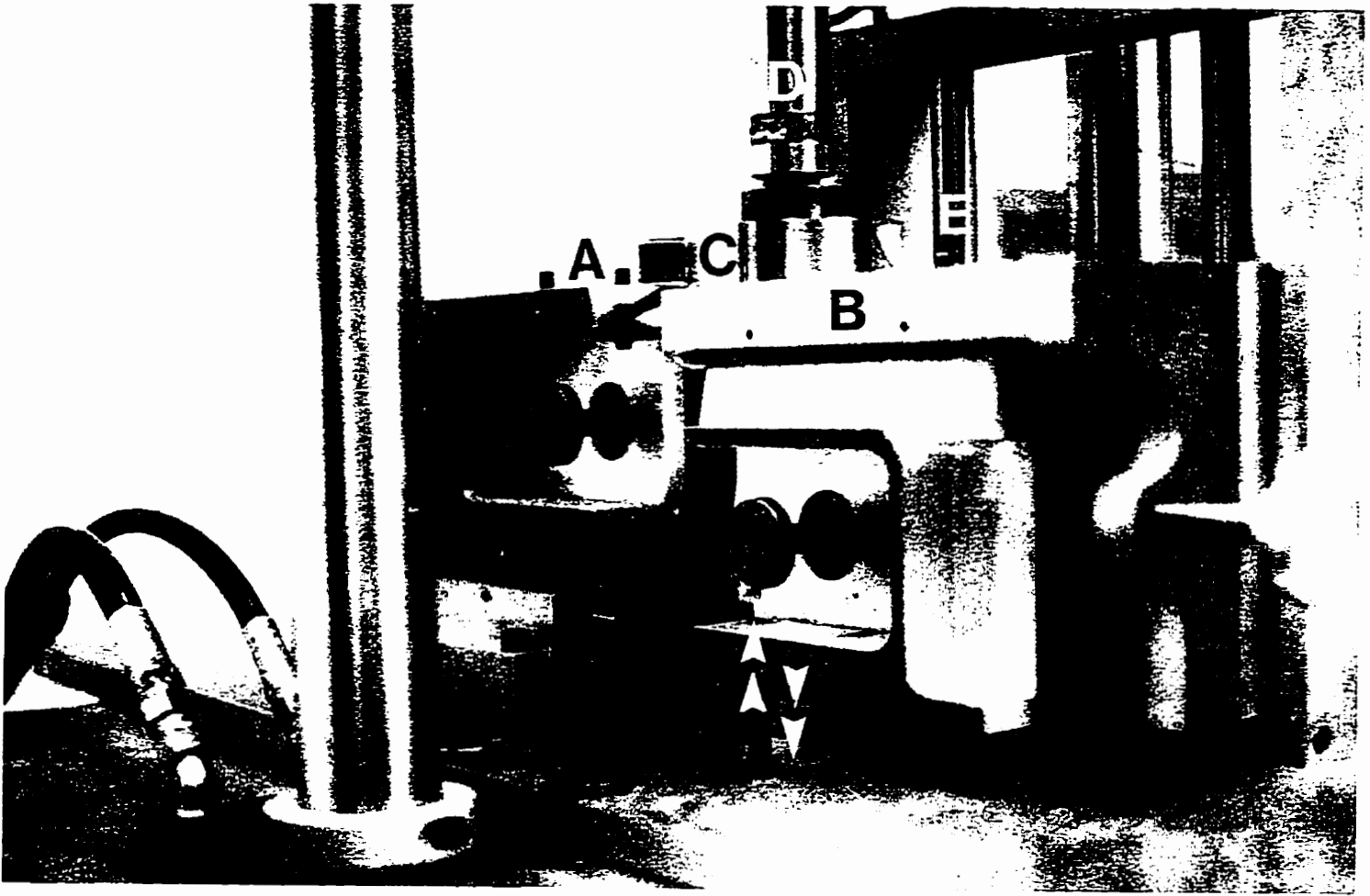
Figure 3: The shear jig was designed to apply pure shear loads to motion segments. The stationary casing holds one vertebra (A) the potting cups are secured using set screws (A) to eliminate movement of the cups. The movable casing (B) is in series with the load cell © and attached to the actuator (D). The casing is mounted on linear bearings (E).

58

3.1.4   Defining Failure

Failure was defined as occurring when the load applied to a specimen exceeds the tolerance of the specimen. Tolerance was defined as the capacity for enduring and or adapting. There is not one tolerance value for a motion segment, the structure will have a different tolerance value for each type of loading; compression and shear loads and torsional and bending moments

. Furthermore, each structure making up the motion segment will have its own tolerance and these structure will interact to affect the tolerance value of the entire motion segment. In order to compare mechanical results between testing protocols, a constant failure point must be defined. A drop in the load signal suggests a failure in a structure resisting shear load.

The severity of injury is dependent upon the definition of failure. The intention was to capture the initial stages of injury in order to document the progression of injury. However, the definition of failure was constrained by the technical limitations of the testing machine. A 6.25 % drop in the feedback load signal occurring within 50 ms was the minimal load drop which was able to be detected by the machine and was used as the definition of failure for the current testing protocols. When this drop in the signal was detected the Instron would abort the test to avoid further damage to the motion segment. The mode of failure was then documented through dissection of the specimen and/or radiology techniques. The break detect mechanism allowed the identification of initial injuries as compared to the massive injuries sustained by motion segments if no break detect was triggered.

3.1.5 Protocol

3.1.5.1 Load Rate and Directional Mechanical Experiments

The cervical spine was initially dissected into two specimens: C3-C4 and C5-C6. One specimen was then mounted into the cups either anteriorly or posteriorly. Anterior mounting allowed the superior vertebra to translate anteriorly while the inferior vertebra remained stationary. Under posterior mounting the superior vertebra translated posteriorly over the stationary inferior vertebra (Figure 4).

The calibrated preload springs on the testing jig were tightened to apply a 300 N preload to the specimen. The break detect and the load rate (slow rate: 100 N/s high rate: Posterior :9454 N/s and Anterior:10810 N/s) for testing were initialized and the specimen was then loaded to failure. Upon the activation of the break detect, the specimen was removed and the type of injury was determined.

3.1.5.2 Serial Tissue Sectional Testing Experiments

The cervical spine was initially dissected into two specimens; C3-C4 and C5-C6. One specimen was then mounted into the cups either anteriorly or posteriorly (see explanation above).

The specimens were tested in four groups, the first three groups in a neutral posture
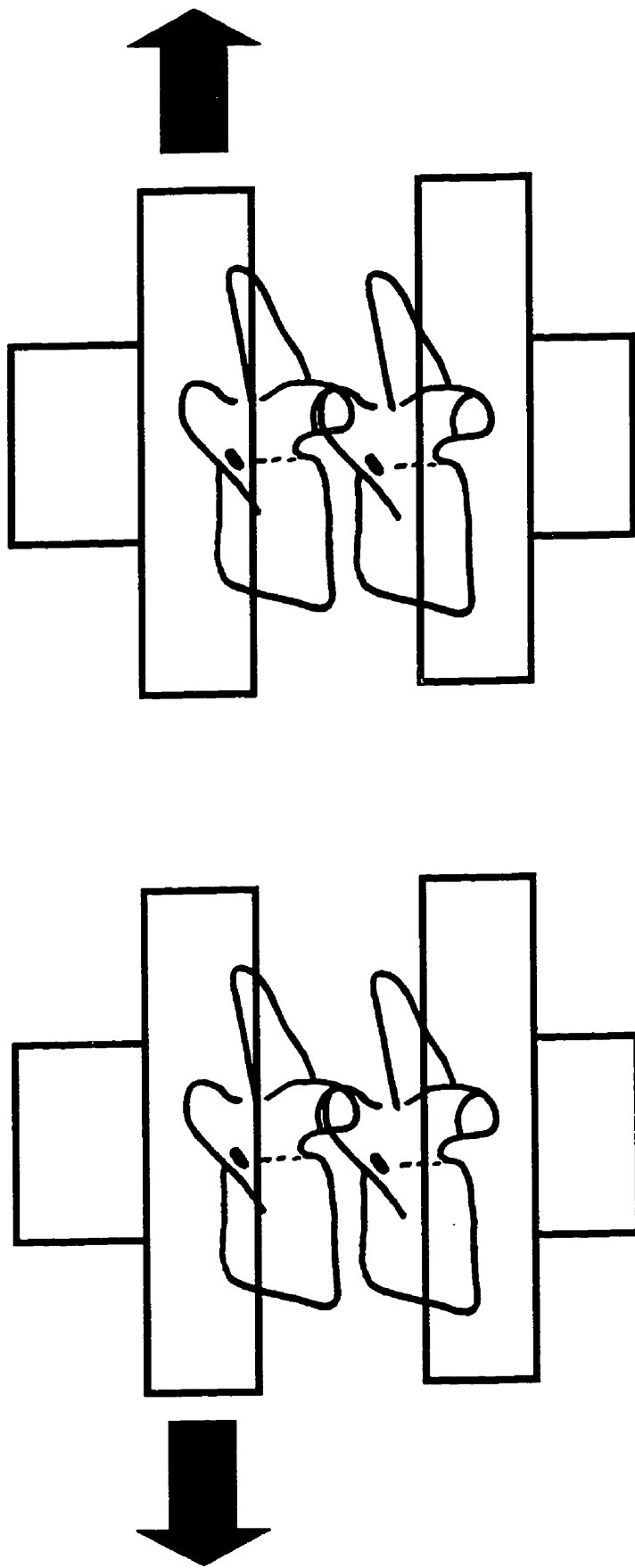
(A) External Anterior Shear Load

(B) External Posterior Shear Load

Figure 4: Schematic diagrams illustrating the application of an externally applied anterior shear load (A) and an externally applied posterior shear load (B) to a cervical porcine motion segment.

with the fourth group in a flexed posture. The first was the whole group (W) with the structure

intact. In the second group (NL), the posterior ligaments (interspinous and supraspinous) were

severed. The third group consisted of specimens with the posterior ligaments severed and the

facet joints removed (NFL), leaving only the intervertebral disc intact. The fourth group

consisted of intact specimens which were tested while in a flexed position (F). The preload

springs on the testing jig were tightened to place a 300 N compressive preload on the

specimen. Five preconditioning cycles were initiated consisting of a triangular waveform with

an amplitude of 4 mm deformation anterior and posterior to increase the repeatability between

tests. This amplitude was within the normal functioning region of the motion segment,

therefore no injuries were expected to result from the preconditioning cycles. The cycles were

loaded at a rate of 100 N/s. Following the preconditioning cycles the break detect and the load

rate (100 N/s) for destructive testing were initialized. The specimen was then loaded to failure.

Upon the activation of the break detect, the specimen was removed and the injury was

documented.

Biomechanical modeling techniques were used to verify load sharing hypotheses for the

motion segment structures under anterior and posterior shear loads.

3.2.6 Data Analysis

Load deformation curves were collected using a computer, A/D sample rate of 50-100

Hz, to obtain the mechanical parameters of the specimen in shear loading. Energy absorbed by

the motion segment, deformation of the motion segment in the plane of the disc. ultimate shear load at failure and stiffness of the specimen were determined from the load-deformation curves. Energy was calculated as the area under the load-deformation curve which is a measure of the energy absorption of the tissue and is an indication of the material's toughness (Ozkaya & Nordin, 1991) (Figure 5). Ultimate shear load at failure was the highest load resisted by the motion segment in the plane of the intervertebral disc before failure (6.25% drop in feedback signal within 50 ms) was detected. Deformation at failure was the translation between the motion segments along the shear plane of the disc measured in millimeters. The stiffness of the motion segment was calculated as the average slope of elastic region of the load-deformation curve. Stiffness represents the rate of change of deformation as a function of load.

The deformation and the load were normalized to 100% for all trials and then averaged over the trials. The average curves were then modeled using a 2nd order polynomial, constrained to a zero intercept.

3.1.7   Statistical Analysis

3.1.7.1   Load Rate and Directional Experiments

Two-way ANOVA's were conducted on the data sets to quantify the effects of differences in direction, anterior and posterior, and for rate of loading, slow (100 N/s) and
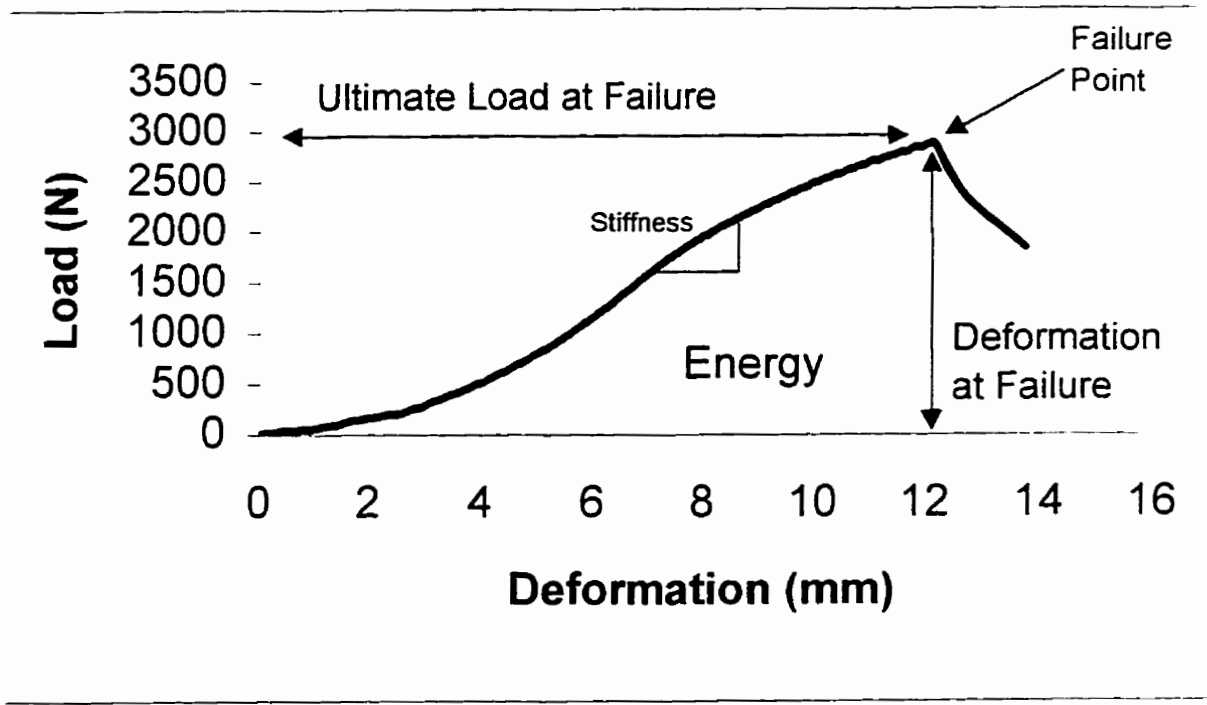
Figure 5: A load-deformation curve identifying the mechanical variables measured or calculated. The average stiffness is the slope of the linear portion of the curve. The energy at failure is the area under the load-deformation curve to the failure point.

fast (Ant:10810 N/s and Post:9454 N/s). The specific variables assessed by the ANOVA were ultimate load at failure, ultimate deformation at failure and energy absorbed at failure and the stiffness of the specimen during the linear region of the test. Data was transformed using a logarithmic transformation to counter the dependance of the standard deviation (SD) to the response size, which is common when analyzing biological data. For example, a larger ultimate load at failure would have larger standard deviation values. Any dependency on response size was determined by plotting the standard deviation against the mean of the response value. The data was checked for any outliers and one response was dropped from the data set. This response had an excessively low stiffness and a large deformation. Each response should account for approximately 3% of the random variance in the test but the outlier response accounted for 30% as determined by the residual mean squares calculated before and after the outlier was removed. After performing the transformations and conducting the ANOVA the stability of the standard deviations was confirmed.

3.1.7.2 Serial Sectional Testing Experiments

Two-way ANOVA's were assessed for differences in the type of specimen preparation: whole specimens (W), specimens with no posterior ligaments (NL), specimens with no posterior ligaments or facet joints (NLF) and anteriorly flexed specimens (F) as well as for any differences in the direction of loading, anterior and posterior. Three response variables were

statistically analyzed: ultimate load at failure, deformation at failure and specimen stiffness. Post hoc tests (LSD) were performed to detect specific differences between each type of specimen preparation for each direction. Data sets were transformed using a logarithmic transformation after an analysis of a plot of standard deviation versus the mean. Values of outliers were checked but no responses were deleted from the data set. Following the transformations and the ANOVA the stability of the standard deviations was checked.

3.1.7.3   Experiments to Assess the Effects of Preconditioning

Two-way ANOVA's were conducted to determine any difference between the preconditioned specimens (P) and the specimens tested without preconditioning (WP) on the three responses: ultimate load to failure, deformation at failure and stiffness of the specimen. Data was transformed using a logarithmic transformation after an analysis of the plot of standard deviations and mean values. One response was deleted from the data set after outlier values were checked. The specimen was noted as being a small specimen at the time of testing. Following the transformations and the ANOVA tests the stability of the standard deviations was checked.

Chapter Four

The Effect of the Direction

of Shear Loading on Joint Behavior

The lumbar motion segment in the anterior-posterior shear plane is not symmetric and is comprised of non homogeneous and anisotropic components. The anterior portion of the motion segment consists of the intervertebral disc and the posterior portion contains the pars interarticularis, the facet joints and the posterior ligaments. These structures are made of different materials which will resist anterior and posterior shear loading in different ways. Anterior shear loading results in the translation of the superior vertebra over the inferior vertebra. It is suspected that the load will be resisted mainly by the stiffness in the pars interarticularis which is initiated as the facets faces compress against one another causing a bending moment in the pars. As well, the intervertebral disc consists of annular fibers which are directly connected to the vertebral body as opposed to the portions of the inner annulus which connect to the endplate. These outer annular fibers will increase their tension as the superior vertebral body translates.

Completely different structures resist external posterior shear loading. The facet faces distract upon shear translation, which increases the tension in the capsular ligaments. This tension in the ligaments may apply a slight bending moment to the pars interarticularis. The

posterior ligaments (interspinous and supraspinous) are aligned in an orientation which suggests that they resist posterior shear loads (Hukins, Kirby, Sikoryn, Aspden, & Cox. 1990). The outer fibers of the annulus appear to resist posterior loading in the same manner as they resist anterior shear loading.

It appears that mainly collagenous tissue structures resist posterior shear loading, compared to the combination of bone and soft tissue that resist anterior loading. The stress-strain curves are different for bone and soft tissue. Soft tissue is comprised of mainly collagen and elastin. Collagen is the primary tensile fiber in tissues and is arranged into right-hand spiral fibers. The behavior has two distinct regions. First, a portion where low stresses result in large deformations as the fibers uncoil. The second portion has a much greater stiffness during which an applied stress results in a more proportional strain (Figure 1). The alignment of collagen fibers within a tissue has a major role in its stiffness capacity. Tissues with the same tensile properties have considerably different load-deformation curves dependant on the arrangement of the collagen fibers (Viidik. 1979). Elastin, which is often termed "biological rubber" is also a spiral fiber (Black. 1988). It is typically seen in a matrix of other fibers such as collagen, which together assemble tendons and ligaments. It is highly elastic and resists minimal stress for maximal strains. Elastin is typically responsible for the elastic region of the stress-strain curve of a structure. The alignment of the fibers within the ligaments and annulus of the motion segment suggest a role of these structures in resisting shear load.

Bone is more stiff and has higher stresses for a given strain compared to soft tissue (Table 1, Figure 1). The vertebral body includes both cortical and cancellous bone. Cortical bone carries the majority of the load in bones, it is moderately viscoelastic and highly

68

anisotropic. Cancellous bone is found in the endochondral areas of long bone and the core of the vertebral body and pars interarticularis, it is made up of trabeculae which is organized directionally and appears to follow Wolff's Law. The bony structure of the pars interarticularis consists of cancellous and cortical bone, with a majority of cortical bone along the thinnest portion of the pars for maximal strength. The addition of the bony stiffness of the pars to anterior loading suggests that a higher stiffness would be found during anterior translations.

The purpose of this study was to quantify the mechanical properties under both anterior and posterior shear loading on a homogenous sample of porcine spinal motion segments.

Global Hypothesis:

> The average stiffness under shear loading to failure will be higher under anterior shear loading than under posterior loading.

Specific Hypotheses:

> The ultimate shear load at failure will be unaffected by the direction of shear loading.
> The deformation to failure will be unaffected by the direction of shear loading.
> The stiffness of the motion segment will be unaffected by the direction of shear loading.
> The energy absorbed at failure will be unaffected by the direction of shear loading.

Table 1: Material properties of collagen, elastin and cortical bone.

Fiber	Elastic Modulus (mPa)	Elastic Limit (%)	Ultimate Strength (mPa)	Ultimate Strain (%)
Collagen	1000	1-2	60	10
Elastin	0.6	60	>0.35	>60
Cortical Bone	10000		10 KN/sq cm(100 mPa)	3

4.1　　　　　　　　　Specific Protocol

The specimens were divided into two groups, one group sustained anterior shear loading (n=10) and the second group, posterior shear loading (n=10). They were mounted in the shear jig connected to the Instron testing machine, and loaded to failure. A 6.25% drop in the load feedback signal defined failure and stopped the test. The load rate was held constant at 100 N/s for both groups. Ultimate load at failure, deformation at failure, stiffness and energy at failure were the dependant variables and were used to compare the tolerance of the specimens under anterior and posterior shear loading. Radiography and dissection techniques revealed the injuries sustained under each type of loading.

4.2　　　　　　　　　Results

The direction of loading significantly affected stiffness ($p < .05$, F=5.01) (Table 2, Figure 2). Anterior stiffness was greater than posterior stiffness (212 N/mm vs 165 N/mm). There was also a significantly ($p < .05$, F=4.95) larger deformation to failure under posterior shear loading compared to anterior shear loading (Table 2, Figure 2). However, the ultimate load to failure and the energy absorbed to failure were not significantly different between anterior and posterior shear loading (Table 2, Figure 2).

Table 2: Mechanical variables at the failure point during anterior and posterior shear loading. mean (SD).

Variable	Anterior (100 N/s)	Posterior (100 N/s)
Load (N)	1980 (390)	1860 (260)
Deformation (mm) *	**9.7 (2.2)**	**12.5 (2.0)**
Stiffness (N/mm) *	**212 (39)**	**165 (24)**
Energy (J)	9794 (3769)	12007 (2788)
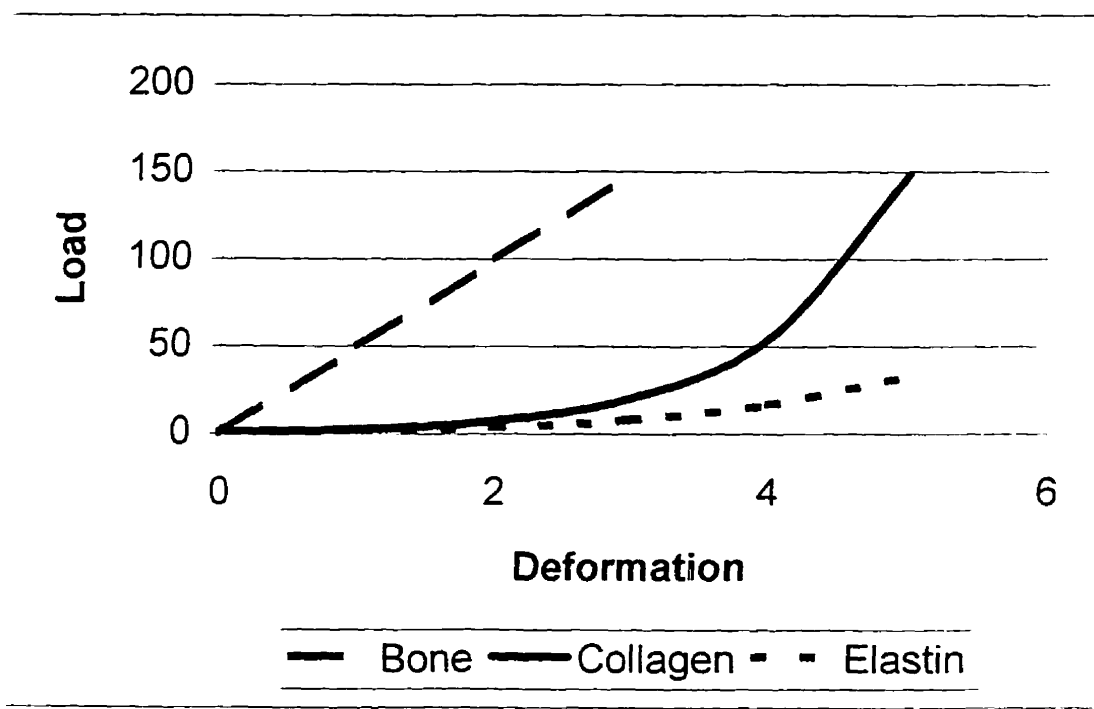
Figure 1: A load-deformation curve illustrating the response of bone, collagen and elastin.
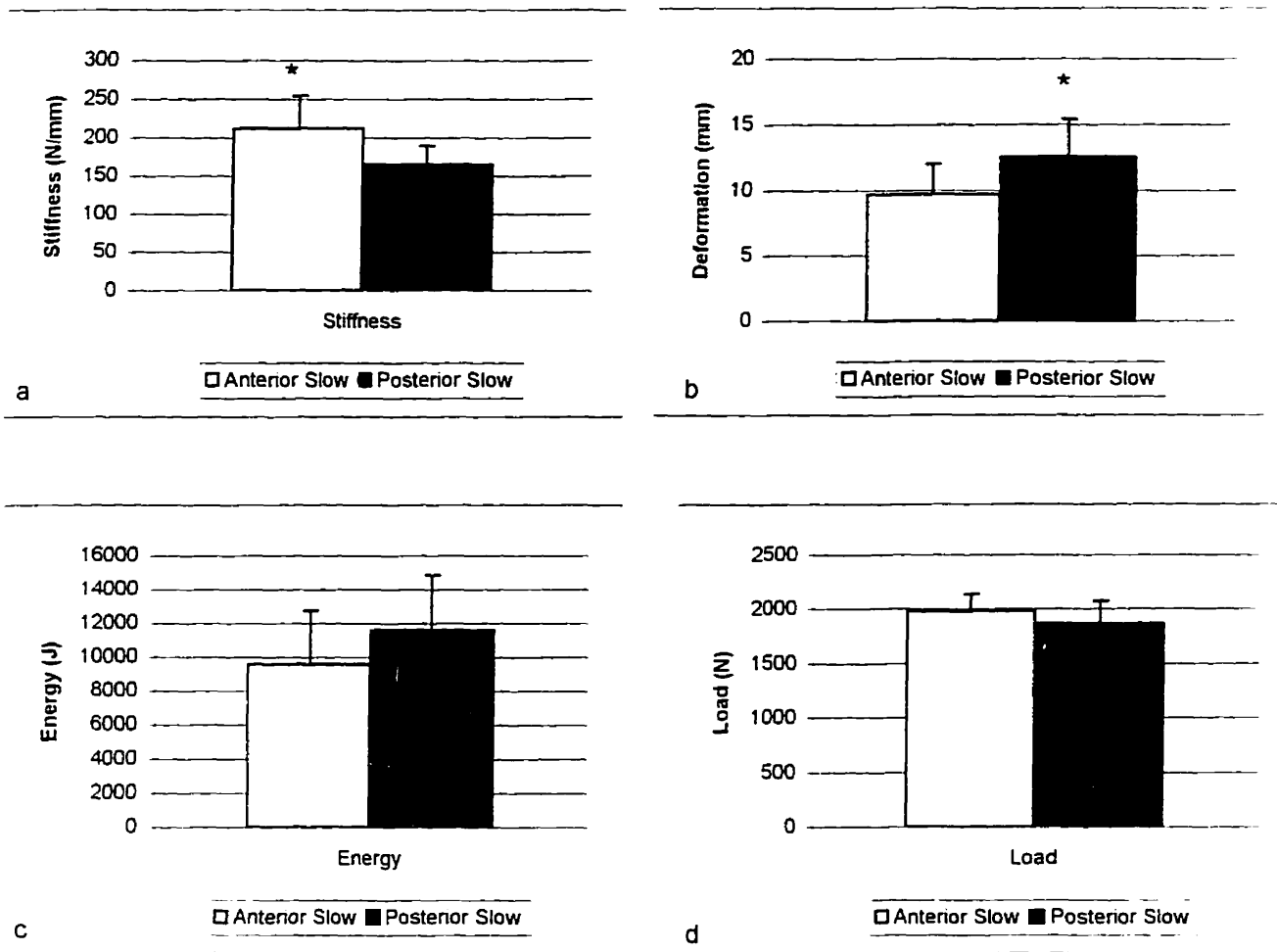
Figure 2: The average values for anterior and posterior loading at 100 N/s. a) average stiffness
b) deformation to failure c) energy absorbed to failure d) ultimate load to failure.

4.3   Discussion

The average anterior stiffness was higher than the average posterior stiffness which is a trend found in other studies. These findings confirm the results of Cripton et. al. (1995) (Cripton, Berleman, Visarius, Begeman, Nolte, & Prasad. 1995), a study which found a lower posterior stiffness (104 (31) N/mm) compared to the anterior stiffness (155 (77) N/mm) under static loading. However, their study used an uncontrolled, nonhomogeneous sample population of human specimens.

The specific hypothesis that the ultimate shear load would not be affected was supported, the ultimate shear loads were similar in both directions. For anterior shear loading the ultimate load at failure was 1980 N and under posterior shear loading the specimens failed at an average of 1860 N. Furthermore, there was no effect found for the energy absorbed at failure. The energy absorbed under anterior loading was on average 9794 J and the energy absorbed under posterior loading was 12007 J. Although this difference is not significant it suggests that the tissues resisting anterior loading and posterior loading absorb the energy of an applied load differently which may suggest that the injuries resulting from these different loadings will also differ. On the other hand, the hypothesis concerning the deformation at failure was rejected. The deformation at failure was significantly larger under posterior loading compared with anterior loading. The deformation values are difficult to compare with values in the literature, as the definitions of failure differ between studies. Previous studies have not attempted to identify the early stages of injury.

The failure point on this study was defined as a 6.25% drop in the load carried by the specimen. This definition of failure allowed a comparison of the mechanical functioning of the motion segment responding to anterior and posterior shear loading. The injury resulting from each failure will result from a similar decrease in functioning of the motion segment.

The stiffness in the posterior shear direction was lower than under anterior loading. therefore, at a constant deformation there was less load on the posterior structures. A common interpretation of this result may be that the motion segment is weaker under posterior loading. This is a misconception as the deformation to failure was different for the directions of loading. The posterior deformation was larger than the anterior deformation, and the ultimate loads at failure were similar. Stiffness is not an accurate measure of ultimate strength in a structure.

It appeared that the stiffness of the pars interarticularis due to its cortical and cancellous bone did significantly affect the stiffness in the anterior direction as well as limit the deformation at failure in the anterior direction compared to soft tissues. which resist posterior loading. Soft tissue, made up of collagen and elastin are less stiff compared to cortical and cancellous bone (Figure 1). The deformation values suggest the stiffness in the pars acts as a mechanical stop which inhibits excessive anterior translation of the superior vertebra over the inferior vertebra.

The ultimate load at failure in the current study was not found to be significantly different between anterior and posterior loading. This could suggest that the intervertebral

disc is important in shear load resistance regardless of the direction of loading. The posterior elements including the pars, the capsular ligaments and the posterior ligaments may have secondary roles in shear loading, possibly a role in stabilizing the disc and in restricting excessive motion. The posterior elements have different functions for anterior and posterior loading. The soft tissue resisting the posterior translation had a lower stiffness value yet a larger deformation, consequently, allowing a higher ultimate load. The pars increases the stiffness during anterior shear and may restrict excessive translations in this direction due to the lower deformation for anterior loading.

Key Findings:

1. The motion segment is more stiff in anterior shear loading than in posterior shear loading.

2. Ultimate load is similar between conditions even though different structures resist the applied loads.

77

Chapter Five

The Effect of the Rate of Loading

on Motion Segment Behavior

The viscoelastic response of a structure is a result of both the mechanical properties of the tissues and the geometrical arrangement of the tissues which comprise a structure. Both the response of the individual tissues comprising the motion segment as well as the response of the entire motion segment to load rate will be reviewed.

The motion segment consists of both soft tissue, ligaments and annular fibers, and bone, both types of tissue may contribute to the viscoelastic response of the motion segment. The posterior ligaments and the annular fibers of the motion segment are made of a combination of collagen and elastin fibers. Despite the time-dependant nature of soft tissue the response of these tissues to loading rate is minimal (Woo, Gomez, & Akeson. 1985). Soft tissue has a relatively minimal increase in stiffness under increased loading rates. Bone, both cortical and cancellous comprise the pars interarticularis. Cortical bone has a greater elastic modulus and ultimate strength when loaded at higher rates. As higher load rates are applied, the bone must increase its energy-absorbing capacity to reduce the possibility of fracture. The increase in elastic modulus and ultimate strength reflect this increase in energy absorption, however, if fracture does occur typically more severe fractures result from this increase in

energy applied to the bone. Cancellous bone also increased the amount of energy absorbed as load rate increases even though the strength and elastic modulus are less than those of cortical bone. Furthermore. this increase may exceed the energy-absorption capacity of cortical bone. which would have an implication in the avoidance of fracture (Carter. 1985). Evans et. al. (1959) stated that the injury produced was a function of the energy absorbed and its rate of absorption. Sammarco et. al. (1971) found increases in the energy absorbed and altered fracture patterns on the tibia as load rate increased during torsional testing. Load rate effects are greater in bone compared with soft tissue and also affect the mode of fracture of the bone.

Soft tissue and bone are typically components of a larger functional structure and the relative response of each tissue may affect the failure of the larger structure. For example, the mode of failure of a bone-ligament-bone specimen is affected by the rate of loading. This effect results from the difference in the response of loading rate between bone and ligament. At lower load rates the bone is weaker and the injury results at the bone-ligament junction. however. at higher load rates the bone becomes much stronger since it is more sensitive to load rate increases, while the ligament does not increase in strength, therefore. the injury results at the ligament (Woo. Gomez, & Akeson. 1985). This difference in load rate response is important in the motion segment, which is a structure containing both types of tissue, and these structures may have an effect on the resulting injury at differing load rates.

Research has focussed on the viscoelastic response of the motion segment, however, the direction of loading and the portion of the segment being tested affected these results. A recent study applying a compressive load to porcine motion segments under a range of load rates (100-16,000 N/s) found an effect when the specimens were loaded at rates higher than 100 N/s.

Little effect was detected as the load rate increased between 3000-16,000 N/s (Yingling et. al., 1996). Kazarian et. al. (1977) were the first to vary the load rate on isolated human thoracic vertebral bodies (.21 in/min [.0889 mm/s], 21 in/min [8.89 mm/s] and 2100 in/min [889 mm/s]). They established that behaviour was dependent on load rate, however, only the vertebral body, which is comprised of cancellous and cortical bone, was tested. A load rate effect would be expected on bone. Hutton et. al. (1979) also varied the load rate (6 mm/min [.1 mm/s] and 300 mm/min [5 mm/s]) on isolated human lumbar vertebral bodies and found higher ultimate compressive loads at failure with increased load rate. Collectively, these studies indicate a trend toward load-rate dependence of the motion segments, however, only the bony portions of the motion segment were tested. These studies all involved only compressive loading, a different effect may be seen in shear loading due to the anisotropic structure of the motion segment. Cripton et. al. (1995) using load deformation rates of 0.5 mm/sec and 50 mm/sec found an increase in stiffness of 37% for unconstrained loading but no difference was found in the maximum load. However, the unconstrained loading was accompanied by sagittal rotation which may confound the results. The lack of a complete analysis of motion segments' response to different shear loading rates motivated this study.

A controversy exists as to the best method of testing for viscoelastic effects in-vitro, load controlled or displacement controlled. Load control involves applying forces and moments to tissues and tracking the resulting deformation patterns, where as, deformation control applies translations and rotations to a tissue and measures the resulting loads. Goel et. at. (1995) contend that load control applies a constant load on the structure regardless of the stiffness or injury state which is similar to situations in-vivo. Also, under load control, creep

will occur in the tissues similar to in-vivo conditions. However, W. T. Edwards (Goel,
Monroe, Gilbertson, & Brinckmann, 1995) maintains that through in-vivo kinematic
measurements, exact movement patterns can be determined and placed on tissues in-vitro. In-
vivo testing, typically involves a constant loading protocol across participants and the
kinematic pattern resulting from the protocol may vary between participants, since the body
has many strategies which may be used for one loading input. The question is how many
deformation patterns could be applied to in-vitro tests to yield meaningful results? In the
opinion of this author the main focus of in-vitro testing should not be to replicate all in-vivo
conditions; this is impossible. In-vitro testing provides information about the mechanical
characteristics of a structure which can explain the tissues' response to in-vivo loading
situations. In-vivo and in-vitro testing create a circle of information and when merged together
may give a full understanding of spinal injury etiology.

The purpose of this experiment was to determine the effect of an increased shear load
rate both in the anterior and the posterior direction on a homogeneous sample of porcine spinal
motion segments.

Global Hypothesis:

> Stiffness and the ultimate shear load at failure of the spinal motion segment will
> increase as load rate increases.

Specific Hypotheses:

The ultimate shear load at failure will be unaffected by loading rate.
The deformation at failure will be unaffected by loading rate.
The stiffness of the motion segment will be unaffected by loading rate.
The energy absorbed at failure will be unaffected by loading rate.

5.1 Specific Protocol

Two groups (n=10 in each group) of specimens were tested at the maximum load rate

of the servo-hydraulic testing machine, however, due to the specimen stiffness the load rates

varied. The average anterior load rate was 10810 N/s (2362 N/s) [The average deformation

rate of the 10 specimens was 49 mm/s] and the average posterior rate was 9454 N/s (1798 N/s)

[average deformation rate: 40 mm/s]. The specimens were mounted in the shear jig and loaded

to failure. A 6.25% drop in the load feedback signal defined failure. Ultimate load at failure,

deformation at failure, stiffness and energy at failure were the dependant variables and were

compared with the results from the shear load tests at 100 N/s [average deformation rates:

anterior:0.47 mm/s, posterior:0.64 mm/s]. Radiography and dissection methods were used to

identify the resulting injuries.

5.2 Results

There was a significant increase in the ultimate load at failure for the faster load rate

when the anterior and posterior direction results are collapsed into one group, a combined

group for the load rate at 100 N/s and another group for the faster load rates ($p < 0.05$, F=2.82) (Table 1, Figure 1). The deformation did not significantly change. The stiffness values for the motion segments were not significant, however, the average values indicate a trend towards an increase in stiffness with an increase in load rate. Energy values were measured as the area under the normalized and averaged curves. The averaged curves were a good representative curve of the average stiffness values from all the trials (Table 2). The area of a triangle was used to calculate the energy values. The energy stored in the structure before failure increased with load rate by 22% under anterior loading and 17% under posterior loading (Table 1, Figure 1). The average graphs illustrate the load rate effect over the entire loading cycle (Figure 2). It is difficult to identify an effect for posterior loading, however, an increase in stiffness during anterior loading is apparent (this technique was used similar to a post-hoc test).

Table 1: Mechanical variables at the failure point during anterior and posterior shear loading at two rates of loading. Mean(SD).

Variable	Anterior 100 N/s	Anterior (avg:10810N/s)	Posterior (100 N/s)	Posterior (avg 9621 N/s)	Significance Load Rate
Load (N)	1980 (390)	2345 (460)	1860 (260)	2150 (408)	0.016 *
Deformation (mm)	9.7 (2.2)	10.0 (2.5)	12.5 (2.0)	12.7 (2.1)	0.75
Stiffness (N/mm)	212 (39)	250 (81)	165 (24)	190 (33)	0.19
Energy (J)	9600	11700	11600	13600	NA

Table 2: A comparison of the average stiffness determined from the equation fit to the experimental data and the stiffness determined from the linear region of each experimental trial.

	Anterior (100 N/s)	Anterior (10810 N/s)	Posterior (100 N/s)	Posterior (9621 N/s)
Equation	Load = 212.34(def)	Load = 242.79(def)	Load =158.85(def)	Load = 161.37(def)
Average Value	212 N/mm	251 N/mm	165 N/mm	186 N/mm
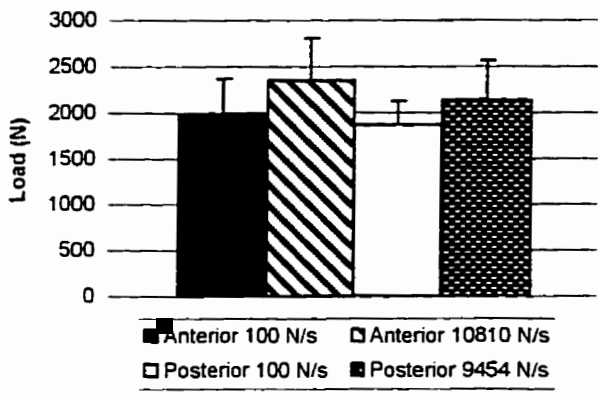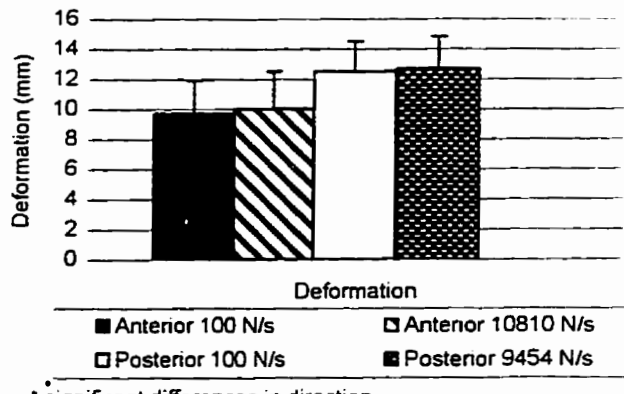
.
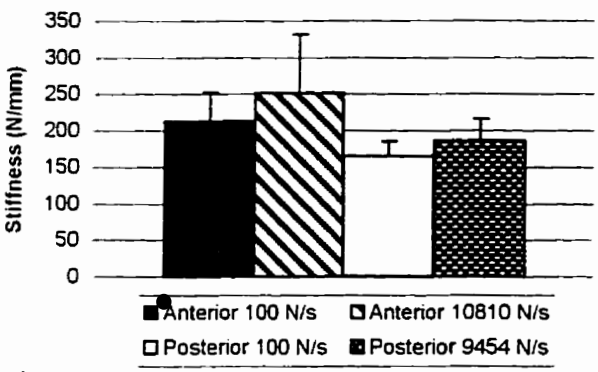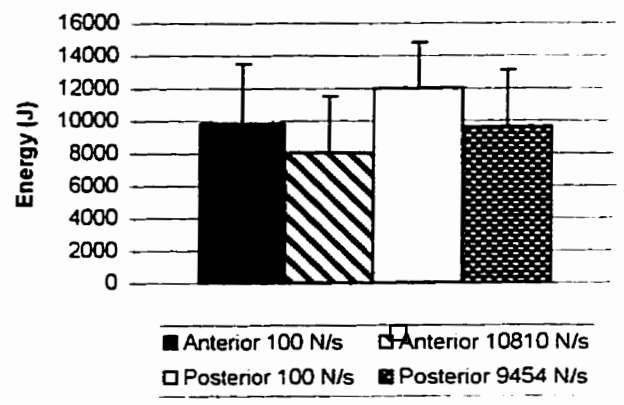
Figure 1: The average values from the anterior slow tests at 100 N/s [deformation rate: 0.47 mm/s], the anterior fast tests at an average load rate of 10810 N/s [49 mm/s], the posterior slow tests at 100 N/s [0.64 mm/s] and the posterior fast tests at an average load rate of 9454 N/s [40 mm/s]. a) Ultimate load at failure, b) Deformation at failure, c) Average stiffness, d) Energy absorbed to failure.
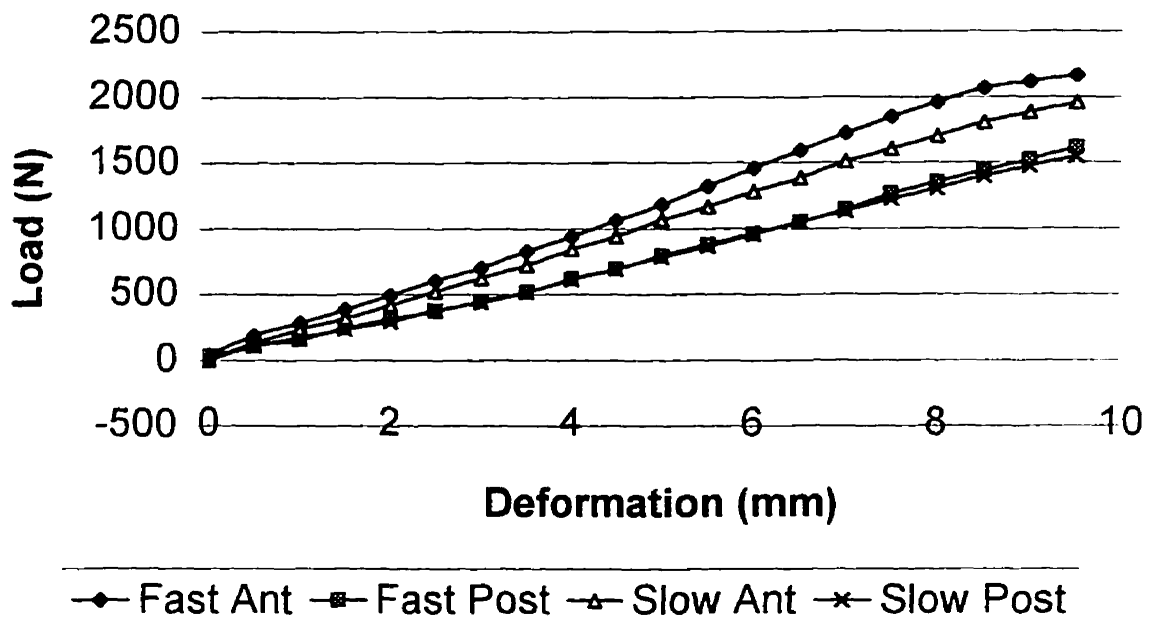
Figure 2: Load-deformation curves for anterior and posterior shear loading at different load rates. The curves are averages of the normalized deformation and load values for all trials (n=10).

5.3　　　　　　　　　　　　Discussion

The results illustrate the dependence of the spinal motion segment on the rate of loading. There was a significant increase in the ultimate load and a trend in the stiffness with the increase in loading rate. This response during anterior loading supports the findings of Cripton et. al. (1995) who found an increase in anterior stiffness for loading cycles up to 1.5 mm shear translation at higher loading rates. The motion segments increased the energy absorbed to failure indicating an attempt to resist the potential for failure, yet the deformation to failure was not affected. Furthermore, the averaged normalized curves diminish the effect of load rate on posterior shear loading.

The response to increased loading rate was similar to the results in other studies. Previous researchers have found a minimal effect of load rate on soft tissue. The relative response to an increase in load rate was relatively small under posterior loading in the current study, which is resisted primarily by soft tissue. There was an increase of 17% in stiffness under anterior shear loading. Anterior shear loading had greater response to the load rate increase as would be expected due to the structures involved in resisting anterior shear loads. The pars, which is made up of cortical and cancellous bone, was involved in the resistance of anterior shear loading. Applied loads on the pars interarticularis at deformation rates of .5 mm/sec and 50 mm/sec found increases in stiffness values and decreases in the deformation values at failure between the different deformation rates (Troup. 1976; Cyron, Hutton, & Troup. 1976). Increases in load rate appear to affect the mechanics under anterior loading but

have minimal effect in posterior loading.

Deformation may be a significant factor in determining failure during posterior shear loading of the motion segment. The deformation at failure was unchanged for an increase in load rate from 100 N/s to 9454 N/s under posterior shear loading. Failure detection was not dependent on the energy absorbed in the structures before failure, therefore, similar load sharing strategies would be expected at different load rates during posterior shear.

The failure of the motion segment under anterior loading is more sensitive to load rate increases. Although the deformation at failure remained constant between the two load rates, the specimen had a significantly higher ultimate load and an increase in stiffness. This suggests a different load sharing strategy between the disc and the pars as load rate increases due to the sensitivity of the bony pars to changes in the rate of loading.

In summary, the increase in loading rate significantly affected the ultimate load at failure for anterior loading possibly due to the increase in stiffness which is suggested by the average curves. This increase in stiffness suggests a variation in the load sharing strategies of the motion segment as the load rate changes.

Key Findings

1. A greater load rate effect for anterior loading compared with posterior shear loading is suggested by the normalized averaged curves.

2. The deformation at failure was not affected by load rate under either anterior or posterior shear loading.

89

Chapter Six

Identification of the Mechanical Roles of

Individual Structures of the Motion Segment

6.0   Tissue Structures

The motion segment resists shear loading as a whole structure but the mechanisms of

injury are based on the capability of the components which share the burden of the applied

load. An applied shear load to the entire motion segment results in a variety of loads on the

individual tissues (Figure 1). Thus, the mechanics of each structure must be appreciated

separately. Motion segments are generally divided into anterior and posterior elements (Figure

2 and 3). The anterior portion consists of the intervertebral disc and bony vertebra. The

posterior portion of the motion segment includes the interspinous and supraspinous ligaments,

the spinous process, and the neural arch (laminae and pedicles). At the junction of the laminae

and pedicle, the superior and inferior facet processes extend vertically. The facets are

connected by the capsular ligaments of the adjacent two vertebrae forming bilateral synovial

joints. Each component of the motion segment is designed to contribute to the functioning of

(A) Anterior Shear Load

(B) Posterior Shear Load

Figure 1: Schematic diagram of sagittal view of the porcine motion segment indicating the types of loads on the individual tissue structures. (A) Under anterior shear loading the annular fibers are under a tensile load A and B. A load C is applied to the inferior facet causing a bending moment D on the pars interarticularis. (B) Under posterior loading the annular fibers are under tensile load A and B. The capsular ligaments C are under a tensile load which may cause a bending moment about the pars interarticularis D. The posterior ligaments are under tensile load E.
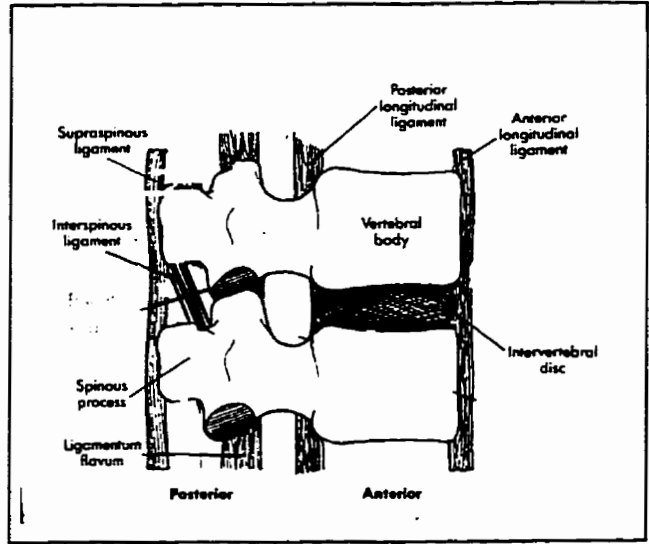
Figure 2: Schematic drawing of the side view
of a lumbar vertebral motion segment.
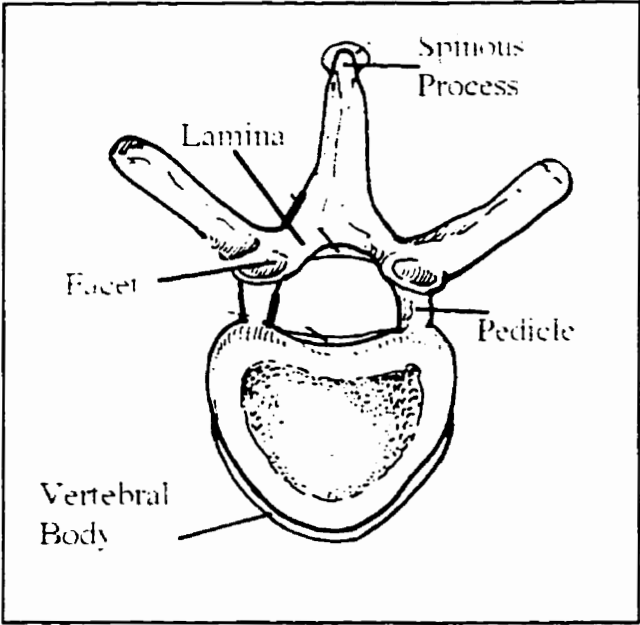
Figure 3: Schematic drawing of the top view of
a vertebral body.

92

the lumbar spine.

6.0.1   Intervertebral Disc

Intervertebral discs have been found to play a major role in resisting applied compressive loads on the spine, but the structure of the disc suggests that it may also perform a role in shear load resistance. The intervertebral disc is a viscoelastic structure between two adjacent bony vertebral bodies; the primary function of the disc is to bind the vertebral bodies together while allowing flexibility in the spine. Three components form the intervertebral disc; the nucleus pulposus, the annulus fibrosus, and the cartilaginous endplates. The nucleus pulposus. a mucopolysaccharide gel. occupies 40-60% of the cross sectional area of the disc. The annulus fibrosus consists of collagenous tissue arranged in concentric lamellae surrounding the nucleus. The inner lamellae attach to the endplates while the outer lamellae attach directly to the cortical shell of the vertebral bodies. The vertebral endplates are made of hyaline cartilage and separate the disc from the bony vertebra. An external shear load applied to the motion segment may be resisted by the disc since the annular fibers are oriented at an oblique angle to the plane of the disc and the outer annular fibers are directly attached to the vertebral body (Bogduk & Twomey. 1991) (Figure 4).

Only the outer portion of the annulus is important to shear loading since no fibrillar connections between the cartilage end-plate and the subchondral trabeculae were found (Inoue. 1981). The inner annular fibers would thus have no effect on shear loading, leaving the shear resistance to the outer fibers, which are connected to the cortical bone. Both the geometry and

93
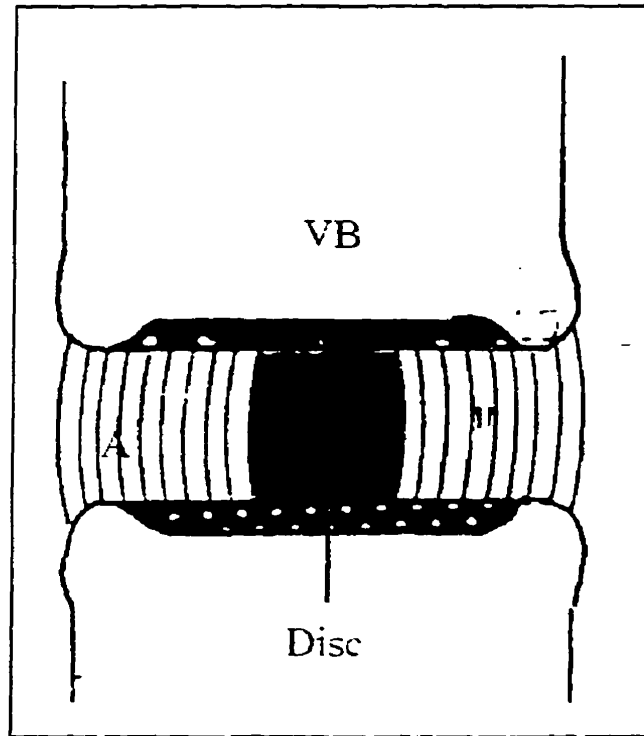
Figure 4: Schematic drawing of the nucleus pulposus of the intervertebral disc (disc). the annulus fibrosus (A) and the vertebral body (adapted from Cailliet. 1995).

histology of the intervertebral disc suggest that the anterior, posterior and lateral portions of the annulus respond differently to an external shear load. The disc is shaped similar to an ellipse, which suggests that the lateral fibers will undergo a greater strain than the anterior or posterior fibers. The difference will also be dependant on the angle of the fibers. Histological analyses of the annular fibers have found that the number of layers of fibers is the largest in the lateral section, (22.9(3) layers), compared with the anterior and posterior regions which have (21.3(3) layers) and (18.8(3) layer) respectively (Marchand & Ahmed. 1990). In a study only considering the outer portion of the annulus, more layers were found anteriorly than in the posterior region (Markolf & Morris. 1974; Tsuji, Hirano, Ohshima, Ishihara, Terahata, & Motoe. 1993; Marchand & Ahmed. 1990). The shape and histology of the annulus suggest a role in both anterior and posterior shear loading.

The weight of the upper body will impose a constant shear loading on the disc during upright standing due to the lordotic curve of the lumbar region of the spine (Figure 5 & 6). The disc has been found to creep under constant compressive loading, but little information is available on the creep characteristics under constant shear loading. Creep in the intervertebral disc during shear loading may shift the load to the facet joints.

6.0.2   Facet Joints

Each lumbar vertebra has four facet processes, two inferior and two superior to the plane of the intervertebral disc. Two bilateral synovial joints are formed between two adjacent

vertebrae. The two facet joints are located posterior to the intervertebral disc creating a triangular three point base for load resistance. The distance of the facet joints behind the disc is of less importance to shear load resistance than the superior-inferior alignment of the joints.

The facet joints have been associated with all types of spinal loading, including compression and shear loads and torsion and flexion moments. In-vitro studies have indirectly measured the amount of compressive load resisted by the facet joints when they impinge on the lamina. A wide range of values have been reported which are dependent on the posture of the motion segment (Yang & King. 1984). Under torsional loading the facet joints and the intervertebral disc collectively resist approximately 90% of the applied load (Farfan, Huberdeau, & Dubow. 1972; Farfan, Cossette, Robertson, Wells, & Kraus. 1970). The facet joints were found to significantly resist flexion moments (Adams, Green, & Dolan. 1994). During flexion the facet joint faces become oblique to one another increasing the distance between the facet faces placing a load on the capsular ligaments (Figure 7).

The facet joints are perpendicular to the transverse plane of the disc thus their main function may be to resist shear load. One study found the facet joints able to resist 1/3 of the applied shear load while the discs resist the remaining 2/3 of the load (Cyron, Hutton, & Stott. 1979). Another study found that the discs resist 77% of the applied shear load (Cripton, Berleman, Visarius, Begeman, Nolte & Prasad. 1995), while a third indicates the facet joints resist the majority of the shear load, 2800 N compared with 900 N for resisted by the intervertebral disc (Farfan. 1988). The relative contribution of the facet joints and intervertebral disc to shear loading appears to depend on the posture of the motion segment and the degenerative state of the disc.

96
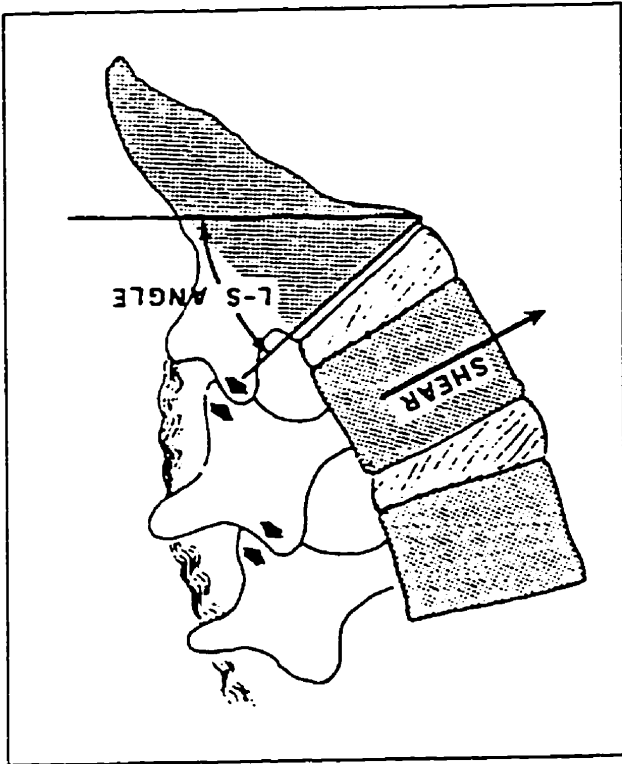
Figure 7: Illustration of the contact of the
surface of the facet joints (F) for a motion
segment in a neutral posture (top) and a flexed
posture (bottom) (adapted from Cailliet, 1995).
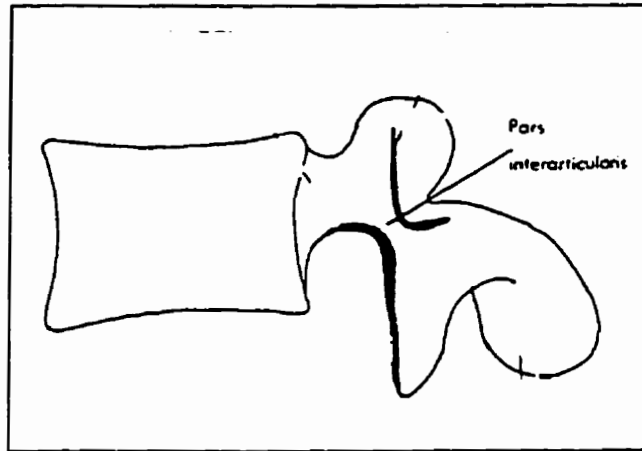
Figure 8: Sagittal view of the vertebral body,
the pars interarticularis is located between the
superior and inferior facets (adapted from
Cyron et. al.. 1976)

6.0.3   Pars Interarticularis

The pars interarticularis is the structure between the superior and inferior facet faces. It consists of two layers of cortical bone joined by thick trabeculae (Figure 8). Loading on the facet faces results in a bending moment of the pars which results in an increase in stiffness in the pars. The cortical bone is thick on the portion of the pars interarticularis where the bending moments occur in order to resist fracture due to the deflexion of the pars during loading (Stewart. 1953; Krenz & Troup. 1973). The shape of the pars is designed to withstand bending moments of (15.6 - 45.6) Nm before failure (Troup. 1976).

Applied shear and torsional loads cause the facets to contact and create a bending moment in the pars interarticularis (Figure 1). The stiffness in the pars from the bending moment may be a significant factor in shear load resistance. A defect in the pars may decrease the pars stiffness and allow an increase in translation of the motion segment. Defects in the pars have been identified to precipitate such conditions as spondylolisthesis.

6.0.4   Ligaments

.

Six ligaments of the motion segment will be reviewed here, the anterior longitudinal ligament (ALL), the posterior longitudinal ligament (PLL), the ligamentum flavum (LF), capsular ligaments of the facet joints (CL), the interspinous ligament (ISL) and the

supraspinous ligament (SSL) (Figure 2). Ligaments allow movement in the spine, yet also help maintain stability in the spine by defining its end range of motion. Ligaments are primarily composed of collagen fibers and resist tensile loads. The function of ligaments depends on the orientation of the collagen fibers as the stiffness of a ligament varies with the alignment of the fibers (Viidik, 1979).

Two ligaments run the entire length of the spine on either side of the vertebral body, the anterior and posterior longitudinal ligaments. The anterior longitudinal ligament provides resistance during extension of the motion segment, one of the few structures of the motion segment which resists extension. It has deep fibers connecting single vertebrae which assist the annulus in the reinforcement of the anterior portion of the disc. The anterior longitudinal ligament has been reported to be twice as strong as the posterior longitudinal ligament. Similar to the anterior longitudinal ligament, the posterior longitudinal ligament is hourglass shaped, thin over the vertebral bodies and thicker over the disc providing protection from posterior disc extrusion during flexion. The deepest and shortest fibers span two intervertebral discs. Its function is primarily to resist the separation of the posterior ends of the vertebral bodies (Bogduk & Twomey, 1991).

The ligaments encasing the facet joints, the capsular ligaments, have two distinct fiber lengths within the ligament, long dorsal fibers and shorter ventral fibers. The capsular ligaments loaded to failure in tension exhibit a two peak load-deformation curve associated with these different fiber lengths (Cyron & Hutton, 1981) (Figure 9). The ligaments were able to resist up to 400 N and had a stiffness of approximately 130-150 N/mm, however, the ligaments were not tested under a loading condition which would be found in-vivo. The

101
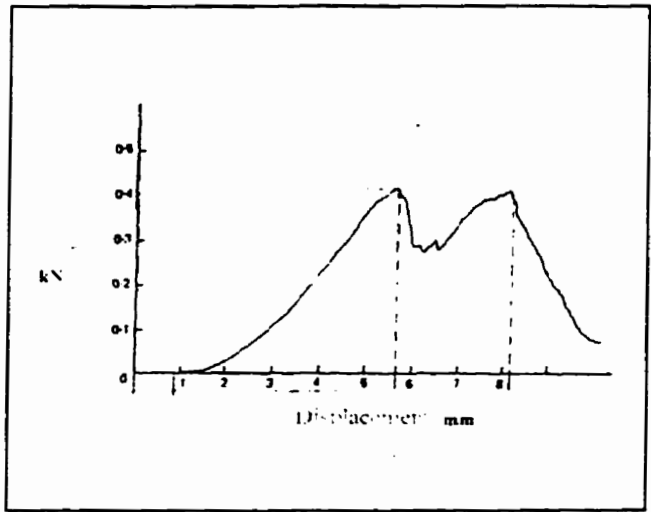
Figure 9: Force-deformation curve of the capsular ligament of the facet joints (Cyron & Hutton. 1981).

ligaments may be involved in shear loading, as the facet faces are forced apart during posterior shear loading, the capsular ligaments would be strained applying a tensile load on the ligament fibers (Figure 1).

The ligamentum flavum, connecting the laminae of adjacent vertebrae. has a high percentage of elastin ensuring that it will not buckle into the spinal canal during extension (Yahia, Drouin, & Newman. 1990). Due to the high elastic content in the ligamentum flavum. it stiffens at a higher deformation compared with other spinal ligaments and may only resist bending moments at full flexion and under large shear loads. The adjacent laminae may translate during large shear loading causing tension in the ligamentum flavum. but due to the large percentage of elastin in this ligament it may only resist excessive posterior shear translations.

The interspinous ligament, running obliquely between adjacent spinous processes. is divided into three regions. The first region blends with the ligamentum flavum. The second region, the major component of the ligament, attaches to the anterior half of the cranial border of the inferior process and the posterior half of the caudal border of the superior process. The third and most dorsal region connects into the supraspinous ligament (Heylings. 1978). The alignment of the fibers has been controversial, previous to Heylings (1978) the fibers were reported to run opposite of what was stated above.

Many studies have corroborated the alignment found in Heylings (1978) (McGill. 1988; Yahia, Drouin, & Newman. 1990; Hukins, Kirby, Sikoryn, Aspden, & Cox. 1990). However, the function of the interspinous ligament remains in contention. Two theories have been introduced. First, the ligament is thought to anchor the thoracolumbar fascia to the spine. The

103

abdominal muscles are thought to produce tension in the fascia which could be transmitted to the spine through the interspinous ligament (Aspden, Bornstein, & Hukins. 1987). Second, the interspinous ligament has been identified with resisting the bending moments in the motion segment since it has the largest moment arm. Some investigators have suggested that the postero-cranial alignment could not aid in flexion resistance since the collagen fibers are not stressed during flexion (Hukins, Kirby, Sikoryn, Aspden, & Cox. 1990). However, Heylings (1978) suggested that if the collagen fibers were vertical between the spinous processes the flexion of the motion segment would be extremely minimal unless the ligaments were very slack in extension. Heylings (1978) suggested that the nearly parallel alignment of the interspinous ligament may function to resist flexion similar to the collateral ligaments of the knee joint, to restrict excessive motion and to guide motion as the facets glide over one another throughout the flexion range. The radially directed ligament fibers would allow flexion while still allowing the collagen fibers to increase in stiffness.

McGill (1988) illustrated the contribution of the interspinous ligament during motion segment bending. The interspinous ligament was the largest contributor to flexion resistance, mainly at larger flexion values possibly due to the crimped nature of the fibers within the ligaments as well as to the radial alignment of the fibers. The role of the interspinous ligament was also illustrated in a study using video fluoroscopy to analyse motion segment flexion and ligament tension during dead lifts performed by experienced power lifters. Cholewicki and McGill (1992) concluded that the motion segments did not reach full flexion. The ligaments would have had their maximal contribution at full flexion, thus their main role was not to contribute maximally but possibly to guide and control the extent of flexion during these

104

maximal lifts. The postero-cranial orientation of the interspinous ligament is also suspected to cause the superior vertebra to shear anteriorly during flexion (Potvin. Norman, & McGill. 1991; McGill. 1988). It is hypothesized by McGill (1988) that this anterior shear may ensure the coupling of the facet faces.

Although the controversy remains as to the function of the interspinous ligament's role in flexion, these studies have verified the posterio-cranial alignment of the ligament. Therefore, a tensile load would be generated in the posterior ligaments from an externally applied shear load which suggests a role of the ligament in resisting posterior shear translations.

6.0.5   Muscle

The mechanical tests in the current study focus on the bony and ligamentous portions of the motion segment of the lumbar spine. However, the abdominal and back musculature has been associated with stabilizing the spine and decreasing anterior shear loads. The back musculature opposes flexor moments and helps to stabilize the spine. Motion segments are not only affected by the muscles directly attached to them but also by the muscles which span them. The forces placed on the segment depend on the orientation of the muscle fascicles as well as the orientation of the motion segment. In the sagittal plane, the muscles place both compressive and shear forces on the spine.

The main function of the back muscles is to counter any flexor moment placed on the body by the abdominal muscles, body weight or external loading. The thoracic fibers of the

105

erector spinae muscles, longissimus thoracis pars thoracis and the illiocostalis lumborum pars thoracic exert 40% - 80% of the total extensor moment (Bogduk, MacIntosh, & Pearcy. 1992). To a lesser extent the multifidus supports the extensor moment (MacIntosh & Bogduk. 1986). The lumbar musculature also imposes compressive loads on the motion segments and is able to counter applied shear loads. These roles are dependent on the angle of insertion of the muscle fascicle and the alignment of the vertebral body. The compressive load on the intervertebral discs is increased by both muscle fascicles directly attaching to the motion segment and fascicles spanning the segment. Many biomechanical models of the lumbar region diminish the role of the back extensor muscles in the resistance of anterior shear loading. These models are single equivalent models with a representative muscle running perpendicular to the plane of the disc, thus having no potential to resist anterior shear loading. The erector spinae muscles, specifically the longissimus thoracis pars lumborum and the illiocostalis lumborum pars lumborum, have individual attachments to the transverse processes of the lumbar spine. Recent studies have represented in detail the anatomy of the lumbar musculature suggesting the potential mechanical role the muscles have in offsetting anterior shear loads (McGill. 1988: MacIntosh & Bogduk. 1987). In addition studies examining the mechanical function of the lumbar musculature have confirmed the muscles' ability to resist increasing applied shear loads (Potvin, Norman, & McGill. 1991; Potvin, McGill, & Norman. 1991; McGill & Norman. 1987).

The functional role of the psoas muscle has been a subject of speculation over the past years. Much of the speculation is due to the inaccessibility of the muscle with surface EMG electrodes. It has been theorized to be a stabilizer of the spine, a controller of lordosis and a

106

source of anterior shear loading on the motion segments. Recent studies have clarified the role of the psoas muscle as a hip flexor based on the activation of the muscle (McGill, Juker, & Kropf. 1995) and the mechanical advantage of the muscle (Santaguida & McGill. 1995). Also. the psoas muscle was shown to have little control over lordosis (Santaguida & McGill. 1995). In addition the anterior shearing potential of the muscle was previously overestimated. substantial anterior shear loads are only placed on the L5-S1 level by the psoas muscle. Stabilization of the lumbar spine using compressive loading and bilateral activation has also been shown to be a function of the psoas muscle (Santaguida & McGill. 1995). Spondylolisthesis may be exacerbated by activation of the psoas due to its imposition of anterior shear at the L5-S1 lumbar levels.

6.0.6 Load Sharing Between the Components of the Motion Segment

In order to understand the mechanism of injury of the motion segment, information is necessary not only on the function of the structures which make up the motion segment but on how these structures share the resistance of an external shear load. Previous studies have shown the load sharing capabilities of tissues during other types of loading. Studies have found the sharing under compressive loading occurred between the disc and the facets (Yang & King. 1984; Prasad, King, & Ewing. 1974; Hakim & King. 1976). The compressive load causes the nucleus to bulge outward into the annular fibers, which resist the bulging with a tensile load. The facets take a portion of this compressive load as the inferior facet process

impinges on the lamina below. The percentage of the load carried by the facets was found to be dependant on the position of the facets, which changes with postural changes of the joint. The percentage was found to be between 0-33% depending on the posture of the motion segment. Torsional loading is shared by the disc (with the longitudinal ligaments) and the facet joints (including the capsular ligaments). Each of these structures carries 45% of the torsional load with the interspinous ligament resisting the remaining 10 % (Farfan, Huberdeau, & Dubow, 1972; Farfan, Cossette, Robertson, Wells, & Kraus, 1970). Shear loads are also shared among the components of the motion segments, however, current data does not support similar strategies between the structures. Farfan (1988) estimated the tolerance of the facet joints to shear loading to be 3100-3600 N with only 900 N being carried by the intervertebral disc. Cripton et. al. (1995) designated the disc with resisting 77% of the applied shear load after the facet joints failed.

The purpose of this experiment was to better identify the function of each structure under shear loading as well as the load sharing of the components of the motion segment .

Global Hypothesis:

Facets joints (pars interarticularis) will resist a greater proportion of an external anterior shear load compared with the disc and posterior ligaments (interspinous and supraspinous).

Specific Hypotheses:

The ultimate shear load at failure will be unaffected by the removal of the facet joints prior to testing.
The deformation at failure will be unaffected by the removal of the facet joints prior to testing.
The average stiffness of the motion segment will be unaffected by the removal of the facet joints prior to testing.

6.1   Specific Protocol

The specimens (C3-C4 and C5-C6) were separated into four types for this testing

protocol, whole specimens (W) (ant n=10, post n=10), posterior ligaments removed (NL) (ant

n=6, post n=6) and posterior ligaments and facet joints removed (NFL) (ant n=10, post n=10)

and whole specimens which were flexed approximately 10 degrees (F) (ant n=10). The

specimens were mounted in the shear jig and loaded to failure at 100 N/s. A 6.25% drop in the

load feedback loop indicated failure. Ultimate load at failure, deformation at failure and

average stiffness of the specimen were used to compare the contributions of the types under

anterior and posterior shear loading. Radiology and dissection techniques revealed the injuries

sustained under each type of loading.

6.2   Results

The stiffness values were significantly different in direction and type ($p < 0.05$, F

=6.54). Post hoc tests showed that for the specimens with no posterior ligaments or facets

(NFL), the average stiffness value was lower than the other three groups, whole (W), no

posterior ligaments (NL) and flexed specimens (F) for anterior loading (Figure 10). Posterior

loading showed no differences except that NL had a lower stiffness than the whole (W)

specimen however, whole (W) and NFL were not significantly different.

The deformation at failure was significant for type and direction ($p < 0.05$, $F = 2.95$) with post hoc tests revealing differences under anterior loading between flexed (F) specimens and NL and NFL specimens, the deformation was lower in these cases. But flexion (F) was not significantly different from the whole (W) specimens. The deformation under posterior loading showed that the whole (W) specimens were not significantly different from NL and NFL however, NFL was significantly lower than NL (Figure 10).

The ultimate load at failure was not significant for the direction of loading but had significant differences in the type of specimen. For posterior loading, the NFL was lower than both the W and NL specimens. Under anterior loading, the NFL was lower from all other types, W, NL, and F, but the flexed specimens (F) are only different from the whole specimen not the NL specimen (Figure 10).

To visualize the shape of the curves between the types of specimens for the entire loading cycle, the trials were normalized, both the deformation and load, and then averaged across all trials. The average curves are shown in Figure 11. The properties of the pars interarticularis were determined by subtracting the no posterior ligament and facet (NFL) curve from the curve for the whole specimen (W), it was assumed that the posterior ligaments had a minimal effect in the resistance of an applied shear load (Figure 12). All the curves were modelled using 2nd order polynomials. The curves were generated from the average curves up to 8 mm to avoid confounding effects of samples not surviving to higher load levels. The equations for anterior loading were:

WHOLE: $\text{LOAD} = 23.286x^2 + 33.041x$ $R^2 = .9959$

DISC: $\text{LOAD} = 13.208x^2 + 45.754x$ $R^2 = .9963$

PARS: $\text{Load} = 10.179x^2 - 12.713x$ $R^2 = .987$

The equations for anterior stiffness were obtained by taking the derivative of the equations above:

WHOLE: $\text{STIFFNESS} = 46.772x + 33.041$

DISC: $\text{STIFFNESS} = 26.416x + 45.754$

PARS: $\text{STIFFNESS} = 20.358x - 12.713$

The largest contributor of stiffness under anterior shear loading was found to be the disc complex, accounting for approximately 70% of the overall stiffness of the motion segment (Figure 13). The pars complex contributed much less to the stiffness, on average 30%. The average load at failure for the disc (NFL) was 1390 N compared to the pars complex (W - NFL) at 830 N.

The posterior curves were also modelled using 2nd order polynomial fits (Figure 13). The capsular ligament graph was obtained by subtracting the no posterior ligament and facet joint (NFL) curve from the whole curve (W). The average load values obtained indicate a load of approximately 420 N carried by the capsular ligaments and any bending in the pars interarticularis. The equations for posterior shear loading were:

111

WHOLE: $\text{L}_{\text{OAD}} = 18.719\text{x}^2 + 10.424\text{x}$ $\text{R}^2 = .9927$

DISC: $\text{L}_{\text{OAD}} = 14.538\text{x}^2 + 6.4254\text{x}$ $\text{R}^2 = .9949$

CAPS LIGS: $\text{L}_{\text{OAD}} = 3.514\text{x}^2 - 4.233\text{x}$ $\text{R}^2 = .9438$

The equations for posterior stiffness were obtained by taking the derivative of the equations above:

WHOLE: $\text{L}_{\text{OAD}} = 37.438\text{x} + 10.424$

DISC: $\text{L}_{\text{OAD}} = 29.076\text{x} + 6.425$

CAPS LIGS: $\text{L}_{\text{OAD}} = 7.027\text{x} - 4.233$

The disc carries approximately 1540 N (74% of the intact specimen) of the ultimate load to failure under posterior loading. The stiffness in posterior loading was again mainly from the intervertebral disc complex, accounting for approximately 85% of the average stiffness. The average displacement under posterior loading decreased significantly when the posterior elements, particularly the facet joints were removed (Figure 10).

The intervertebral disc has similar mechanical properties whether it is loaded to failure at 100 N/s under anterior or posterior shear loading (Figure 14). The average deformation to failure is approximately 10 mm for both anterior and posterior loading (Figure 10). The stiffness and the ultimate load to failure are also similar between the two conditions. The average anterior stiffness was 236 N/mm compared with a posterior stiffness of 249 N/mm. An ultimate anterior load of 1385 N was found with a posterior load of 1537 N.

112

A significant difference was found between the whole (W) and flexed (F) specimens for the ultimate load at failure. There was no significant difference in the deformation. however. a trend of increased deformation at failure for the flexed specimens was identified. Stiffness between the whole (W) and flexed (F) specimens was not significantly different (Figure 15).

Preconditioning cycles had a significant effect on the average values for the deformation at failure, the ultimate load at failure and the stiffness of the specimens (Figure 16). Average deformation values at failure increased 19.6% for anterior loading and 5% for posterior loading following the preconditioning cycles. Ultimate load values increased 7% for anterior loading and 10% for posterior loading. A 49.5% increase was found in the anterior stiffness value and 76% increase for posterior loading. The significance of these results is illustrated in the average curves for the preconditioned specimens and those without preconditioning (Figure 16), a toe region is introduced followed by an increase in the stiffness in the linear portion of the load-deformation curve (Figure 17).
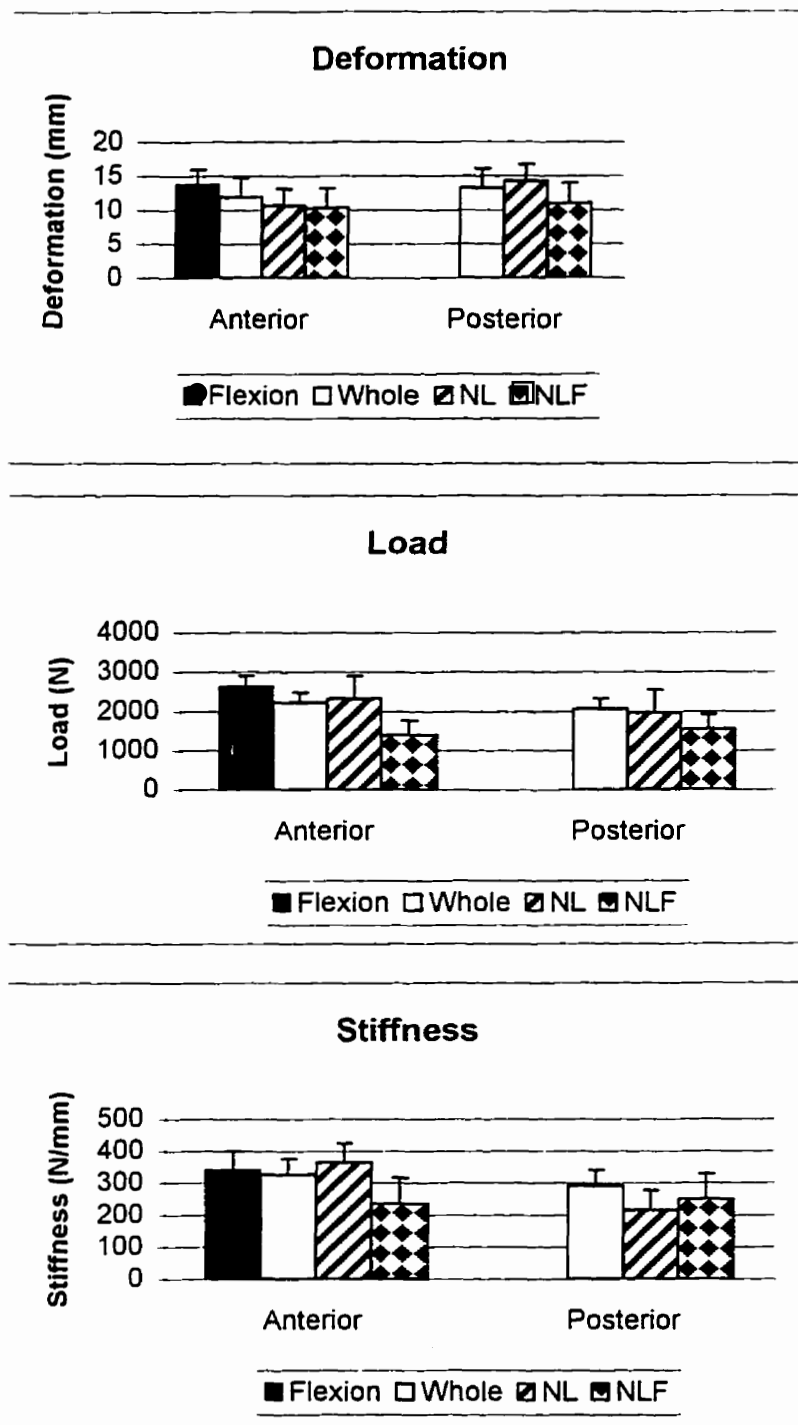
Figure 10: Average values for deformation at failure, ultimate load at failure and the stiffness for flexed specimens (Flexion), whole neutral specimens (Whole) specimens without posterior ligaments (NL) and specimens without both posterior ligaments or facet joints (NFL).

Anterior Shear Loading

Whole —■—NFL —△—Pars

Posterior Shear Loading

—◆—Whole —△—Disc (NLF) —✕—Capsular Ligs
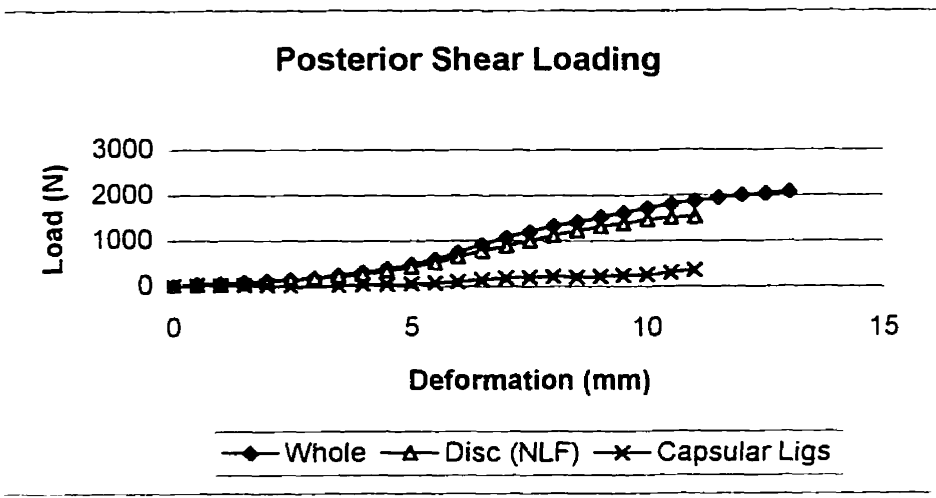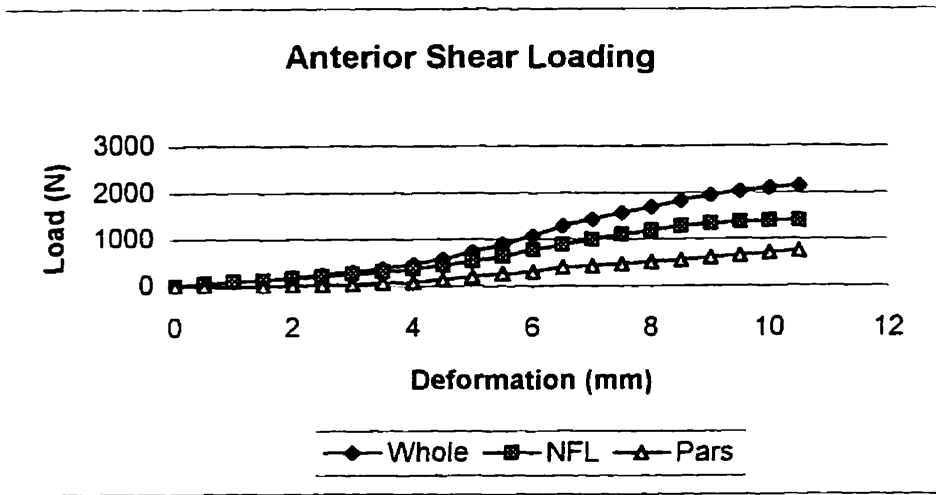
Figure 11: Averaged curves for the anterior shear loading trials and the posterior shear loading trials. Illustrates the partitioning of the applied shear load between the structures comprising the motion segment. For anterior shear loading the pars interarticularis and the intervertebral disc resisted the load. For posterior loading, the intervertebral disc and the capsular ligaments share the loading.
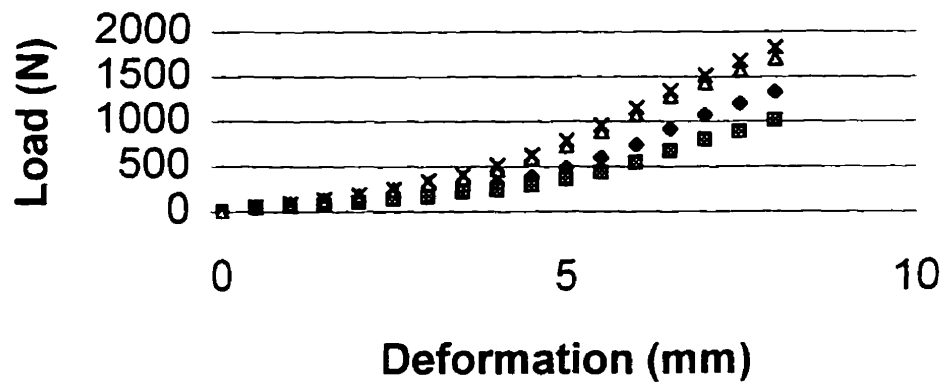
Figure 12: Averaged curves showing the similarity between the whole specimens and specimens with their posterior ligaments severed.

Anterior Shear Loading

Poly. (Whole) ▪ ▪ ▪ Poly. (Disc (NFL)) — —Poly. (Pars)

Posterior Shear Loading

Poly. (Whole) — —Poly. (Capsular Ligs) ▪ ▪ ▪ Poly. (Disc (NLF))
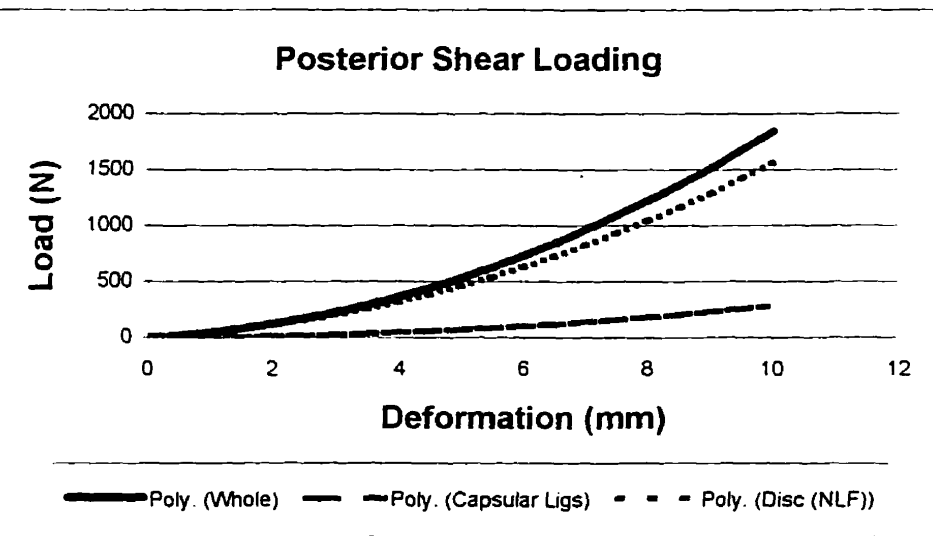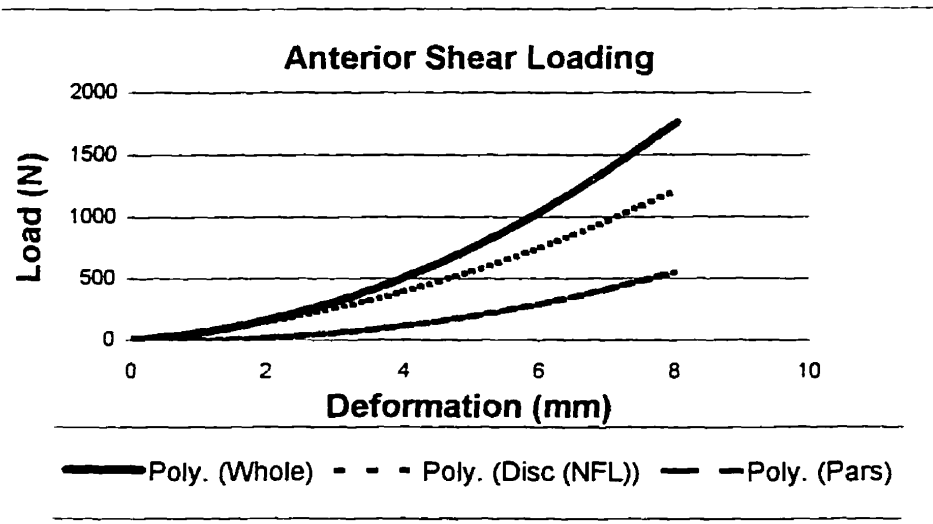
Figure 13: Experimental data modelled using 2nd order polynomial curves. The curves illustrate the partitioning among the structures of the motion segment.
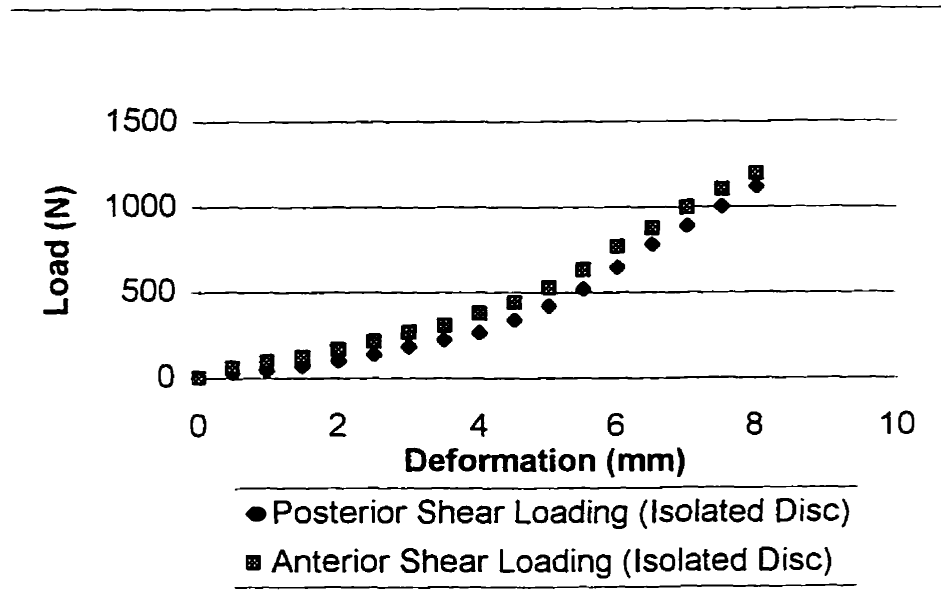
Figure 14: Averaged data of the isolated disc under the anterior and posterior shear loading conditions up to 8 mm of deformation. The response of the intervertebral disc was similar under both conditions.
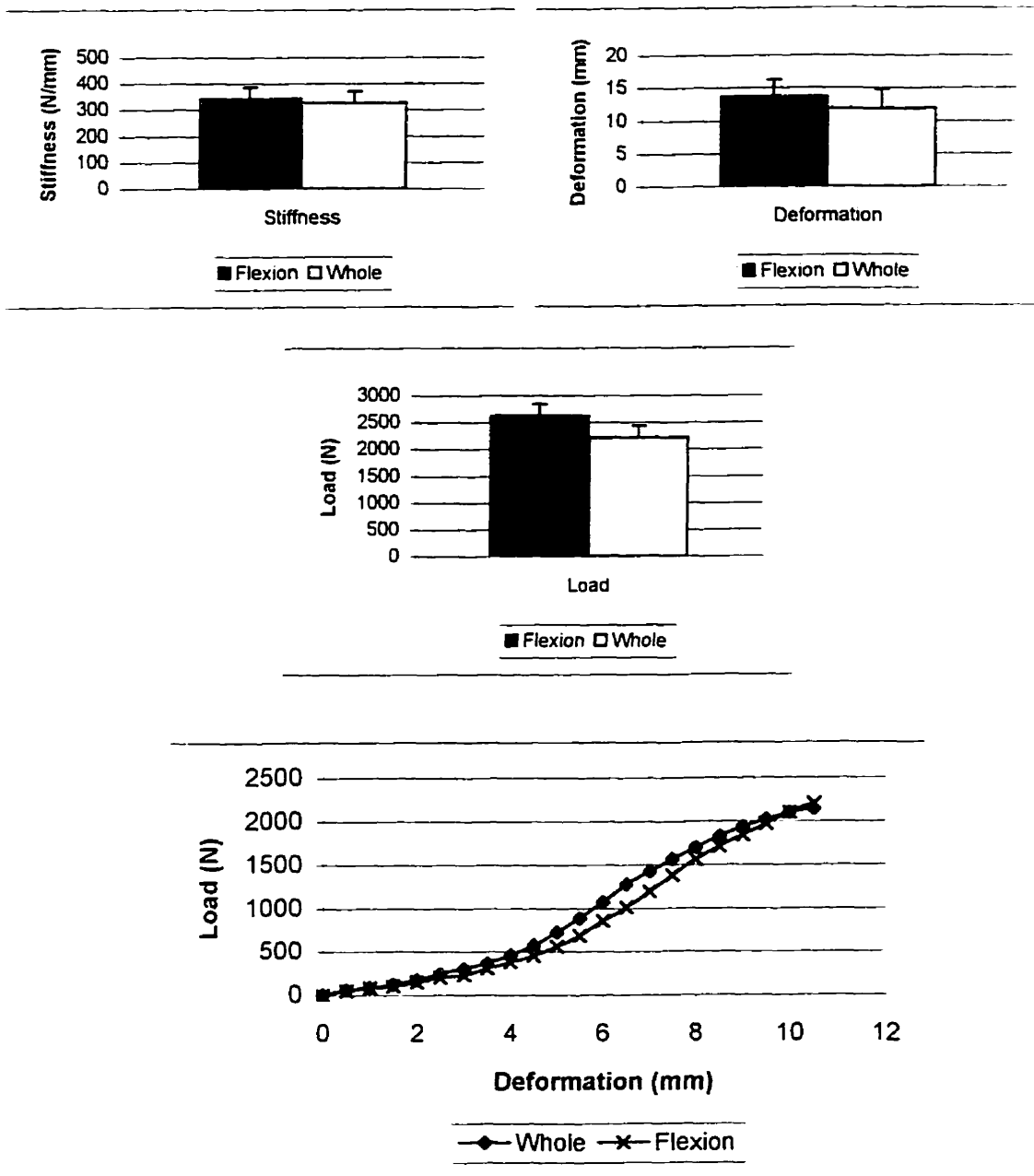
Figure 15: A comparison of the whole specimens with the specimens in a flexed posture. The barcharts illustrate the differences in the stiffness, the deformation at failure and the ultimate shear load at failure for the conditions (top). The load-deformation curve shows the differences in the shape of the response between the conditions (bottom).

119

Deformation
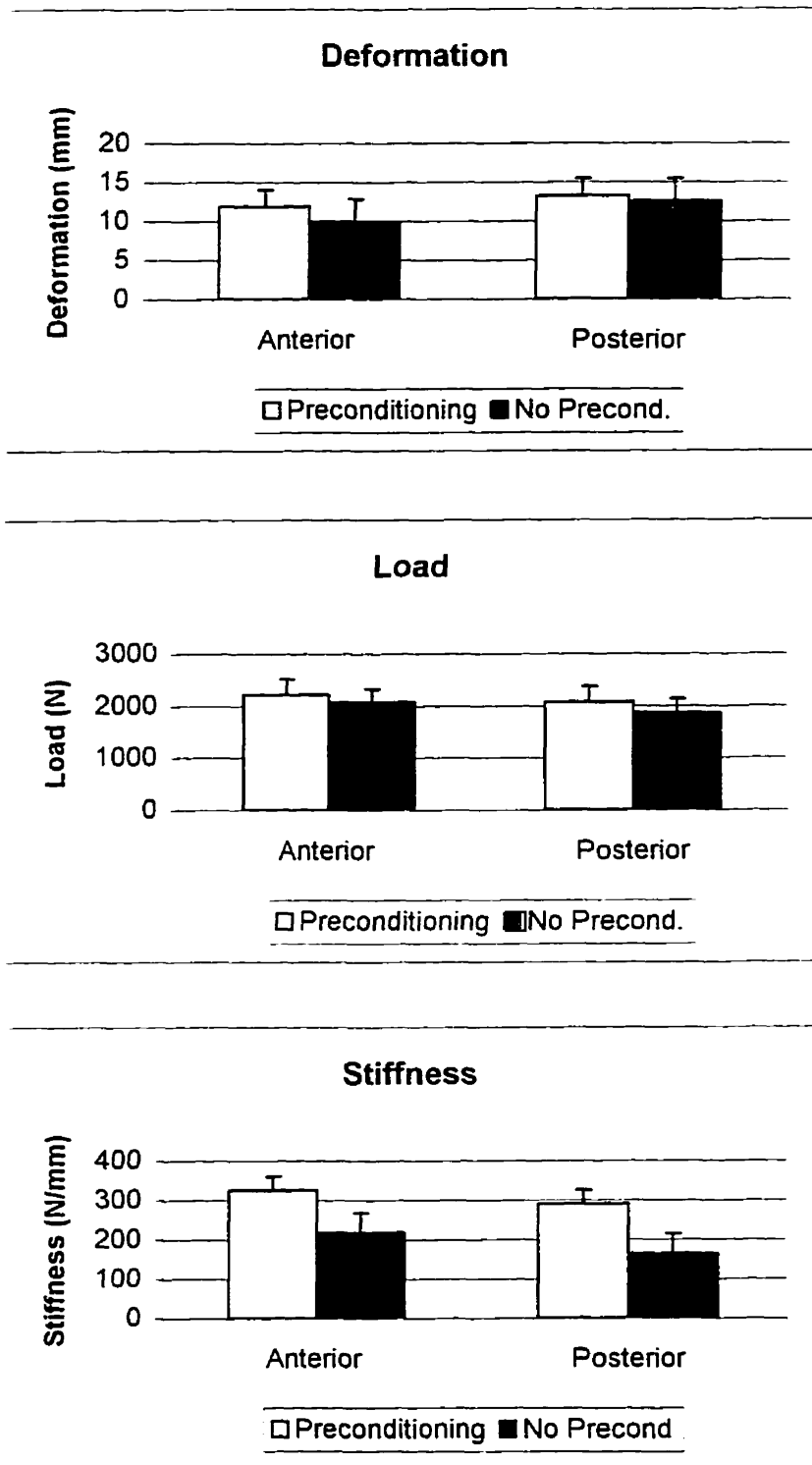
Load

Stiffness

Figure 16: Average values for the deformation at failure, the ultimate load at failure and the stiffness for specimens which were preconditioning with 5 cycles and specimens with no preconditioning.

Anterior Shear Loading

Whole Ant Precond — Slow Ant

Posterior Shear Loading

Slow Post — Whole Posterior Precond
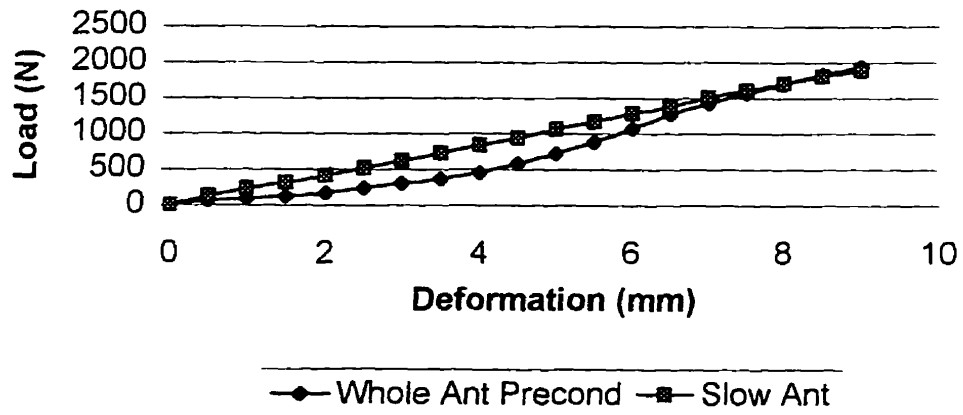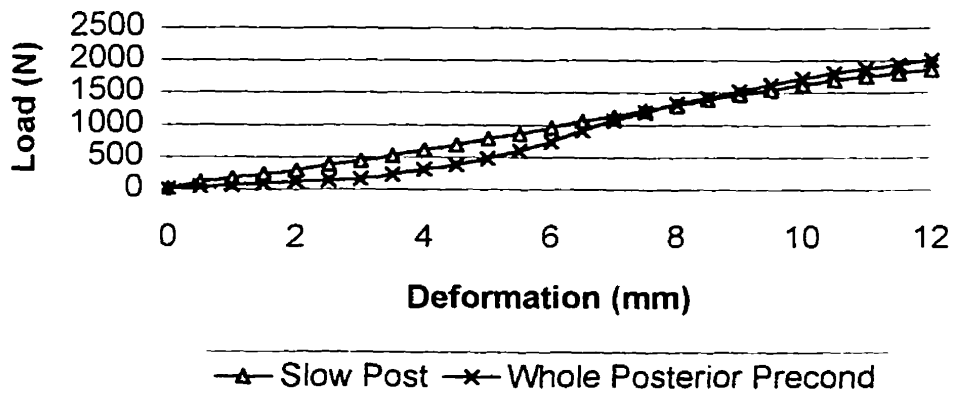
Figure 17: Average curves for anterior and posterior shear loading for preconditioned specimens and those without preconditioning. There was an increase in the toe-region and the average stiffness following preconditioning cycles.

6.3   Discussion

The facet joints were not the main shear load resisting structure as was hypothesized. The intervertebral disc resisted the majority of shear load, approximately 62.5% of the anterior load and 74% of the posterior load. This finding supports the results of Cripton et. al. (1995). 77% of the shear load was associated with the disc in their study. These results are in opposition to Farfan, which associated the majority of an applied shear load to the facets. The testing protocols may have an influence on the results. The testing jig as well as preconditioning of the specimens may also affect the results.

The specific hypotheses pertaining to stiffness and deformation were partially supported. For anterior shear loading the stiffness was minimized by the removal of the facet joints, however, the deformation was not significantly lower than the intact specimens. Under posterior shear loading, the deformation appears to be lower after the posterior elements are removed and the stiffness values were not significantly lowered.

Preconditioning cycles applied to the specimens prior to destructive testing appear to have introduced a neutral zone to the specimen, as well as increase the stiffness during the linear portion of the load-deformation curve. Previous studies have reported that there was no neutral zone in shear loading, however, preconditioning cycles were not applied to these specimens (Cripton, Berleman, Visarius, Begeman, Nolte, & Prasad. 1995). A toe region was introduced which delayed the increase in the stiffness until approximately 4 mm of deformation. This phenomenon appears to be due to the viscoelastic properties of biological

122

tissues. The current thought is that soft tissue undergoes a residual viscous flow during early testing or that certain components rupture and are not available for future cycles (Butler, Noyes, & Grood. 1978). All three variables increased following the five preconditioning cycles (Figure 16), however, the main differences were the emergence of the toe region and the increase in the stiffness in the linear region (Figure 17).

The posterior ligaments even under posterior shear loading were found to have minimal effect in resisting shear loads (Figure 12). The result may be due to the laxity in the ligaments due to the compressive preload (300 N) on the motion segment during testing. The collagenous fibers in the ligament may not have sustained enough translation to surpass the toe region of the ligament to attain an increase in the load bearing capacity of the ligament. The role of the interspinous ligament has been suggested to be a collateral ligament which guides the motion of the spine. however, it is not load bearing until extreme flexion or shear loading. Cripton et. al. (1995) reported posterior ligament damage resulting from shear loading tests. however. the testing situation was unconstrained which allowed sagittal rotation of the motion segment when the facet faces contacted one another. The lumbar spine in-vivo is partially constrained due to the weight of the upper body and the muscles surrounding the spine, therefore this injury may not be seen in-vivo. As well, there was no preload applied prior to testing which may have allowed a load on the posterior ligament which would not be evident during the in-vivo preloaded state. These results supply further evidence that the posterior ligaments' function is to limit the flexion of the motion segment.

The results of the sectioned testing reveal insights into the functioning of the structures making up the motion segment under loading situations not including impact situations. First,

the intervertebral disc appears to be the primary load bearing structure during both anterior and posterior shear translations. Second, the pars interarticularis adds to the stiffness of the disc under anterior loading but is not a primary load bearing structure. Third, the capsular ligaments are able to bear some of the transferred load of the disc at its maximal deformation to increase the deformation under posterior translation before failure.

The deformation at failure after the posterior elements were removed for both posterior and anterior loading was expected to increase. However, the deformation remained constant under anterior loading and decreased under posterior loading following the removal of the posterior elements. McGlashen et. al. (1987) found a 1.66 fold increase in anterior shear translation after the posterior elements were removed. This study involved static testing and the measurements were taken 60 s after the load was applied. The dynamic loading effects on the stiffness of tissue and the effect of creep due to the 60 s lag in recording the measurements may explain their increase in translation. The structures resisting shear translations are viscoelastic so they do increase their stiffness under dynamic loading. The intervertebral disc under dynamic conditions fails at similar deformations under both anterior and posterior shear loading.

The disc was found to be the primary shear load resisting structure. The maximum deformation for both anterior and posterior translation was approximately 10 mm with a maximum load of 1385 N for anterior loading and 1537 N for posterior loading. The stiffness values also support the isotropy of the disc in the coronal plane, with an average value of 236.5 N/mm for anterior loading and 249.2 N/mm for posterior loading. Although the mechanical properties of the disc were isotropic in the anterior-posterior shear plane; the structure of the

124

disc is anisotropic. The outer fibers of the annulus are directly connected to the vertebral body and it is these fibers which are responsible for resisting shear loading. The lateral fibers of the annulus are similar in number of layers and in thickness of fiber, but the anterior and posterior fibers differ. The posterior section of the disc has fewer layers and thinner fibers. It is important to consider that although the intervertebral disc may be able to resist the majority of applied shear loads, the posterior elements may resist a portion of the load in order to protect the intervertebral disc from injury.

Cripton et. al. (1995) showed that during an applied shear test while intervertebral disc pressure was measured there was an increase in disc pressure only after failure in the facet joints. The injured structure was retested and the intervertebral disc was able to resist 77% of the applied load. This series of tests suggests that although the intervertebral disc is capable of sustaining a majority of the shear load, it may only do so after an injury to the posterior elements.

The pars interarticularis was not found to be the primary shear load resisting structure. The pars was only responsible for approximately 35% of the load during shear loading at 100 N/s. The pars does not increase the deformation to failure of the motion segment, but it does increase the stiffness by 27% and the ultimate load at failure by 37%. The pars increases the stiffness of the motion segment after the facet faces make contact and initiate a bending moment on the pars. The lag in the stiffness is due to any space between the facet faces and to the articular cartilage which must be compressed. The stiffness of the pars was added to the motion segment after approximately 4mm of translation.

The pars interarticularis may be able to sustain a larger load. One study found the pars

able to sustain up to 2000 N and deflect 8-10 mm before failure (Troup. 1976) at deformation rates of .5mm/sec. The pars may decrease the injury sustained by the disc by withstanding more load at later deformations of the motion segment or possibly by sustaining more load during the entire loading cycle.

The pars and the disc were modelled to illustrate the response of the motion segment to an applied anterior shear load. The disc was modelled as a 2nd order polynomial curve. The pars was separated into an initial toe region and a linear stiffness, the toe region was ignored due to its minimal affect on the overall response (Appendix A). The constant stiffness of the pars, 108 N/mm is added to the stiffness of the disc at 3.5 mm of deformation to create the whole segments load-deformation response to an anterior shear load. The response of the two component model compares well with the experimental response of whole segments (Figure 18).

Partitioning the anterior shear load in this manner requires two assumptions. The anterior and posterior longitudinal ligaments are included in the model of the intervertebral disc which negates their individual contributions to shear resistance. The pedicles were assumed to be rigid in order to identify the contribution of the pars. The pedicles have been found to sustain bending moments, however, the moments are considerably less than the moments in the pars.

The pars interarticularis is the only bony tissue resisting anterior translation and therefore the effect of load rate may increase the stiffness in the pars. The load rate effect was explored by increasing the linear stiffness of the pars which was added to the stiffness of the disc. An increase in the pars stiffness by 17% changed the partitioning between the disc and

126

the pars (Figure 19). At a deformation of 8 mm, the disc contributed 65% of the load of 1830

N, with the pars accounting for 35%. The load rate effect of the pars altered the partitioning of

the load between the disc and the pars and increased the overall load sustainable in the motion

segment.

Although the stiffness and the load at a constant deformation are increased with

increases in load rate, it is still uncertain if this is beneficial in avoiding shear injuries. The

effect of load rate alters the load sharing strategy of the motion segment structures. The

deformation at failure may remain constant but the severity of the injury sustained is increased

(McElhaney, Fogle, Byars, & Weaver. 1964). Evidence suggests that although the motion

segment deformation remains constant the deformation of the structures may vary. Testing on

the pars at higher deformation rates 50mm/sec resulted in a reduction of the deformation at

failure from 8-10 mm at .5mm/sec to 3-5mm at the higher load rate. Load rate may contribute

a beneficial margin of safety increase for tasks which apply minimal deformations to the

motion segment.

The flexion of the motion segment altered the mechanical response of the specimen

particularly the realignment of the pars. Flexion of the motion segments resulted in increases

in deformation at failure and the ultimate load at failure while the stiffness remained the same

as whole neutral specimens during anterior loading (Figure 15).

The contact between the facet faces is altered during flexion. An increase in the

distance between the facet faces as well as an increase in the moment arm between the center

of rotation of the pars and the application of force occurred. The change in facet face

orientation was determined using coordinates from Cholewicki and McGill (1995) (Appendix

127

B). The L4 coordinates were flexed through a range from 0-10 degrees and the facet face position was determined. The moment arm increased 5 mm and the distance between the facet faces increased by only 0.4 mm (Figure 20). The alteration of the vertebrae orientation may affect the motion segments response to shear loading. The increase in the toe region may be attributed to the the slight increase facet face difference. As well, the overall increase in deformation of the motion segment may be due to the increase in moment arm of the pars and thus an increase in the deflection of the pars (Appendix B).
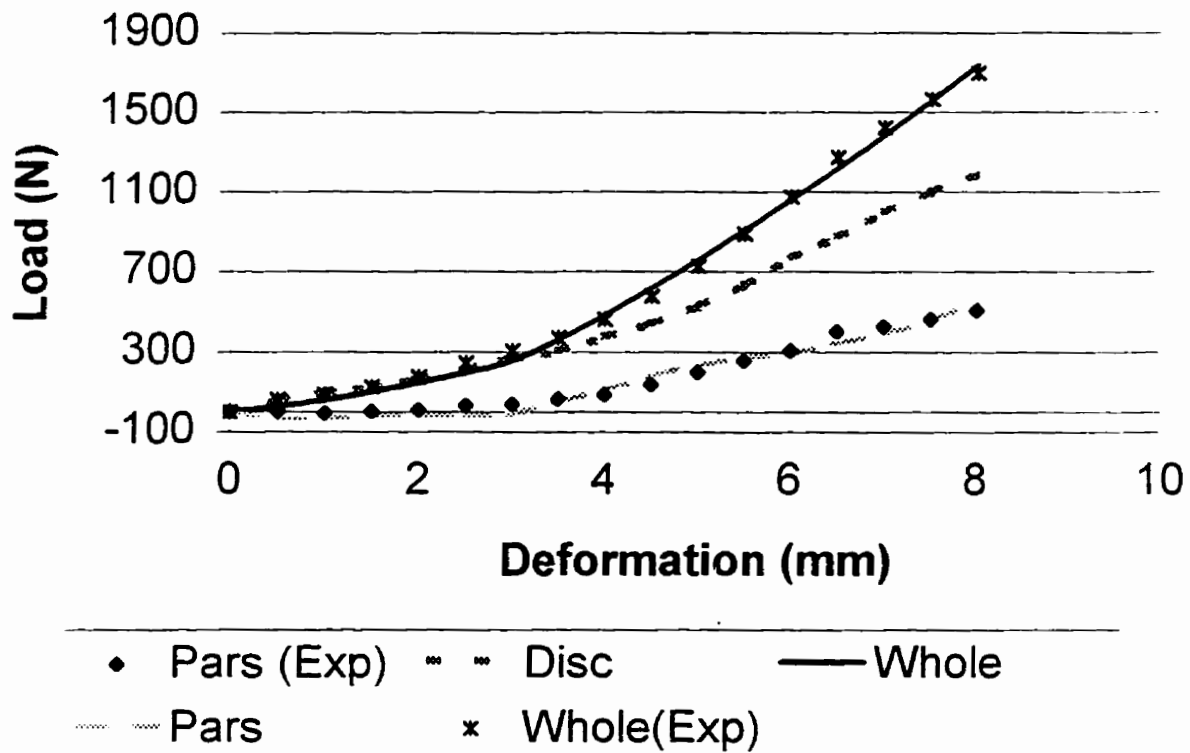
Figure 18: Model for anterior shear loading partitioned between the intervertebral
disc and the pars interarticularis. Comparison of modelled curves with the
experimental data. Pars(Exp) is the data from subtracting the isolated disc data
from the whole experimental data. Disc is the equation expressing the isolated disc data.
Whole is the equation expressing the experimental data. Pars is the equation for the
linear stiffness portion of the pars data. Whole(Exp) is the experimental data from
intact specimens.

129

Pars Stiffness of 108 N/mm

17 % Increase in Pars Stiffness
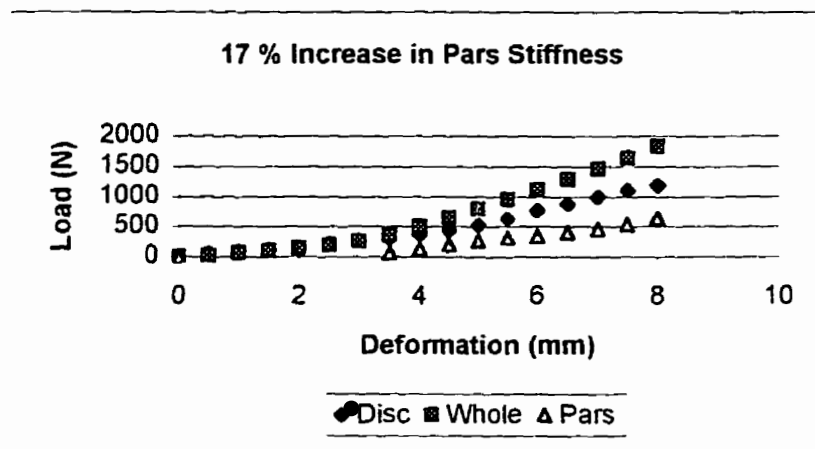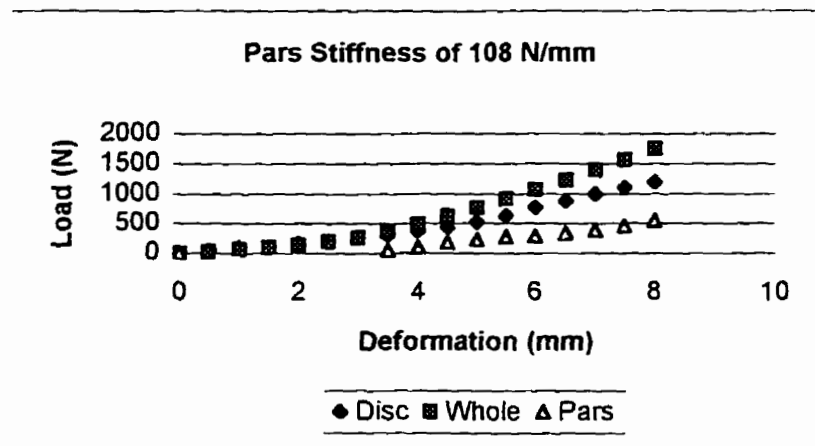
Figure 19: Load sharing differences resulting from a 17 % increase in pars stiffness due to an increase in load rate for 100 N/s to 10810 N/s for anterior shear loading.
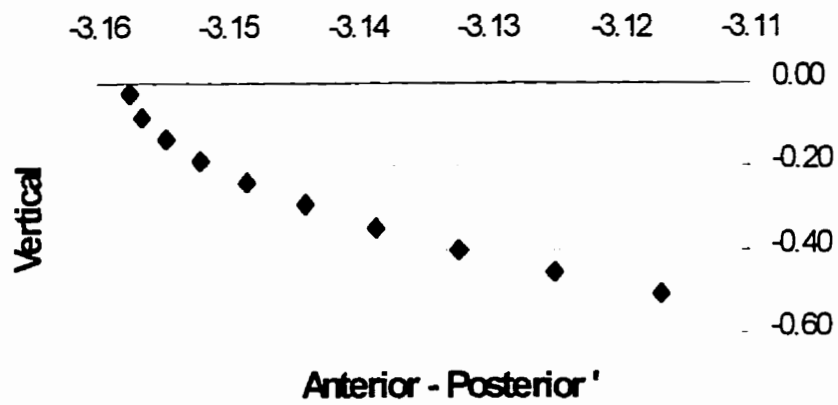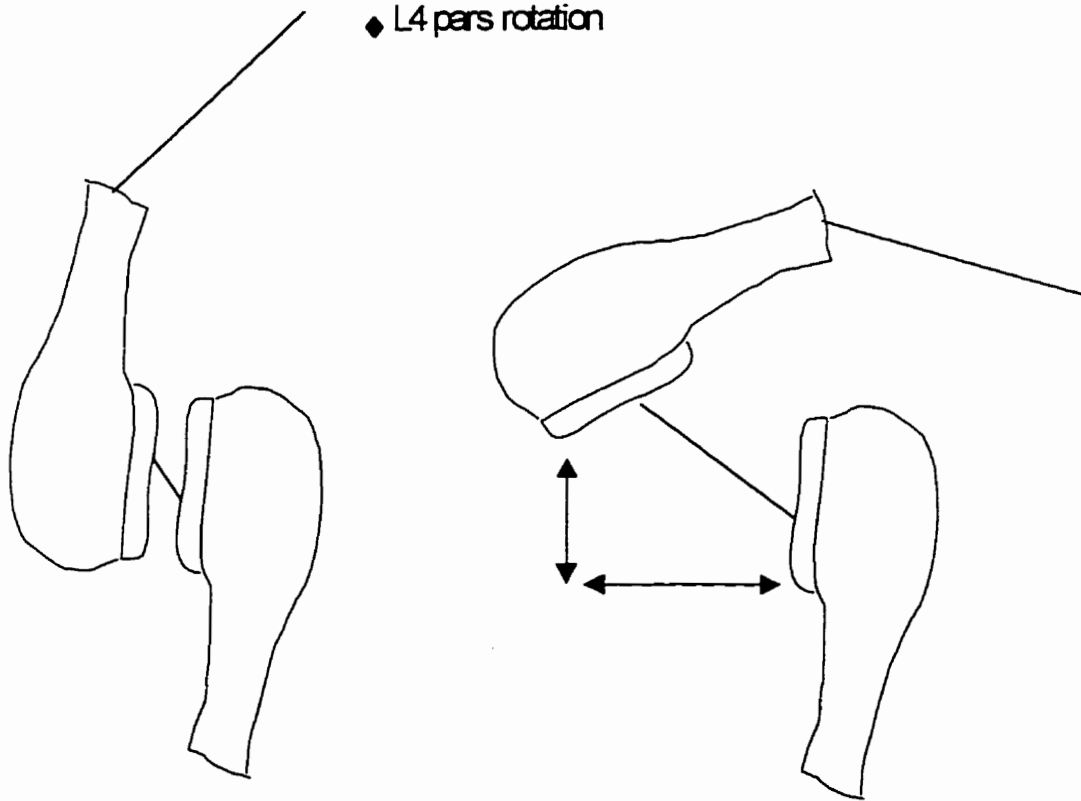
Figure 20: An illustration of the relative movement of the facet faces during a rotation of 10 degrees. The vertical distance increased by 5 mm and the anterior-posterior distance increased by .4 mm. (The schematic diagram is not to scale.)

Under posterior shear loading the capsular ligament and the pars do not increase the stiffness of the motion segment but they may be involved in load sharing with the intervertebral disc. The disc under posterior shear loading accounts for 85% of the load with the capsular ligaments and pars resisting the remainder. However, there is an increase in the deformation at failure when the posterior element is intact. The increase in deformation accompanies a 25% increase in the ultimate load at failure. The intervertebral disc alone fails at 10 mm of deformation and approximately 1500 N of load. After 10 mm of deformation the disc would be expected to level off or see a decrease in its load carrying capacity. The capsular ligaments and the pars sustain the load needed during the increase in deformation to failure (Figure 11, bottom). The increase in deformation is achieved thorough the extension of the ligaments and by deflection of the pars.

The increase in deformation and load in the intact motion segment could also be a result of the capsular ligaments and the pars relieving the disc of some of the load during the entire loading cycle. The disc would then be carrying less load for each deformation than was observed on the tests with the whole disc alone, which would allow the segment to sustain a larger deformation and achieve a higher ultimate load without compromising the disc.

In summary, the intervertebral disc sustained the majority of both anterior and posterior applied shear loading. However, the posterior elements alter the functioning of the disc. The pars interarticularis increases the stiffness and ultimate load to failure of the motion segment. The capsular ligaments and pars interarticularis increase the deformation at failure of the intact motion segment. These structures may lessen to load on the disc which allows the deformation to increase without injury to the disc.

132

Key Findings

1. The intervertebral disc accounts for the majority of stiffness during anterior and posterior shear loading.

2. The intervertebral disc has a similar response for anterior and posterior shear loading.

3. The pars interarticularis accounts for the increase in stiffness during anterior loading compared with posterior loading.

4. The pars interarticularis and the capsular ligaments may share the load of the disc after 10 mm deformation or may relieve the load on the disc during the entire loading cycle.

5. The distance between the facet faces increases with flexion.

6. The moment arm of the pars interarticularis increases with flexion.

7. Preconditioning cycles prior to testing increase the stiffness in motion segment.

Chapter Seven

Documentation of Specific Injuries

from Shear Loading

In order to prevent injury to the lumbar spine, the etiology of injury must first be understood. By purposefully injuring the motion segments one can begin to understand the progression of injury and combined with the mechanical understanding of the motion segment, the mechanisms of injury can be identified.

7.0 Clinical Injuries

Spondylolisthesis, disc degeneration and facet injury have been linked with shear loading (Troup. 1976; Taillard. 1976; Hutton, Stott, & Cyron. 1977). Few studies have isolated shear loading to recreate these injuries. The majority of the information concerning injuries from applied shear loads are epidemiological in nature and contain many confounding variables. The common belief, that a connection exists between shear loading and injury, motivates further research to clarify injury mechanisms under isolated shear loading.

7.0.1   Spondylolisthesis

Spondylolisthesis, predominately occurring in the lumbar spine, is the translation of the

body of the superior vertebra on its adjacent inferior vertebra (Cailliet. 1995). This translation

is considered to result from mechanical loading, yet the nature of the load is not fully

understood (Kelsey & White. 1980). The literature on congenital and degenerative

spondylolisthesis indicates that repetitive shear stress on the facets and pars interarticularis may

be a contributing factor to the onset and progression of this injury (O'Neil & Micheli. 1989;

Troup. 1976; Wiltse, Windell, & Jackson. 1975).

Spondylolisthesis is classified into five categories as follows:

Type I (Isthmic):

Adolescents are typically diagnosed with this common form of spondylolisthesis. An

anatomic defect is discovered in the pars interarticularis conceivably resulting from falls early

in life often connected with the toddler phase. This defect in the pars is weakened by repetitive

loading and spondylolisthesis may not be detected for some years (Cailliet. 1995).

Type II (Congenital):

A structural inadequacy, congenital or acquired, typically at the L4, L5 and S1 level of

the lumbar spine is a precursor to the translation of the vertebra in this frequently occurring

type of spondylolisthesis.

Type III (Degenerative):

This type is a frequently occurring condition with 72.5% of the cases occurring in women and 27.5% in men (Newman. 1963). Cases of degenerative spondylolisthesis are usually detected in individuals over 40 years. Repetitive loading may be the mechanical etiology, beginning with a soft tissue lesion followed by facet damage. eventually resulting in slipping of the superior vertebrae (Neugebauer. 1976). The interspinous and supraspinous ligaments may be the site of the soft tissue lesion which precedes degenerative spondylolisthesis. This assertion is supported by the work of Rissanen (1960) which indicated that ruptures in these ligaments (interspinous and supraspinous) are common in persons over 40 years of age.

Type IV (Pathological):

A rare occurrence often arising from a disease. resulting in bone insufficiency. weakening the pars interarticularis and the facets.

Type V (Traumatic):

This form of Spondylolisthesis rarely occurs. A trauma to the facet and/or pars interarticularis results from a sudden large anterior shear force. The shear load resisted by the facet joints results in a bending stress on the pars. Failure in the pars interarticularis precipitates spondylolisthesis.

In-vitro studies have attempted to recreate the injuries associated with

136

spondylolisthesis. a study conducted by Cyron et. al. (1976) examined the resistance of the

vertebral body to loads applied to the facets. A force was applied to the inferior articular facets

of 44 human lumbar vertebrae free of bone disease (26-75 yrs of age) to produce a bending

moment across the pars interarticularis. Fractures, similar to those found in spondylolisthesis.

occurred after a load between 2000-2800 N was applied to the inferior facet at load rates of

0.05 cm/s and 5.0 cm/s. Displacements of the pars ranged from 0.3 cm to 1.21 cm which may

be sufficient to transfer the shear resistance burden to the intervertebral disc even before failure

of the pars develops. These results may have been affected by the storage methods of the

specimens which was a combination of freezing at -20°C for 3 specimens and storage in 10%

formaldehyde in saline for the remaining specimens; the effect of storage methods on the

mechanical properties of tissue remains controversial (Callaghan & McGill. 1995).

7.0.2 Disc Degeneration and Facet Injury

The mechanics of the intervertebral disc and facet joints are closely coupled; an injury

in one structure contributes to the injury of the other structures. Disc degeneration may lead to

misalignment and increased loading on the facet joints, however. damage to the facet joints

will increase the shearing translation of the intervertebral disc leading to disc degeneration

(Kirkaldy-Willis. 1988). A link has been established between osteoarthritis of the facet joints

and osteophytic lipping of the vertebra, common in degenerative disc disease (Lewin, 1964).

The degenerative process of the intervertebral disc and the two facet joints is a

progressive disease which may initiate from a trauma or repeated loading to one of the three structures. Kirkaldy-Willis (1988) modelled the degenerative process into three phases, dysfunction, unstable phase and stabilization. Dysfunction is the interruption of normal function by an injury to either the facet joints or the intervertebral disc. The unstable phase is indicated by an increase in the movement of the motion segment. During this phase, the disc suffers a loss of fluid which results in the narrowing of the disc space. Narrowing of the space between the discs of the spine affects the alignment and the peak pressure (Dunlop, Adams, & Hutton, 1984) of the facet joints. The increase in the compressive force on the face of the facet joints may initiate the osteoarthritis process, a common disorder of synovial joints. Stabilization is marked by fibrosis in both the facet and intervertebral joints, increasing the stiffness and stability of the motion segment. Osteophytes on the rim of the vertebrae and fibrosis around the facet joints also increase the stiffness of the motion segment.

Shear loading may be a source of injury to the facet joints and intervertebral disc when the equilibrium among the three structures is altered. An applied shear load on the motion segment is resisted by both the disc and the facet joints. A gradual eroding or a traumatic injury of the facet joints will cause a laxity in the joints which in turn increases the proportion of applied shear load which the intervertebral disc must resist. The redistribution of load resistance may initiate the degenerative process described above.

The purpose of this section was to identify the injuries resulting from the previously described mechanical tests, including the directional test, the load rate test and the sectional test.

Global Hypothesis: Injuries resulting from anterior shear loading will be primarily pars interarticularis fractures, as opposed to predominately disc injuries resulting from posterior shear loading.

7.1   Specific Protocol

After the motion segments were loaded to failure, injuries were identified through a combination of dissection techniques and radiography. Primarily, planar X-ray is used in clinical settings to detect injury, however, a recent study discovered many injuries found during surgery were not detected on X-ray (Jonsson, Cesarini, sahlstedt & Rausching, 1994). X-ray techniques including slicing the specimens to obtain a clearer view of the injured structure were used in this study as well as a specially designed jig which was able to place a load and a bending moment on the specimen to help reveal all injuries. The specific settings for the Mercury Modular X-ray unit (Raymax of Canada) are as follows: Whole specimen 64 kvp at 5 mas; Sectioned specimen 60 kvp at 4-5 mas. The specimens were also dissected to locate injuries and finally boiled to remove all soft tissue to gain a better view of the bony structures. The combination of X-ray techniques and dissection proved to be capable of finding injuries in each specimen.

7.2   Results

The injuries documented for anterior and posterior shear loading differed by both direction and load rate (Figure 1). Anterior shear loading at 100 N/s resulted in a majority of pars interarticularis fractures mainly single fractures compared to bilateral fractures. These fractures were either complete or partial fractures of the pars (Figure 2 & 3). Anterior loading also resulted in endplate avulsions, which is the tearing of the cartilaginous endplate from the cancellous vertebral body (Figure 4 & 5). Posterior loading at 100 N/s resulted in solely endplate avulsions (Figure 1).

The vertebral motion segments are comprised of viscoelastic structures whose mechanical properties are affected by load rate and consequently the injuries at failure also differed with increases in shear load rate. At higher anterior load rates (10810 N/s) endplate avulsions accompanied all the pars injuries in the motion segments. The appearance of bilateral fractures increased in occurrence at the faster anterior loading rate (Figure 1). At an increased posterior loading rate, an edge fracture appeared (Figure 6).

The injuries resulting from the whole specimens from the sectioning tests were similar to the previous injuries, a combination of pars fractures and endplate avulsions during anterior loading and endplate avulsions during posterior loading (Figure 7). Flexion of the motion segments before shear loading did not significantly change the type of injuries detected, they were similar to both whole (W) specimens and those with their posterior ligaments severed. After the severing of the posterior ligaments and the facet joints, the injuries were all endplate

avulsions. The majority of endplate avulsions included the lateral fibers either in isolation of in conjunction with the anterior or posterior fibers. Posterior loading resulted in some facet face avulsions of the capsular ligaments.
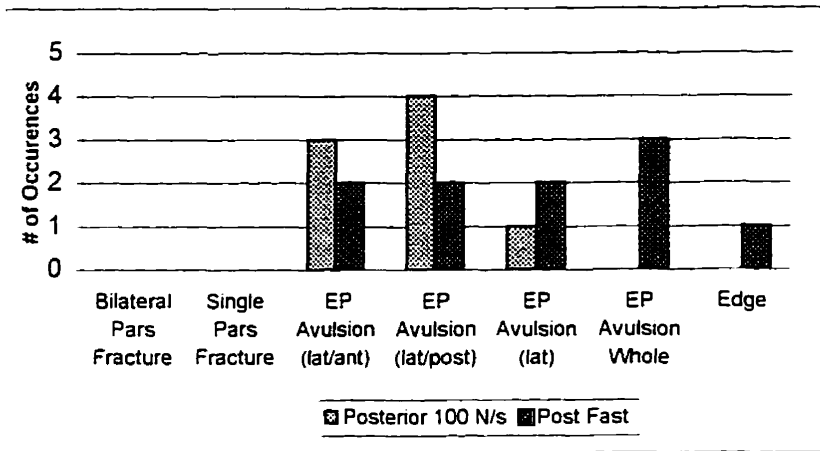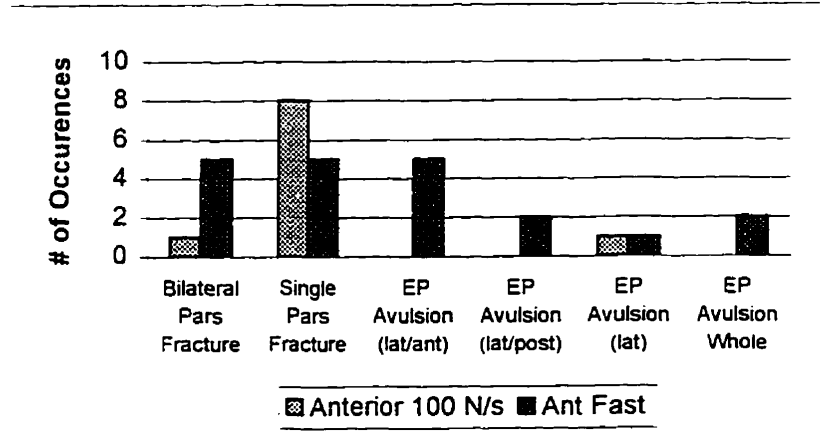
Figure 1 : The number of occurences of bilateral pars fractures, single pars fractures and endplate avulsions for anterior and posterior shear loading at slow (100N/s) and fast (post:9454 N/s, ant: 10810 N/s).

Figure 2: A sliced specimen with a bilateral pars fracture and an endplate avulsion. The pars fracture results from the bending moment placed on the pars. the fracture begins on the inner surface of the pars where a tensile load is placed on the bone. The endplate avulsion results from the tensile load on the annular fibers.

Figure 3: An X-ray revealing a pars fracture and an endplate avulsion.

144

Figure 4: A rearview of a specimen with an endplate avulsion in the posterior lateral region of the annulus. The avulsion results from the tensile load in the annular fibers which is greater than the fiber-bone attachment site.
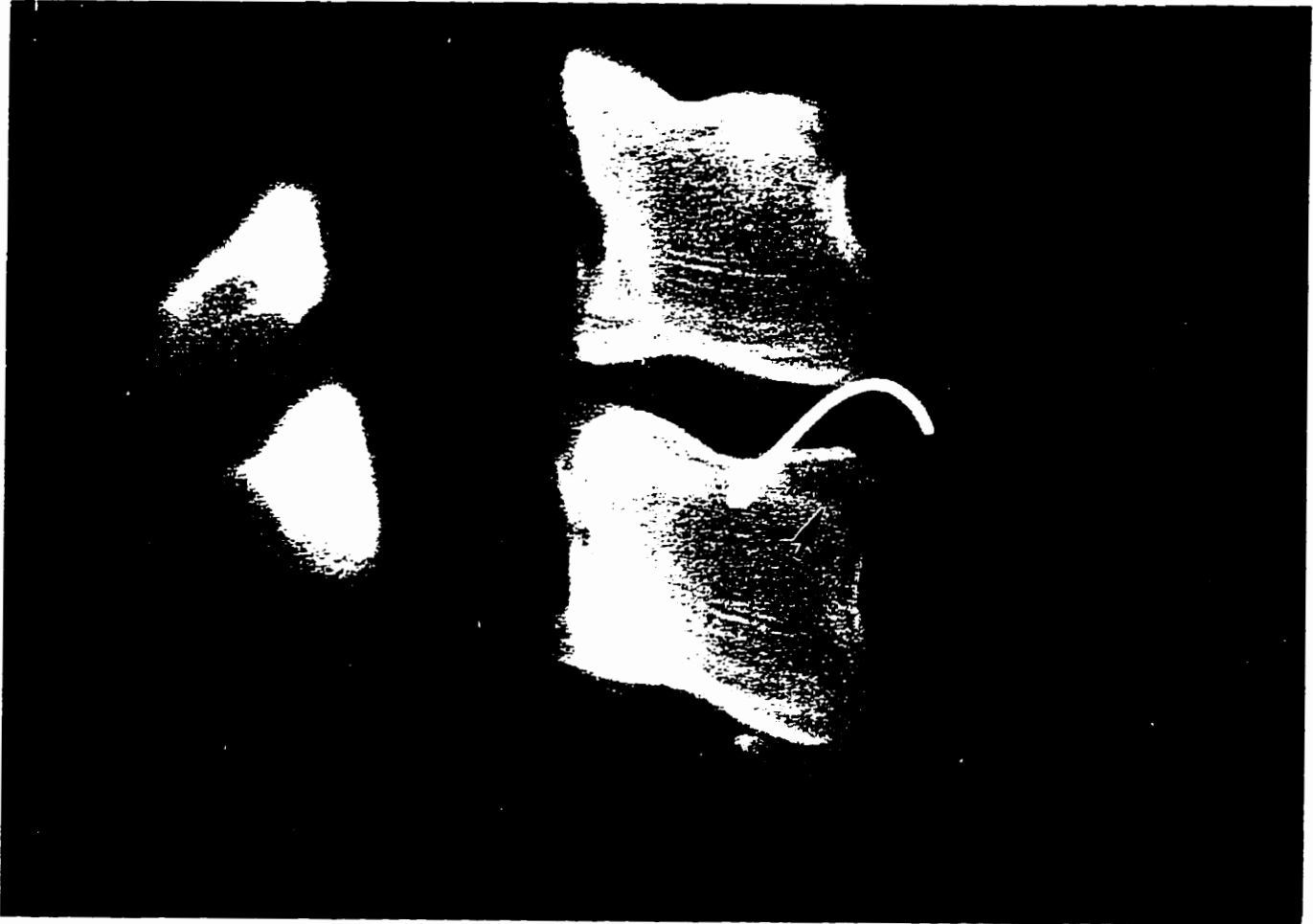
Figure 5: A sagittal view X-ray of an anterior endplate avulsion.
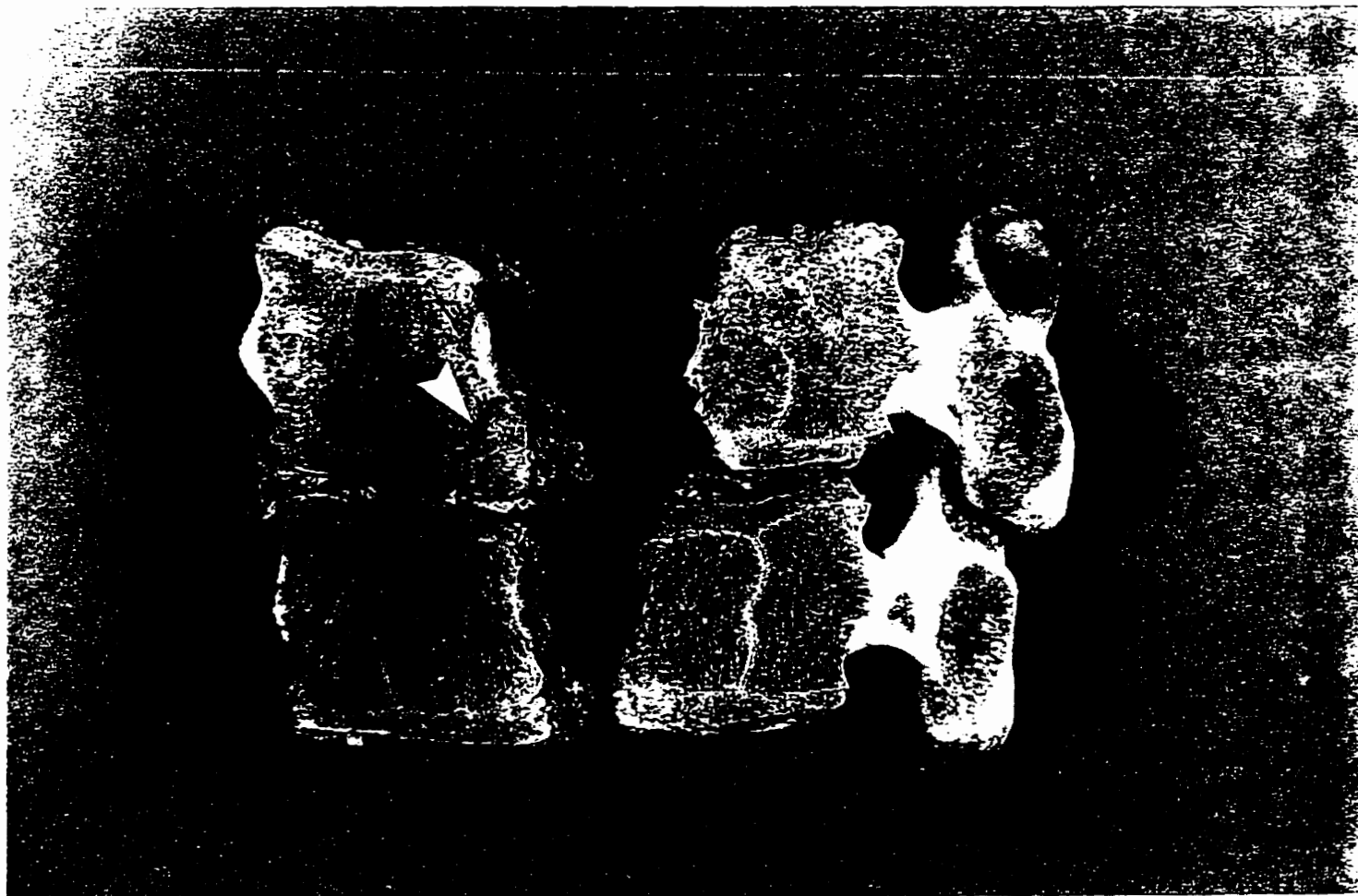
Figure 6: A sagittal view of an edge fracture. A center slice of the specimen shows the

edge fracture on the posterior edge of the inferior vertebra (right).

Anterior Shear Loading

Pars □ Annular avulsion ⧄ Endplate off

Posterior Shear Loading

■ Pars ⊠ Facet Avulsion □ Annular Avulsion ⧄ Endplate off
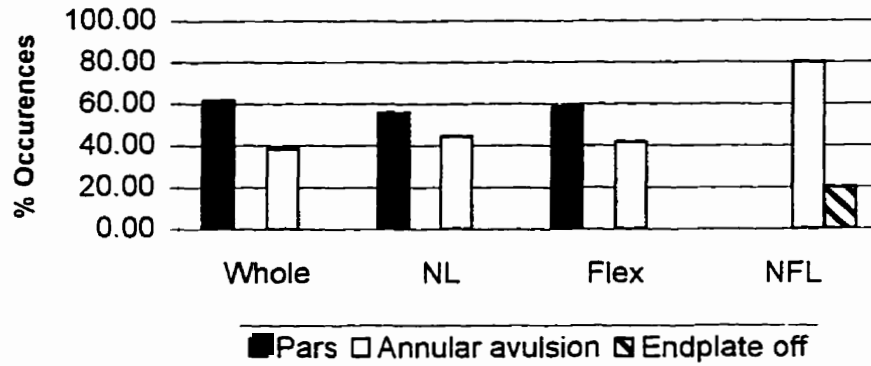
Figure 7: Injuries resulting form the sectioned testing, whole (W), specimens with the posterior ligaments severed (NL), specimens with the posterior ligaments and the facet joints severed (NFL) and flexed specimens (F) under anterior and posterior loading.
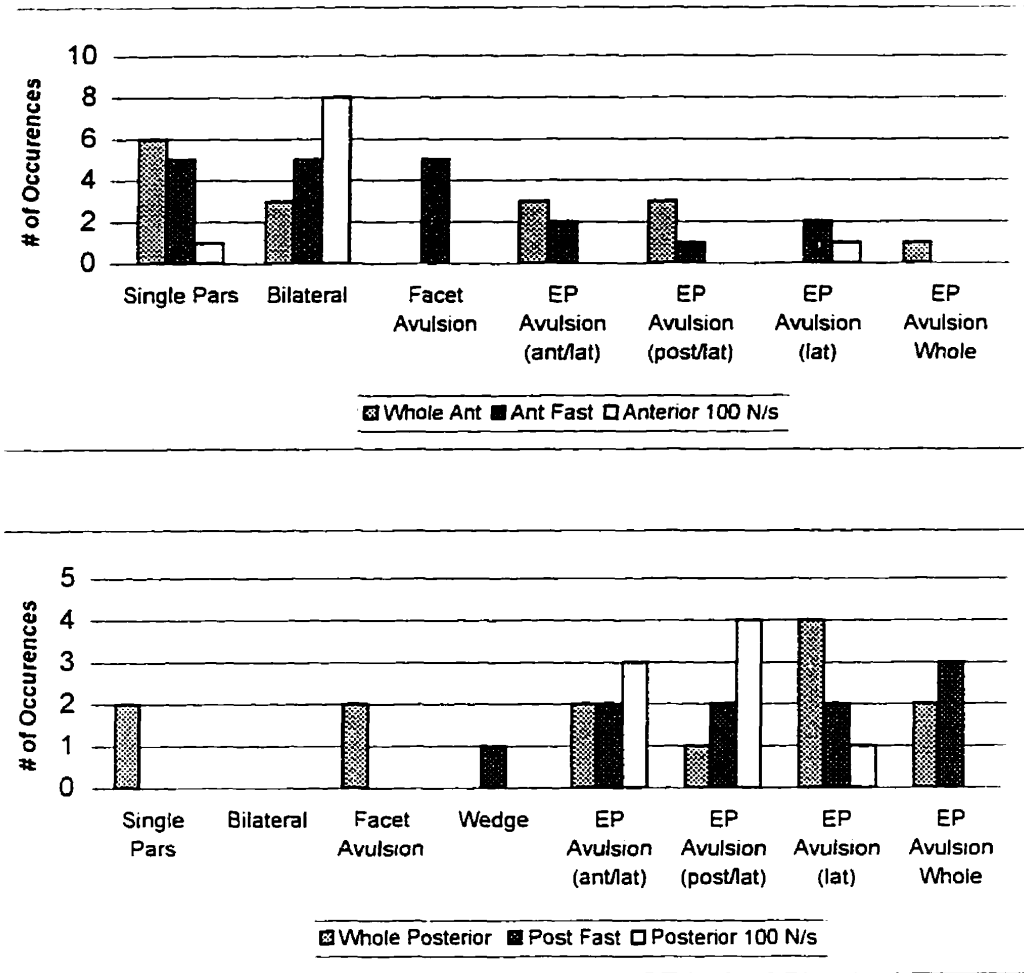
Figure 8: Injuries resulting from preconditioning cycles. A comparison of the injuries which result after preconditioning cycles and those from high load rates and from low load rates. The injuries after preconditioning and at high load rates are similar.

7.4   Discussion

The hypothesis was supported since the majority of pars fractures occurred as a result

of anterior shear loading. Posterior shear loading resulted in predominately endplate avulsion

injuries.

Understanding mechanisms of injury is a complex task since the failure point may vary

as a function of the magnitude of load, the direction of loading and/or the rate of loading. The

injuries found on porcine specimens were located in the same structures as injuries found on

human vertebrae. The resulting pars interarticularis injury from anterior shear loading is a

fracture originating at the posterior facing aspect of the superior facet below the facet face and

on the anterior portion of the inferior facet above the facet face (Cyron, Hutton, & Troup.

1976). A segmental analysis of the pars interarticularis found two dense layers of cortical bone

on the anterior face of the inferior process to the inferior border of the pedicle and on the

posterior portion of the superior process extending into the lamina (Krenz & Troup. 1973).

Cortical bone which is stronger than cancellous bone is hypothesized to be in portions of the

pars which are subject to tensile stress from bending moments placed on the pars

interarticularis and pedicle. Previously it was thought that genetic factors predisposed

individuals to pars defects which resulted in fractures (Krenz & Troup. 1973), however,

mechanical factors are currently associated with fractures of the pars interarticularis. An

applied shear load to the intervertebral joint introduces a bending moment on the pars

interarticularis and the pedicles resulting in failure. The moment about the pedicles is less than

about the pars interarticularis. Results of one study (Cyron, Hutton, & Troup. 1976) found 1/3

as many fractures across the pedicles than in the pars during in-vitro testing.

Pars injuries are not only found in-vitro, injuries have been found in-vivo on cricket bowlers. The study of 22 bowlers resulted in 6 bilateral and 6 unilateral pars defects being detected (Hardcastle, Annear, Foster, Chakera, McCormick, Khangure & Burnett. 1992). Injuries found in-vivo in clinical assessments of Spondylolisthesis patients also suggest injuries of the pars interarticularis (Newman. 1963; Grobler, Novotny, Wilder, Frymoyer, & Pope. 1994). As well, a study of skeletons from Alaskan natives verified that every second skeleton showed one or more defective neural arches. The defects were considered defects of the neural arch but did not specify whether they were defects to the pedicle or to the pars interarticularis. The fracture in the pars interarticularis is difficult to detect using radiographs unless the fracture is a massive injury since the fracture is typically not through the entire thickness of the pars interarticularis.

Porcine in-vitro shear testing also resulted in endplate avulsions. This injury occurs when the load on the annular fibers connected with the endplate exceeds the force connecting the endplate to the vertebral body. Cripton et. al. (1995) also reported avulsion injuries on human vertebrae after in-vitro testing.

The viscoelastic nature of the motion segment affected the mode of injury of the motion segment. There was a shift in the injury type to include endplate avulsion injuries and bilateral facet fractures under faster anterior load rates. Under anterior loading the deformation to failure did not change between the load rate conditions, however, there was an increase in stiffness and thus a slight increase in ultimate load at failure. The increase in stiffness in the peripheral fibers of the annulus was greater than the strength at the bone-fiber insertion point.

151

This suggests that the failure point defined in the current studies may be triggered due to deformation, yet, the tissues have absorbed more energy which must be released. which results in more severe failures. Although a large mechanical effect was not seen under posterior loading at a higher load rate. edge failures and whole endplate avulsions occurred.

Preconditioning cycles prior to testing appeared to have the same effect on injury as an increase in loading rate for anterior shear loading (Figure 8) . The prevalence of endplate avulvions with pars fractures was apparent. As well, bony failures resulted after preconditioning in the posterior shear tests. The load sharing between the intervertebral disc and the pars may have shifted towards less load being carried by the pars as opposed to during testing conditions prior to preconditioning of the specimens.

The injuries seen in the endplate were in three main categories: anterior and lateral. posterior and lateral or lateral (Figure 6). Anterior or posterior avulsions in isolation were not detected. This suggests that the initiation of the endplate avulsions are in the lateral region. This can be supported using an elliptical model of the annulus which illustrates an increase in deformation in the lateral regions of the annulus (Appendix C). A larger deformation in the neutral posture as well as during translation suggest that these fibers may be resisting more of the shear load than the anterior and posterior regions. The layers of the annulus are constructed of layers of fibers which change their angle every layer (Bogduk & Twomey. 1991; Tsuji, Hirano. Ohshima, Ishihara, Terahata. & Motoe. 1993). At the lateral portions of the annulus, the angle restricts the contributions of the fibers aligned against the translation. However, the number of layers in this area of the annulus are more abundant than in the anterior and posterior regions and the thickness of the fibers is greater (Marchand & Ahmed. 1990; Tsuji,

Hirano, Ohshima. Ishihara, Terahata. & Motoe. 1993). The increase in fibers and thickness

seems to be needed considering that during small translations only a portion of the fibers are

aligned optimally to resist shear loading. The fibers also appear to sustain more deformation in

this region.

It appears that the posterior elements attempt to protect the intervertebral disc from

injury. The injuries to the disc appear to follow pars failure. Intervertebral disc injuries are

always accompanied by facet fracture. However, during the low rate anterior testing. pars

fractures were detected without injury to the disc. The pars has been reported to sustain up to

2000 N before failure, the structure has the capacity to resist larger portion of an applied shear

load in order to avoid injury to the disc. A similar strategy exists for posterior loading. the

capsular ligaments and the pars share some of the applied shear load to increase the

deformation of the intact motion segment. Injuries were mainly identified in the disc however.

any injury to the capsular ligaments was difficult to identify.

The mechanical variable which seems to be associated with injury was the energy

absorbed at failure. The mechanical data from the load rate test suggest that deformation was

the predictor of injury, since it remained constant between the testing at a low load rate and at a

higher load rate. Yet, the injuries both from anterior and posterior loading differed between the

load rate conditions. Therefore, deformation cannot predict the severity of injury. Injuries

identified under anterior loading at 100 N/s consisted of mainly pars fractures, however, at a

higher load rate the endplate was also injured. Posterior loading at 100 N/s had mainly

endplate avulsions but at the higher load rate an edge fracture was identified. Stiffness was not

a predictor of the severity of injury since the stiffness value did not significantly increase for

posterior loading with an increase in load rate. There was an increase in ultimate shear load at failure for both anterior and posterior loading as well as an increase in the energy absorbed to failure with an increase in load rate. However, posterior and anterior loading resulted in similar ultimate load values during testing at 100 N/s while sustaining very different injuries. The energy values, on the other hand, were different between anterior and posterior loading which suggest this variables' association with injury identification.

Key Findings:

1. Both the pars interarticularis fractures and endplate avulsions occur at high rate anterior shear loading. There is also an increase in the occurrence of bilateral pars fractures.

2. The lateral region of the annulus may be the site of failure initiation.

Chapter Eight

Summary

8.0   Hypotheses Evaluation

In addressing the hypotheses and formulating conclusive statements, the use of porcine spines for the mechanical testing should be considered.

Hypothesis 1:

The ultimate shear load at failure will be higher under anterior shear loading than under posterior loading.

The hypothesis was rejected. Although the average stiffness was higher under anterior shear loading. the ultimate load at failure was similar for anterior and posterior shear loading. The tissue structures resisting anterior and posterior loads are different which may account for the difference in deformation at failure. Anterior shear loads are resisted by the bony pars which increases the stiffness of the motion segment by 30%. The stiffness of the motion segment under posterior shear loads is not increased by the posterior elements which are mainly soft tissue, the capsular ligaments and the posterior ligaments. The functioning of the motion segment was different for the resistance of anterior shear loads as opposed to posterior shear loads.

Hypothesis 2:

A flexed posture will sustain a lower ultimate shear load at failure compared with a neutral posture.

The hypothesis was rejected. The ultimate load to failure was higher under flexion and the stiffness remained the same. During flexion the facet faces glide over one another and increase the moment arm approximately 5 mm for 10° of flexion which may increase the deflection of the pars. The increase in deflection of the pars may allow a higher ultimate load at failure to be reached during flexed postures.

Hypothesis 3:

Cyclic preconditioning both anterior and posterior decreases the ability of the motion segment to resist shear loading.

The hypothesis was partially rejected. Preconditioning increases the average stiffness, the deformation at failure and the ultimate shear load at failure. The load and deformation values increased at failure which would suggest a higher tolerance, however, the injuries detected at failure were similar to those found at the high loading rate. The mechanical tolerance may be increased by preconditioning, yet there is a possibility of increasing the severity of injury at failure.

Hypothesis 4:

Stiffness and the ultimate shear load at failure of the spinal motion segment will increase as load rate increases.

The hypothesis was partially rejected. The ultimate load to failure was significantly increased with an increase in load rate. However, the increase in stiffness was not significant. there was only a trend in the stiffness values. Furthermore, this trend was mainly seen during anterior loading. The averaged normalized curves for posterior loading did not reveal an effect for the increase in load rate. Previous studies have suggested that the load rate effect for soft tissue was minimal. It would then be expected that anterior shear loading would have a larger effect due to the bony pars interarticularis which is an important structure in anterior shear load resistance.

Hypothesis 5:

Facet joints will resist a greater proportion of an external anterior shear load compared with the disc and posterior ligaments (interspinous and supraspinous).

The hypothesis was rejected. The intervertebral disc was the primary load resisting structure for both anterior and posterior shear loads. The facet joints increase the stiffness of the intact motion segment by 30% compared with the stiffness of the isolated disc. However, the most common site of injury resulting from anterior loading is the facet joints. The posterior elements appear to protect the intervertebral disc from excessive loading which would result in injury.

157

The structures of the motion segments resist anterior and posterior shear loading using different strategies. Different mechanical values and injuries result from anterior and posterior shear loading. Load rate modified the mechanical parameters for anterior shear loading, with no effect on posterior loading. The intervertebral disc was the significant shear load resisting structure for both anterior and posterior loading. The posterior elements appear to modulate the injury and the mechanical variables. The pars interarticularis increased the stiffness and the ultimate shear load at failure and appears to increase the tolerance of the specimen at higher loading rates. The capsular ligaments and the pars interarticularis increase the deformation at failure in the intact motion segment and relieve the disc of some loading to reduce the possibility of injury.

Specific contributions are stated as follows:

1. The motion segment is not weaker during posterior shear loading compared to anterior shear loading even though the stiffness value is lower. Similar ultimate load values at failure were achieved in both loading directions.

2. Load rate affects the response to shear loads in the anterior direction. The pars interarticularis may increase the margin of safety for the motion segment.

3. Fractures were found in the pars similar to the site of spondylitic fractures found clinically. The injuries occurred below the facet faces.

158

4. The intervertebral disc is the main component resisting anterior and posterior shear loading. The posterior elements function to reduce the possibility of injury to the disc.

5. The increase in deformation in posterior shear loading between the isolated disc test and the intact motion segment testing is due to load sharing by the capsular ligaments and the pars interarticularis. These structures decrease the load on the disc thus allowing the segment to reach a higher deformation before injury occurs.

6. During flexion the increase in deformation and increase in ultimate load may be due to an increase in the moment arm of the pars and an increase in distance between the facet faces.

7. Energy absorbed to failure may be the associated with the severity of injury.

8.1   Future Directions

1. Is the main function of the pars interarticularis to protect the intervertebral disc from injury?

The data from the current study suggest that the pars may increase the tolerance of the motion segment under anterior shear loading as the loading rate increases. In addition, the isolated pars has been found to sustain more loading than was calculated in the current study, suggesting a potential for more load resistance during applied shear loading (Troup. 1976). As well, studies have shown an increase in the disc pressure following facet fracture, implying that

the disc does not significantly increase its load capacity until failure of the pars (Cripton, Berleman, Visarius, Begeman, Nolte, & Prasad, 1995). The pars interarticularis could be tested in isolation in a set-up similar to in-vivo. The intervertebral disc pressure could be measured during anterior shear loading to determine when the intervertebral disc resists shear loads.

2. How much do the capsular ligaments and pars interarticularis resist an applied posterior load?

The current data suggests the posterior elements allow the disc to achieve a larger deformation before mechanical failure is detected. Measuring the intervertebral disc pressure during posterior loading may determine the timing of the load sharing between the structures.

3. Following failure in the facet joints, does the creep increase significantly in the anterior direction?

A constant shear load is applied to the lumbar spine due to its lordotic curvature. An increase in creep following the failure of the pars interarticularis may exacerbate the progression of conditions such as spondylolysthesis.

4. What is an appropriate threshold limit value (TLV) for anterior and posterior shear loading?

NIOSH has attempted to create a threshold limit value (TLV) for compressive loading on the lumbar spine which is a single value. The TLV has limitations such as its insensitivity

160

to age, gender, loading rate and spine posture. A shear value should attempt to consider modulators such as direction of loading. One value cannot be identified for shear loading but a value for anterior and posterior loading should be developed. Load rate has been found to affect anterior shear load values. The posture of the spine should be considered since flexion altered the mechanical response of the segment.

References

Adams, M.A., Green. T.P., & Dolan, P. (1994). The strength in anterior bending of lumbar intervertebral discs. *Spine*, *19(19)*, 2197-2203.

Adams, M.A., & Hutton, W.C. (1983). The mechanical function of the lumbar apophyseal joints. *Spine*, *8*, 327-330.

Adams, M.A., Hutton, W.C., & Stott, J.R.R. (1980). The resistance to flexion of the lumbar intervertebral joint. *Spine*, *5(3)*, 245-253.

Aspden. R.M., Bornstein. N.H., & Hukins. D.W.L. (1987). Collagen organization in the interspinous ligament and its relationship to tissue function. *Journal of Anatomy*, *155*, 141-151.

Black, J. (1988). *Orthopaedic biomaterials in research and practice*. New York: Churchill Livingstone.

Bogduk, N., MacIntosh, J.E., & Pearcy, M.J. (1992). A universal model of the lumbar back muscles in the upright position. *Spine*, *17*, 897-913.

Bogduk, N., & Twomey, L. (1991). *Clinical anatomy of the lumbar spine*. Melbourne:

Churchill Livingston.

Brinckmann, P., Biggemann, M., & Hilweg, D. (1989). Prediction of the compressive strength of human lumbar vertebrae. *Clin Biomech, 4, Suppl 2,* s1-s27.

Broberg, K.B., & vonEssen, H.O. (1980). Modeling of intervertebral discs. *Spine, 5(2),* 155-167.

Butler. D.L., Noyes. F.R., & Grood, E.S. (1978). Measurement of the mechanical properties of ligaments. In B.N. Feinberg & D.G. Fleming (Eds.), *CRC handbook of engineering in medicine and biology.* (pp. 279-314). West Palm Beach: CRC Press, Inc.

Cailliet, R. (1995). *Low back pain syndrome.* Philadelphia: F.A. Davis Company.

Callaghan, J.P., & McGill, S.M. (1995). Frozen storage increases the ultimate compressive load of porcine vertebrae. *Journal of Orthopaedic Research,*

Carter, D.R. (1985). Biomechanics of bone. In H.M. Nahum & J. Melvin (Eds.), *Biomechanics of trauma.* (pp. 135-165). Norwalk, Connecticut: Appleton Century Crofts.

Cheung, K.M.C., Ruan, D., Chan, F.L., & Fang, D. (1994). Computed tomographic osteometry

of Asian lumbar pedicles. *Spine. 19.* 1495-1498.

Cholewicki, J., McGill, S.M., & Norman, R.W. (1991). Lumbar spine loads during the lifting of extremely heavy weights. *Medicine and Science in Sports and Exercise. 23.* 1179-1186.

Cresswell, A.G., & Thorstensson, A. (1993). Intra-abdominal pressure and force during isokinetic lifting and lowering. *Proceedings of the International Society of Biomechanics XIVth Congress.* 290-291.

Cripton, P., Berleman, U., Visarius, H., Begeman. P.C., Nolte, L.P., & Prasad, P. (1995). Response of the lumbar spine due to shear loading. *Symposium: Injury prevention through biomechanics.* 111-126.

Cyron, B.M., & Hutton, W.C. (1981). The tensile strength of the capsular ligaments of the apophyseal joints. *Journal of Anatomy, 132,* 145-150.

Cyron, B.M., Hutton, W.C., & Stott, J.R.R. (1979). The mechanical properties of the lumbar spine. *Engineering in Medicine. 8,* 63-68.

Cyron, B.M., Hutton, W.C., & Troup, J.D.G. (1976). Spondylolytic fractures. *Journal of Bone and Joint Surgery (Am.), 58-B,* 462-466.

Dunlop. R.B.. Adams. M.A.. & Hutton, W.C. (1984). Disc space narrowing and the lumbar

facet joints. *Journal of Bone and Joint Surgery (B). 66-B(5).* 706-710.

Farfan, H.F. (1988). Biomechanics of the lumbar spine. In W.H. Kirkaldy-Willis (Ed.).

Managing low back pain. (pp. 15-29). New York: Churchill Livingstone.

Farfan, H.F., Cossette. J.W., Robertson. G.H., Wells, R.V., & Kraus, H. (1970). The effects of

torsion on the lumbar intervertebral joints: The role of torsion on the production of disc

degeneration. *Journal of Bone and Joint Surgery (Am.), 52-A(3),* 468-497.

Farfan, H.F.. Huberdeau, R.M., & Dubow, H.I. (1972). Lumbar intervertebral disc

degeneration. *Journal of Bone and Joint Surgery (Am.). 54-A(3).* 492-510.

Galante. J.O. (1967). Tensile properties of the human lumbar annulus fibrosus. *Acta Orthop*

Scand, Suppl # 100, 5-91.

Goel, V.K., Monroe. B.T.. Gilbertson. L.G., & Brinckmann, P. (1995). Interlaminar shear

stresses and laminae separation in a disc. *Spine, 20(6),* 689-698.

Grobler, L.J., Novotny, J.E., Wilder, D.G., Frymoyer, J.W., & Pope, M.H. (1994). L4-5

isthmic spondylolisthesis. *Spine, 19(2),* 222-227.

Hakim, N.S., & King, A.I. (1976). Static and dynamic articular facet loads. *Proceedings of the 20th Stapp Conference*, 607-640. (abstract)

Hardcastle, P., Annear, P., Foster, D.H., Chakera, T.M., McCormick, C., Khangure, M., & Burnett, A. (1992). Spinal abnormalities in young fast bowlers. *J Bone Jt Surg. 74B*, 421-425.

Hayes, W.C., & Myers, E.R. (1994). Biomechanics of fractures. In B.L. Riggs & L.J.I. Melton (Eds.), *Osteoporosis: Etiology, diagnosis, and management*. (pp. 2-56). New York: Raven Press.

Heylings, D.J.A. (1978). Supraspinous and interspinous ligaments of the human lumbar spine. *Journal of Anatomy, 125*, 127-131.

Hickey, D.S., & Hukins, D.W.L. (1980). Relation between the structure of the annulus fibrosus and the function and failure of the intervertebral disc. *Spine, 5(2)*, 106-116.

Hukins, D.W.L., Kirby, M.C., Sikoryn, T.A., Aspden, R.M., & Cox, A.J. (1990). Comparison of structure, mechanical properties, and functions of lumbar spinal ligaments. *Spine, 15(8)*, 787-795.

Hutton, W.C., & Adams, M.A. (1982). Can the lumbar spine be crushed in heavy lifting? *Spine, 7*, 586-590.

Hutton, W.C.. Cyron. B.M.. & Stott. J.R.R. (1979). The compressive strength of lumbar vertebrae. *Journal of Anatomy, 129,* 753-758.

Hutton, W.C., Stott, J.R.R., & Cyron. B.M. (1977). Is spondylolysis a fatigue fracture? *Spine. 2(3),* 202-209.

Inoue, H. (1981). Three-dimensional architecture of lumbar intervertebral discs. *Spine. 6(2).* 139-146.

Janevic, J., Ashton-Miller, J.A., & Schultz, A.B. (1991). Large compressive preloads decrease lumbar motion segment flexibility. *J Orthop Res, 9.* 228-236.

Johnstone. B.. Urban, J.P.G.. Roberts. S.. & Menage, J. (1992). The fluid content of the human intervertebral disc. *Spine, 17(4).* 412-416.

Jonsson. H.. Cesarini, K.. Sahlstedt, & Rauschning, W. (1994) Findings and outcome in whiplash-type neck distortions. *Spine, 19(24).* 2733-2743.

Kazarian, L., & Graves, G.A. (1977). Compressive strength characteristics of the human vertebral centrum. *Spine, 2(1),* 1-14.

Kelsey, J.L., & White, A.A.I. (1980). Epidemiology and impact of low-back pain. *Spine, 5(2),*

133-140.

Kirkaldy-Willis, W.H. (1988). *Managing low back pain.* New York: Churchhill Livingstone.

Krenz, J., & Troup, J.D.G. (1973). The structure of the pars interarticularis of the lower lumbar vertebrae and its relation to the etiology of spondylolysis. *Journal of Bone and Joint Surgery (B). 55-B.* 735-741.

MacIntosh, J.E.. & Bogduk, N. (1986). The biomechanics of the lumbar multifidus. *Clin Biomech. 1.* 205-213.

MacIntosh. J.E., & Bogduk. N. (1987). The morphology of the lumbar erector spinae. *Spine. 12.* 658-668.

Marchand, F., & Ahmed, A. (1990). Investigation of the laminate structure of lumbar disc annulus fibrosus. *Spine, 15(5),* 402-410.

Markolf, K.L., & Morris, J.M. (1974). The structural components of the intervertebral disc. *Journal of Bone and Joint Surgery (Am.), 56-A(4),* 675-687.

McElhaney, J., Fogle, J., Byars, E., & Weaver, G. (1964). Effect of embalming on the mechanical properties of beef bone. *J Appl Physiol, 19,* 1234-1236.

McGill, S.M. (1988). Estimation of force and extensor moment contributions of the disc and ligaments at l4-l5. *Spine, 13,* 1395-1402.

McGill, S.M. (1997). The biomechanics of low back injury implications on current practice in inductry and the clinic. *Journal of Biomechanics, 30(5).* 465-475.

McGill, S.M.. Juker, D., & Kropf, P. (1995). Indwelling EMG of psoas: Clinical inplications for low back injury and rehabilitation. *American Society of Biomechanics,* 87-88. (abstract)

McGill, S.M., & Norman, R.W. (1986). Partitioning of the L4/L5 dynamic moment into disc. ligamentous, and muscular components during lifting. *Spine, 11,* 666-677.

McGill, S.M., & Norman, R.W. (1987). Effects of an anatomically detailed erector spinae model on L4/L5 disc compression and shear. *Journal of Biomechanics, 20,* 591-600.

Miller, J.A.A.. Haderspeck. K.A.. & Schultz, A.B. (1983). Posterior element loads in lumbar motion segments. *Spine, 8(3),* 331-337.

Moroney, S.P., Scultz, A.B., & Miller, J.A.A. (1988). Analysis and measurement of neck loads. *J Orthop Res, 6,* 713-720.

Nachemson, A., & Evans, J.H. (1968). Some mechanical properties of the third lumbar

interlaminar ligament (ligamentum flavum). *J Biomech. 1.* 211-220.

Neugebauer, F.L. (1976). The classic: A new contribution to the history and etiology of spondylolisthesis. *Clinical Orthopaedics and Related Research, 117.* 4-21.

Newman, P.H. (1963). The etiology of spondylolisthesis. *Journal of Bone and Joint Surgery (B). 45-B(1).* 39-59.

Norman, R., Wells, R., Neumann, P., Frank, J., Shannon, H.Kerr, M. (1997). A comparison of peak vs cumulative physical work exposure risk factors for the reporting of low back pain in the automotive industry. Submitted.

O'Neil. D.B.. & Micheli. L.J. (1989). Postoperative radiographic evidence for fatigue fracture as the etiology in spondylolysis. *Spine, 14(12),* 1342-1355.

Osvalder, A.L., Neumann, P., Lovsund, P., & Nordwall, A. (1993). A method for studying the biomechanical load response of the (in-vitro) lumbar spine under dynamic flexion-shear loads. *Journal of Biomechanics, 26(10),* 1227-1236.

Oxland, T.R., Panjabi, M.M., Southern, E.P., & Duranceau, J.S. (1991). An anatomic basis for spinal instability: a porcine trauma model. *J Orthop Res, 9,* 452-462.

Penning, L. (1992). Acceleration injury of the cervical spine by hypertranslation of the head. *European Spine Journal, 1,* 13-19.

Potvin, J.R., McGill, S.M., & Norman, R.W. (1991). Trunk muscle and lumbar ligament contributions to dynamic lifts with varying degrees of trunk flexion. *Spine, 16,* 1099-1107.

Potvin, J.R., Norman, R.W., & McGill, S.M. (1991). Reduction in anterior shear forces on the L4/L5 disc by the lumbar musculature. *Clin Biomech, 6,* 88-96.

Prasad, P., King, A.I., & Ewing, C.L. (1974). The role of articular facets during +Gz acceleration. *Journal of Applied Mechanics,* 321-326.

Santaguida, P.L., & McGill, S.M. (1995). The psoas major muscle: A three-dimensional geometric study. *Journal of Biomechanics, 28(3),* 339-345.

Sedlin, E.D., & Hirsch, C. (1966). Factors affecting the determination of the physical properties of femoral cortical bone. *Acta Orthop Scand, 37,* 29-48.

Shirazi-Adl, A., Ahmed, A.M., & Shrivastava, S.C. (1986). A finite element study of a lumbar motion segment subjected to pure sagittal plane moments. *Journal of Biomechanics, 19(4),* 331-350.

Shirazi-Adl, A., Shrivastava, S.C., & Ahmad, A.M. (1984). Stress analysis of the lumbar disc-body unit in compression A three-dimensional nonlinear finite element study. *Spine, 9(2),* 120-134.

Sikoryn, T.A., & hukins, D.W.L. (1990). Mechanism of failure of the ligamentum flavum of the spine during in vitro tensile tests. *Journal of Orthopaedic Research, 8,* 586-591.

Smeathers, J.E., & Joanes, D.N. (1988). Dynamic compressive properties of human lumbar intervertebral joints: A comparison between fresh and thawed specimens. *Journal of Biomechanics, 21(5),* 425-433.

Stewart, T.D. (1953). The age incidence of neural-arch defects in alaskan natives, considered from the standpoint of etiology. *Journal of Bone and Joint Surgery (Am.), 35-A,* 937-950.

Taillard, W.F. (1976). Etiology of spondylolisthesis. *Clinical Orthopaedics and Related Research, 117,* 30-39.

Troup, J.D.G. (1976). Mechanical factors in spondylolisthesis and spondylolysis. *Clinical Orthopaedics and Related Research, 117,* 59-67.

Tsuji, H., Hirano, N., Ohshima, H., Ishihara, H., Terahata, N., & Motoe, T. (1993). Structural variation of the anterior and posterior anulus fibrosus in the development of human lumbar

intervertebral disc. *Spine. 18(2).* 204-210.

Viidik, A. (1979). Biomechanical behavior of soft connective tissues. In N. Akkas (Ed.).

Progress in biomechanics. (pp. 75-113). Alphen aan den Rijn: Sijthoff & Noordhoff.

White, A.A.I., & Panjabi, M.M. (1990). Physical properties and functional biomechanics of the

spine. In Anonymous, *Clinical biomechanics of the spine.* (pp. 1-83). Philadelphia:

J.B.Lippincott Company.

Wiltse, L.L., Windell, E.H., & Jackson, D.W. (1975). Fatigue fracture: The basic lesion in

isthmic spondylolisthesis. *Journal of Bone and Joint Surgery (Am.), 57-A(1).* 17-22.

Woo, S.L.-Y., Gomez, M.A., & Akeson, W.H. (1985). Mechanical behaviors of soft tissues:

Measurements, modifications, injuries, and treatment. In H.M. Nahum & J. Melvin (Eds.),

Biomechanics of trauma. (pp. 109-133). Norwalk, Connecticut: Appleton Century Crofts.

Yahia, H., Drouin, G., & Newman, N. (1990). Structure-function relationship of human spinal

ligaments. *Z mikrosk anat forsch Leipzig, 104,* 33-45.

Yang, K.H., & King, A.I. (1984). Mechanism of facet load transmission as a hypothesis for

low-back pain. *Spine, 9(8),* 557-565.

Yingling, V.R., Callaghan, J.P., & McGill, S.M. (1997). Dynamic loading affects the

mechanical properties and failure site of porcine spines. *Clinical Biomechanics,*

.

Appendix A

Anterior Shear Loading Model of the Motion

Segment

The model of the motion segment under anterior loading was formed using the experimental data from the intact motion segments and the data from the isolated intervertebral disc under shear loading. The experimental data was modeled using a 2nd order polynomial equation. To identify the influence of the pars interarticularis the equation of the intervertebral disc was subtracted from the equation for the intact motion segment. The three equations are:

WHOLE: $LOAD = 23.286x^2 + 33.041x$ $R^2 = .9959$

DISC: $LOAD = 13.208x^2 + 45.754x$ $R^2 = .9963$

PARS: $Load = 10.179x^2 - 12.713x$ $R^2 = .987$

The pars interarticularis equation consists of a toe region followed by a stiffness of 108.92. The pars was represented as the linear stiffness portion of the equation. which was added to the equation of the disc at 3.5 mm of translation (Figure 1). The response of an intact motion segment aquired by adding the intervertebral disc to the linear pars stiffness. was similar to the experimental values from the intact specimens (Figure 2). As well. the average stiffness values from the experimental data were similar to the average stiffnesses calculated

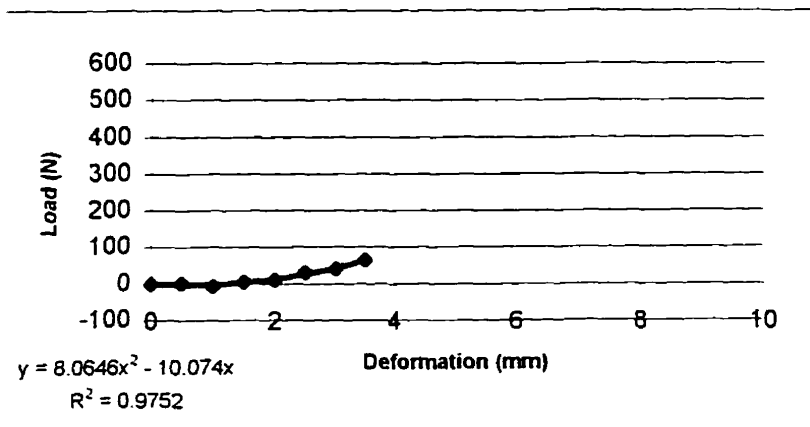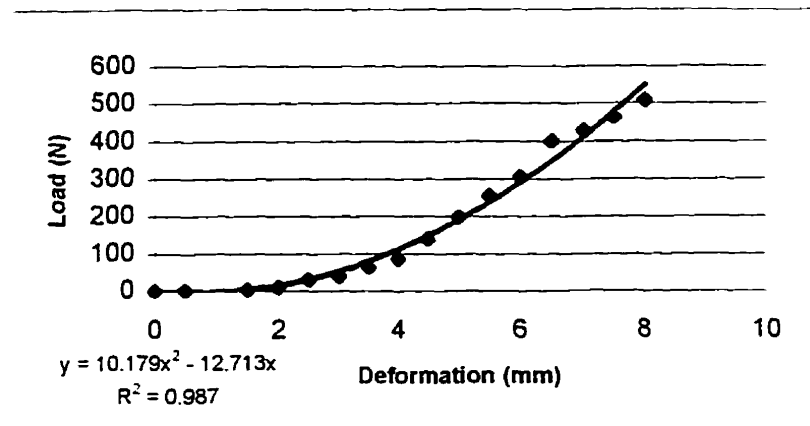from the equations (Table 1).
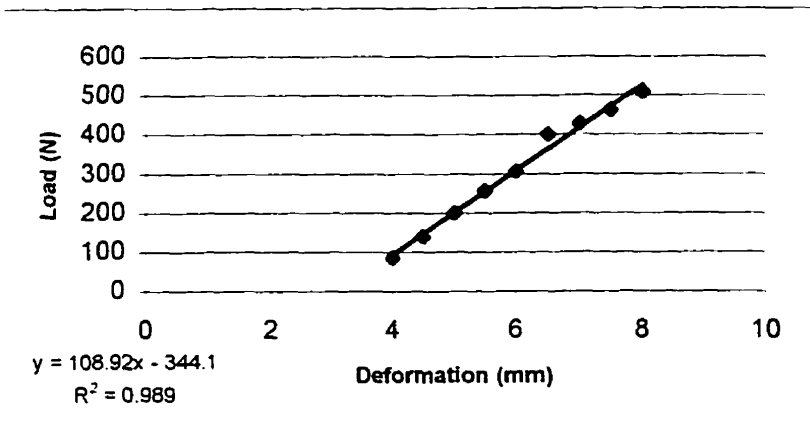
Figure 1: Partitioning of the pars interarticularis data into an initial toe region and a linear portion. The toe region was minimal therefore only the linear portion was used as the pars interarticularis model.
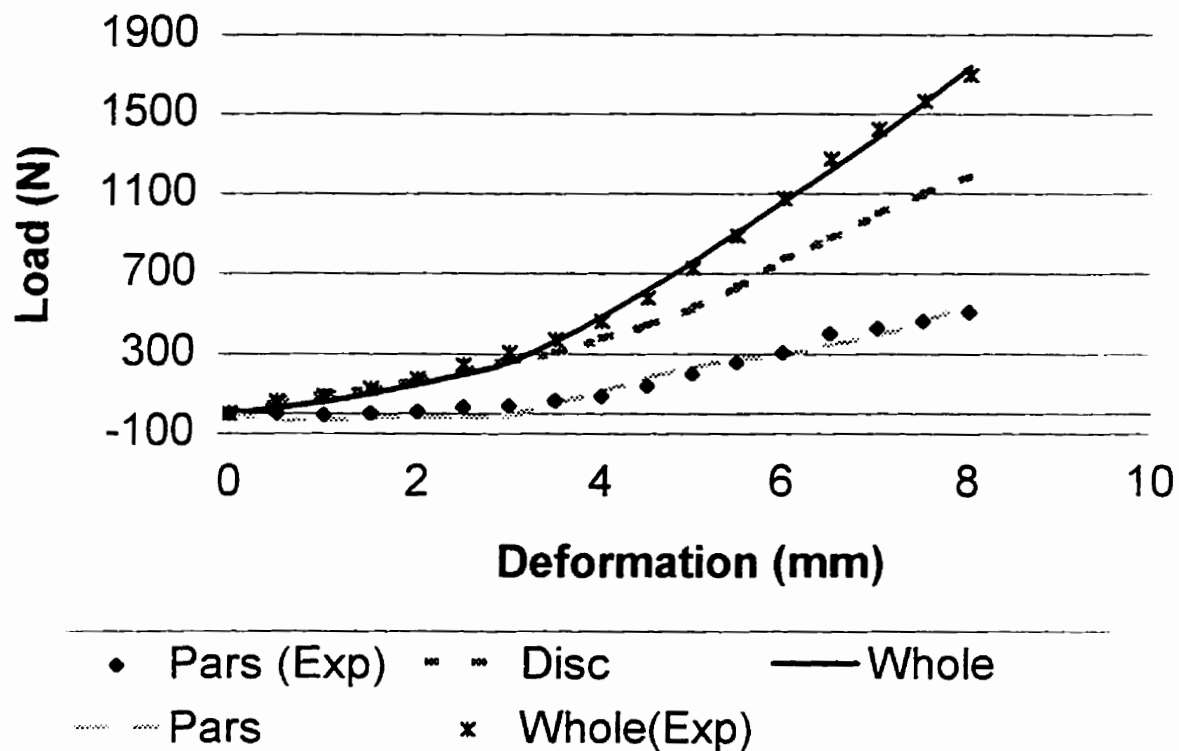
177

Figure 2: Model for anterior shear loading partitioned between the intervertebral disc and the pars interarticularis. Comparison of modelled curves with the experimental data. Pars(Exp) is the data from subtracting the isolated disc data from the whole experimental data. Disc is the equation expressing the isolated disc data. Whole is the equation expressing the experimental data. Pars is the equation for the linear stiffness portion of the pars data. Whole(Exp) is the experimental data from intact specimens.

Table 1: The comparison of the average stiffness values from the experimental data to the average stiffness values calculated from the equations representing the whole specimen and the intervertebral disc.

Type of Specimen	Average Stiffness from Experimental Data (N/mm)	Average Stiffness from the Equations (N/mm)
Whole Specimens	326	337
Isolated Disc	236	217

Appendix B

Effect of Flexion on the Facet Face Alignment

The effect of flexion on the alignement of the pars interarticularis was determined using coordinates for important landmarks on the L4 and L5 vertebrae (McGill & Norman. 1987). These points were then rotated around the z-axis to yield the relative location of the facet faces. Figure 1 illustrates the effect of flexion on the facet face alignment. The vertical distance. or the moment arm of the pars interarticularis, increased by 5 mm. The anterior-posterior distance between the facet faces increased by .4 mm.

The increase in moment arm affects the deflection of the pars. The pars interarticularis can be modelled as a cantilever beam. Using the flexure formula, the deflection of the beam can be calculated as follows:

$$\text{Deflection} = \text{Load}_{pars} * \text{Moment Arm}^3 / 3 * E * I$$

Figure 2 illustrates the change in moment for 10 mm of deformation of the motion segment as well as the deflection of the pars interarticularis with an increase in moment arm of 5 mm.
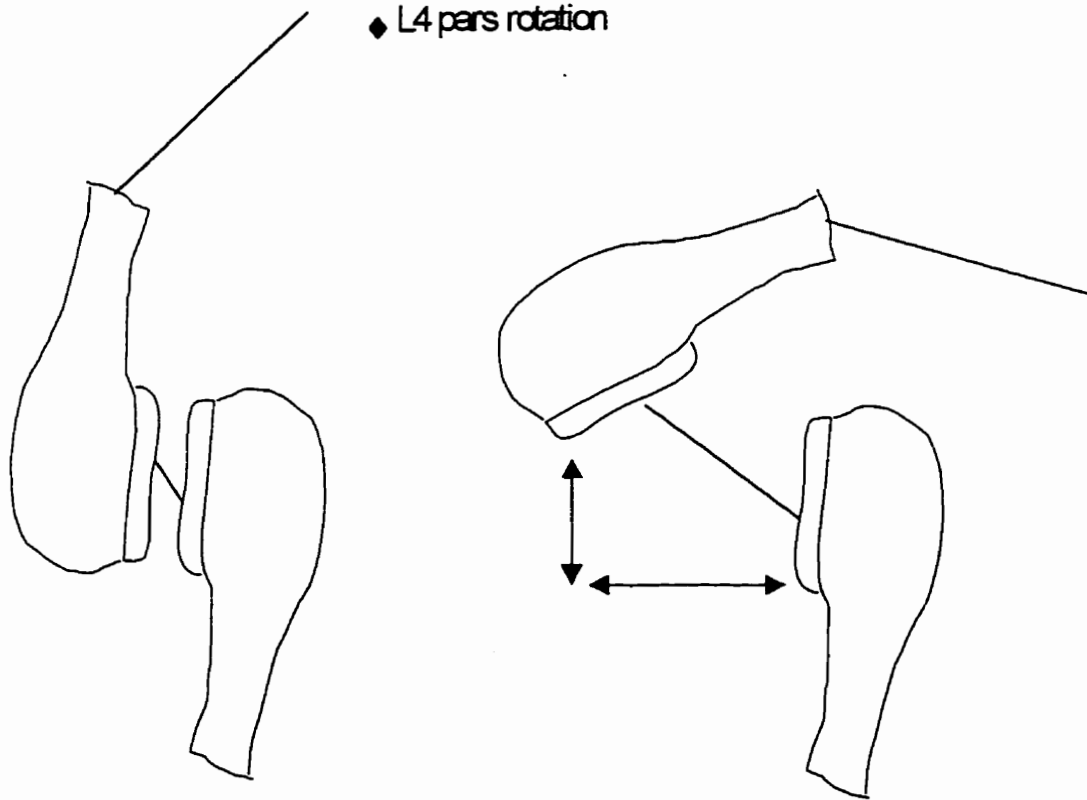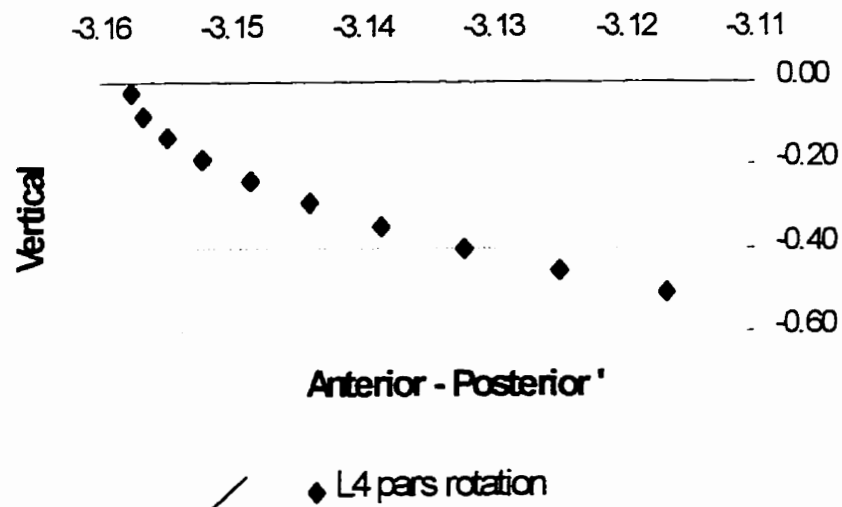
Figure 1: An illustration of the relative movement of the facet faces during a rotation of 10 degrees. The vertical distance increased by 5 mm and the anterior-posterior distance increased by .4 mm. (The schematic diagram is not to scale.)
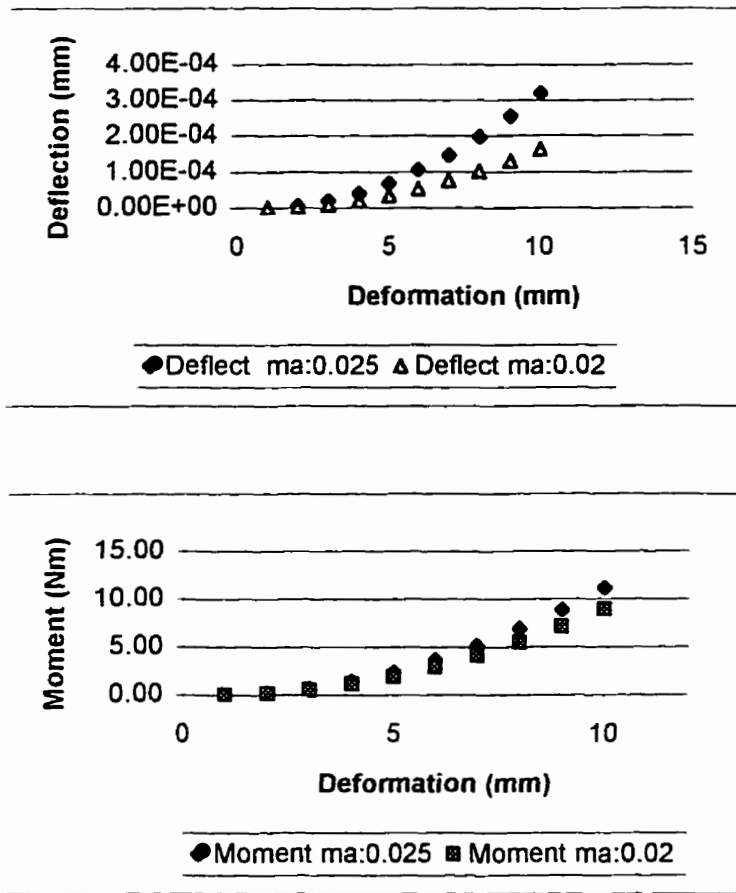
181

Figure 2: The effect on pars deflection of a 5 mm increase in moment arm. The Elastic Modulus was 10000 MPa, the load on the pars was taken from the experimental data, a square beam was used for moment of inertia calculations. The bottom graph illustrates the change in the moment about the pars interarticularis with a 5mm increase in moment arm.

Appendix C

Model of Annulus

The purpose of this model was to identify any regions of the annulus which may expereince more load and/or deformation from an anterior or posterior translation resulting from anterior or posterior shear loading.

The intervertebral disc has been thought to be shaped as an ellipse. An ellipse was used to model the disc in an attempt to identify the effects of the lateral curvature on the functioning of the annulus. Previous models of the disc have used cylindrical or circular models (Broberg & vonEssen. 1980), however, for shear translations these models do not describe the mechanics of the disc adequately. The fiber angle and fiber length vary in an elliptical structure especially when a translation occurs, however, in a circular model the fiber angles and fiber lengths remain constant implying all areas of the structure are equally loaded. The histology also suggests that differences in annular regions exist. The fiber thickness and the number of layers of fibers differ, with the lateral annulus having the most layers followed by the anterior portion and then the posterior region (Tsuji, Hirano, Ohshima, Ishihara, Terahata, & Motoe. 1993; Marchand & Ahmed. 1990).

The intervertebral disc was modelled as an ellipse with a major axis of 4.9 cm and a minor axis of 3.4 cm (Hickey & Hukins. 1980). Seventy-two equally spaced points were generated for each elliptical structure (representing the upper and lower endplates). The fibers

were connected from the lower ellipse to a point on the upper ellipse which was shifted one point to the right and to the left to represent the opposite fiber angles in the structure. Twenty-five to thirty degrees is a commonly reported angle in the literature (Bogduk & Twomey. 1991), however, the angle is actually random as shown in morphological studies (Tsuji. Hirano. Ohshima. Ishihara. Terahata. & Motoe. 1993: Marchand & Ahmed. 1990). The modelled fibers range from 28-35 degrees.

The lateral fibers in a neutral position were longer than the fibers in the anterior and posterior region (Figure 1). As the upper ellipse translated in the x-direction. the effect of the fiber angle on the lateral fibers was evident. The two layers of the annulus were not contributing to the same extent as was the case in the anterior and posterior fibers due to the opposite fiber angles and the shape of the ellipse on the lateral sides (Figure 2).

The top ellipse was then flexed around the z-axis to simulate a flexion posture to identify the differences in fiber length. The x-axis is the anterior-posterior axis. the z-axis is the medial-lateral axis and the y-axis is the verticle axis. Figure 3 illustrates the affect on the fiber lengths for a 10° flexion of the superior ellipse.
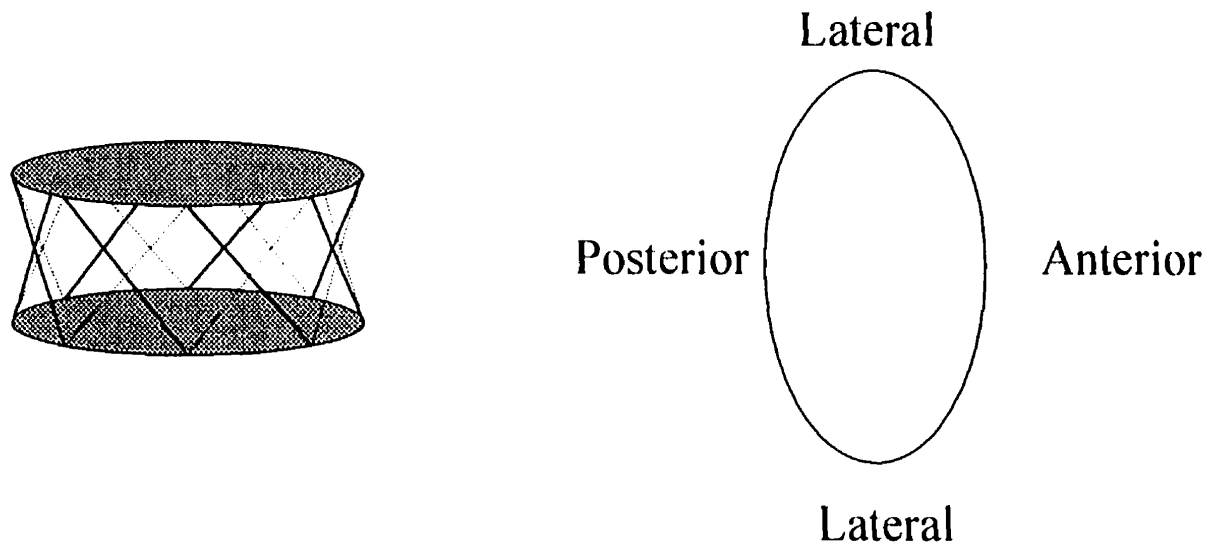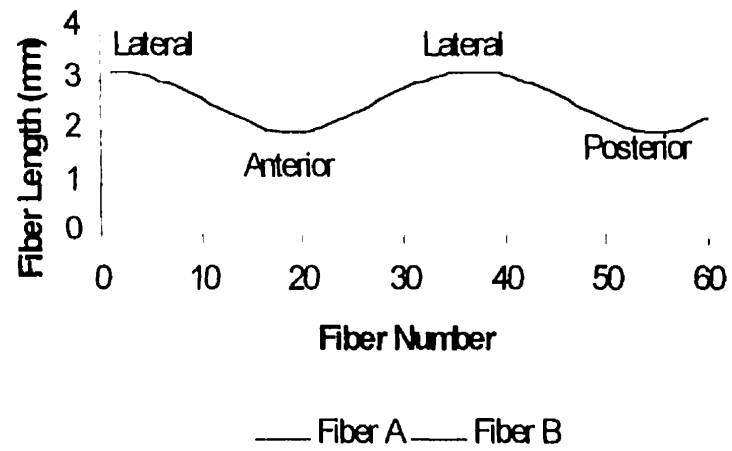
Figure 1: The graph illustrates the difference in the lengths of the fibers due to the elliptical geometry of the intervertebral disc. The lateral fibers are longer than the anterior and posterior fibers in a neutral position with no translation. Fiber A and Fiber B represent the opposite angles of the fibers in the annulus
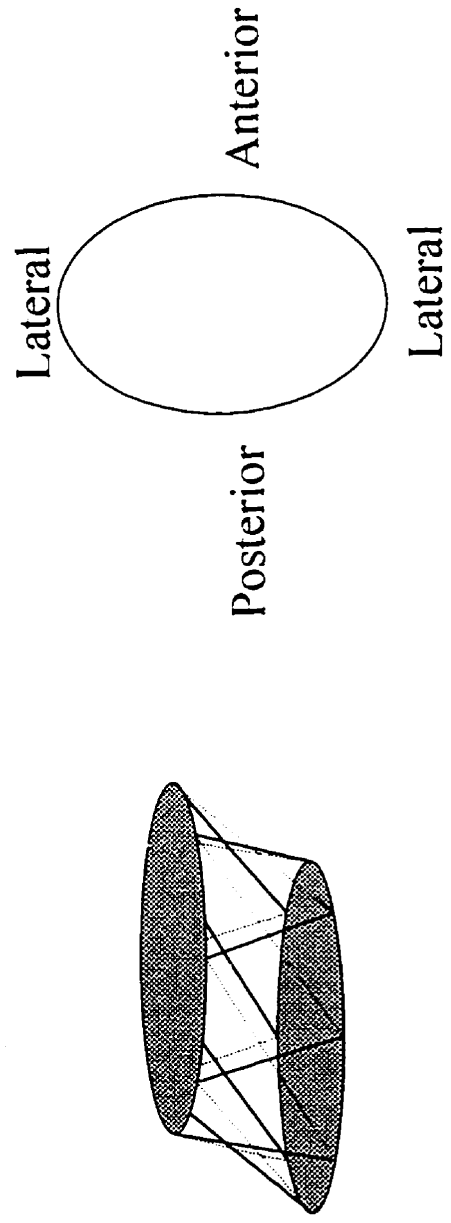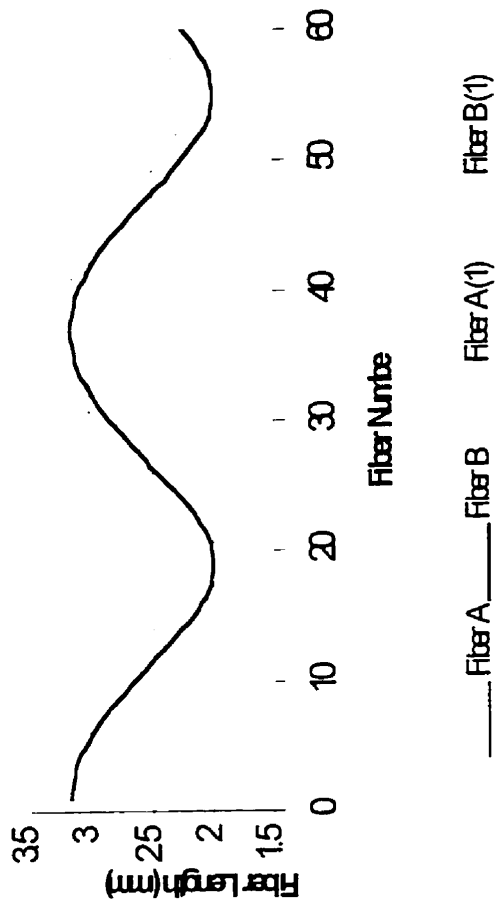
Figure 2: This graph illustrates the difference in fiber lengths due to the elliptical geometry after the superior vertebra was translated 1 mm. The lateral fibers are longer and the variation in angle direction affects the length of the fiber. Fiber A (1) is shorter in the lateral and anterior portions (Fiber 1-20) and is longer for the posterior and opposite lateral fibers (Fiber 35-55)
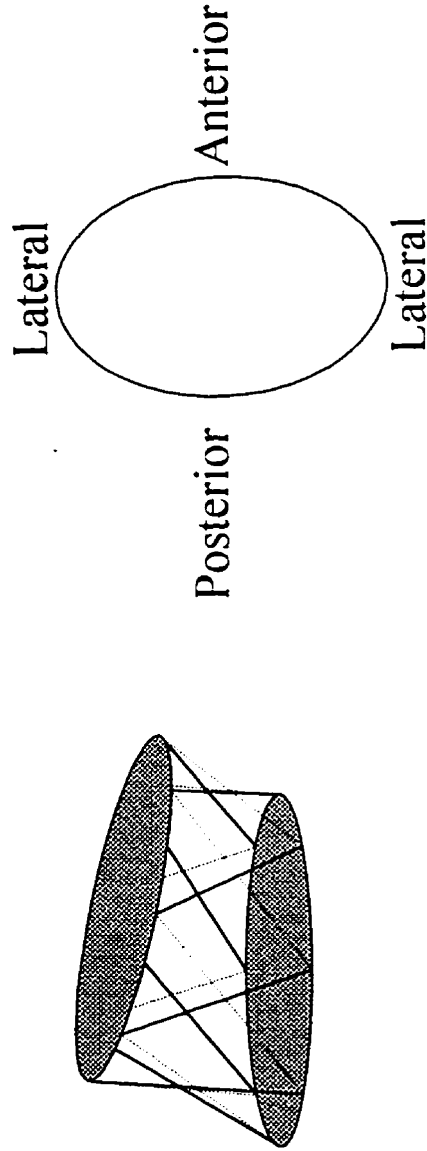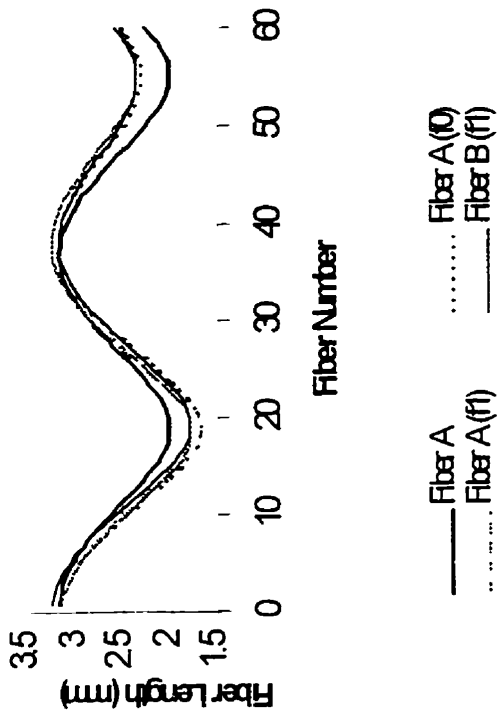
Figure 3: The graph illustrates the difference in the fiber length due to the elliptical geometry of the intervertebral disc in a neutral position, flexed 10 degrees and flexed and translated 1 mm. FiberA and Fiber B overlay one another, they are the neutral fiber lengths, Fiber A (fo) and Fiber B (fo) also overlay one another and are the fiber lengths following 10 degrees of flexion, Fiber A(fl) and Fiber B (fl) are the fiber lengths after 10 degrees of flexion and 1 mm of translation. During translation the layers with different fiber angles function differently in the lateral region.